

ISSN:2454-1311



# International Journal of Advanced Engineering Management and Science

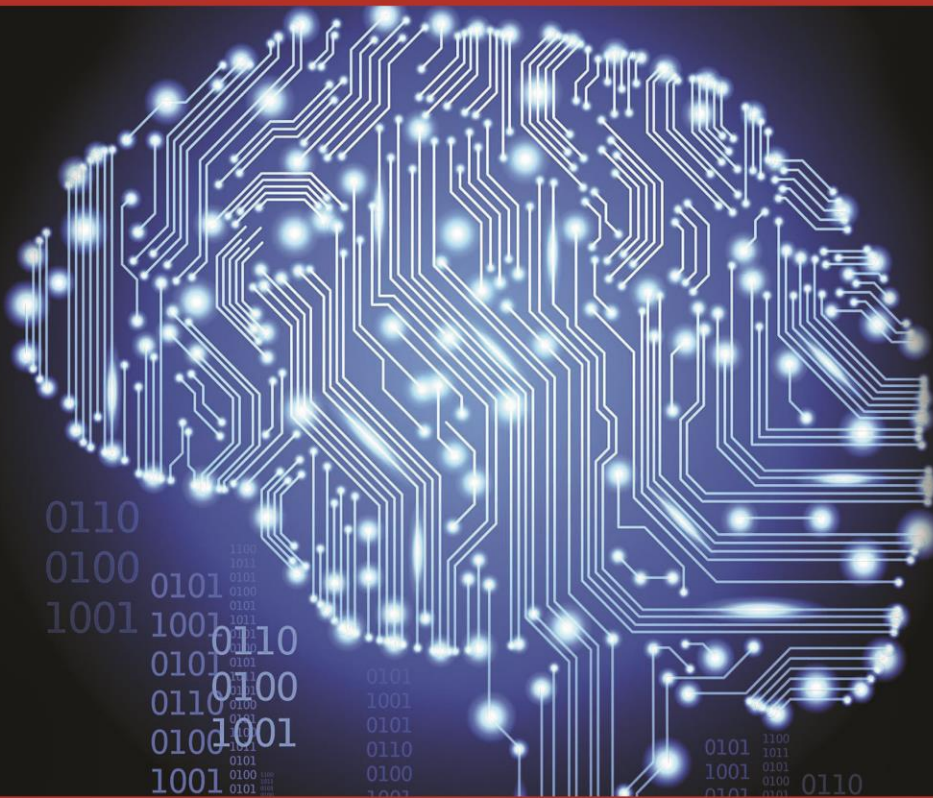
(IJAEMS)

An Open Access Peer Reviewed International Journal

Vol. -4

Issue -7

July, 2018



Journal DOI: 10.22161/ijaems

Issue DOI: 10.22161/ijaems.4.7



<http://www.ijaems.com/> | [editor@ijaems.com](mailto:editor@ijaems.com)

# Editorial Board

**Dr. Zafer Omer Ozdemir**

*Energy Systems Engineering Kirklareli, Kirklareli University, Turkey*

**Dr. H.Saremi**

*Vice- chancellor For Administrative & Finance Affairs, Islamic Azad university of Iran, Quchan branch, Quchan-Iran*

**Dr. Ahmed Kadhim Hussein**

*Department of Mechanical Engineering, College of Engineering, University of Babylon, Republic of Iraq*

**Mohammad Reza Kabaranzad Ghadim**

*Associated Prof., Department of Management, Industrial Management, Central Tehran Branch, Islamic Azad University, Tehran, Iran*

**Prof. Ramel D. Tomaquin**

*Prof. 6 in the College of Business and Management, Surigao del Sur State University (SDSSU), Tandag City, Surigao Del Sur, Philippines*

**Dr. Ram Karan Singh**

*BE.(Civil Engineering), M.Tech.(Hydraulics Engineering), PhD(Hydraulics & Water Resources Engineering), BITS- Pilani, Professor, Department of Civil Engineering, King Khalid University, Saudi Arabia.*

**Dr. Asheesh Kumar Shah**

*IIM Calcutta, Wharton School of Business, DAVV INDORE, SGSITS, Indore  
Country Head at CrafsOL Technology Pvt.Ltd, Country Coordinator at French Embassy, Project Coordinator at IIT Delhi, INDIA*

**Dr. Uma Choudhary**

*Specialization in Software Engineering Associate Professor, Department of Computer Science Mody University, Lakshmanagarh, India*

**Dr. Ebrahim Nohani**

*Ph.D.(hydraulic Structures), Department of hydraulic Structures, Islamic Azad University, Dezful, IRAN.*

**Dr.Dinh Tran Ngoc Huy**

*Specialization Banking and Finance, Professor, Department Banking and Finance, Viet Nam*

**Dr. Shuai Li**

*Computer Science and Engineering, University of Cambridge, England, Great Britain*

**Dr. Ahmadad Nabih Zaki Rashed**

*Specialization Optical Communication System, Professor, Department of Electronic Engineering, Menoufia University*

***Dr.Alok Kumar Bharadwaj***

*BE(AMU), ME(IIT, Roorkee), Ph.D (AMU),Professor, Department of Electrical Engineering, INDIA*

***Dr. M. Kannan***

*Specialization in Software Engineering and Data mining, Ph.D, Professor, Computer Science,SCSVMV University, Kanchipuram, India*

***Dr.Sambit Kumar Mishra***

*Specialization Database Management Systems, BE, ME, Ph.D,Professor, Computer Science Engineering Gandhi Institute for Education and Technology, Baniatangi, Khordha, India*

***Dr. M. Venkata Ramana***

*Specialization in Nano Crystal Technology, Ph.D,Professor, Physics,Andhara Pradesh, INDIA*

***Dr.Swapnesh Taterh***

*Ph.d with Specialization in Information System Security, Associate Professor, Department of Computer Science Engineering Amity University, INDIA*

***Dr. Rabindra Kayastha***

*Associate Professor, Department of Natural Sciences, School of Science, Kathmandu University, Nepal*

***Amir Azizi***

*Assistant Professor, Department of Industrial Engineering, Science and Research Branch-Islamic Azad University, Tehran, Iran*

***Dr. A. Heidari***

*Faculty of Chemistry, California South University (CSU), Irvine, California, USA*

***DR. C. M. Velu***

*Prof.& HOD, CSE, Datta Kala Group of Institutions, Pune, India*

***Dr. Sameh El-Sayed Mohamed Yehia***

*Assistant Professor, Civil Engineering(Structural), Higher Institute of Engineering -El-Shorouk Academy, Cairo, Egypt*

***Dr. Hou, Cheng-I***

*Specialization in Software Engineering, Artificial Intelligence, Wisdom Tourism, Leisure Agriculture and Farm Planning, Associate Professor, Department of Tourism and MICE, Chung Hua University, Hsinchu Taiwan*

***Branga Adrian Nicolae***

*Associate Professor, Teaching and research work in Numerical Analysis, Approximation Theory and Spline Functions, Lucian Blaga University of Sibiu, Romania*

***Dr. Amit Rathi***

*Department of ECE, SEEC, Manipal University Jaipur, Rajasthan, India*

***Dr. Elsanosy M. Elamin***

*Dept. of Electrical Engineering, Faculty of Engineering. University of Kordofan, P.O. Box: 160, Elobeid, Sudan*

# FOREWORD

I am pleased to put into the hands of readers Volume-4; Issue-7: July, 2018 of “**International Journal of Advanced Engineering, Management and Science (IJAEMS) (ISSN: 2354-1311)**”, an international journal which publishes peer reviewed quality research papers on a wide variety of topics related to Science, Technology, Management and Humanities. Looking to the keen interest shown by the authors and readers, the editorial board has decided to release print issue also, but this decision the journal issue will be available in various library also in print and online version. This will motivate authors for quick publication of their research papers. Even with these changes our objective remains the same, that is, to encourage young researchers and academicians to think innovatively and share their research findings with others for the betterment of mankind. This journal has DOI (Digital Object Identifier) also, this will improve citation of research papers.

I thank all the authors of the research papers for contributing their scholarly articles. Despite many challenges, the entire editorial board has worked tirelessly and helped me to bring out this issue of the journal well in time. They all deserve my heartfelt thanks.

Finally, I hope the readers will make good use of this valuable research material and continue to contribute their research finding for publication in this journal. Constructive comments and suggestions from our readers are welcome for further improvement of the quality and usefulness of the journal.

With warm regards.

**Dr. Uma Choudhary**

Editor-in-Chief

Date: Aug, 2018

## Vol-4, Issue-7, July, 2018

Sr No.	Title
1	<p><a href="#"><u>Comprehensive Review of the Investigation of Anthropogenic and Naturally Occurring Radionuclides in Different Parts of Bangladesh</u></a>  <b>Author:</b> M. N. Islam, H. Akhter, M. Begum, M. Kamal   <b>DOI:</b> <a href="https://doi.org/10.22161/ijaems.4.7.1"><u>10.22161/ijaems.4.7.1</u></a></p> <p style="text-align: right;"><b>Page No:</b> 490-495</p>
2	<p><a href="#"><u>Design of charging station for electric vehicle batteries</u></a>  <b>Author:</b> Kusum, Chetan Parveer   <b>DOI:</b> <a href="https://doi.org/10.22161/ijaems.4.7.2"><u>10.22161/ijaems.4.7.2</u></a></p> <p style="text-align: right;"><b>Page No:</b> 496-509</p>
3	<p><a href="#"><u>Identification of Cocoa Pods with Image Processing and Artificial Neural Networks</u></a>  <b>Author:</b> Sergio A. Veites-Campos, Reymundo Ramírez-Betancour, Manuel González-Pérez   <b>DOI:</b> <a href="https://doi.org/10.22161/ijaems.4.7.3"><u>10.22161/ijaems.4.7.3</u></a></p> <p style="text-align: right;"><b>Page No:</b> 510-518</p>
4	<p><a href="#"><u>Intellectual Capital Impact on Organizations' Performance</u></a>  <b>Author:</b> Sayyed Khawar Abbas, Hafiz Ali Hassan, Zair Mahmood Hashmi, Hafiz Muhammad Junaid, Sikandar Majid, Tanzila Ijaz   <b>DOI:</b> <a href="https://doi.org/10.22161/ijaems.4.7.4"><u>10.22161/ijaems.4.7.4</u></a></p> <p style="text-align: right;"><b>Page No:</b> 519-524</p>
5	<p><a href="#"><u>Optimization of Cutting Rate for EN 1010 Low Alloy Steel on WEDM Using Response Surface Methodology</u></a>  <b>Author:</b> Munish Giri, Manjeet Bohat, Ravinder Chaudhary, Anish Taneja   <b>DOI:</b> <a href="https://doi.org/10.22161/ijaems.4.7.5"><u>10.22161/ijaems.4.7.5</u></a></p> <p style="text-align: right;"><b>Page No:</b> 525-533</p>
6	<p><a href="#"><u>Optimization of Surface Roughness for EN 1010 Low Alloy Steel on WEDM Using Response Surface Methodology</u></a>  <b>Author:</b> Munish Giri, Manjeet Bohat, Ravinder Chaudhary, Anish Taneja   <b>DOI:</b> <a href="https://doi.org/10.22161/ijaems.4.7.6"><u>10.22161/ijaems.4.7.6</u></a></p> <p style="text-align: right;"><b>Page No:</b> 534-542</p>
7	<p><a href="#"><u>Development of Interactive E-Module for Global Warming to Grow of Critical Thinking Skills</u></a>  <b>Author:</b> Wayan Suwatra, Agus Suyatna, Undang Rosidin   <b>DOI:</b> <a href="https://doi.org/10.22161/ijaems.4.7.7"><u>10.22161/ijaems.4.7.7</u></a></p> <p style="text-align: right;"><b>Page No:</b> 543-549</p>
8	<p><a href="#"><u>Multi-Index Bi-Criterion Transportation Problem: A Fuzzy Approach</u></a>  <b>Author:</b> Dr. Samiran Senapati   <b>DOI:</b> <a href="https://doi.org/10.22161/ijaems.4.7.8"><u>10.22161/ijaems.4.7.8</u></a></p> <p style="text-align: right;"><b>Page No:</b> 550-556</p>

9	<p><b><u><a href="#">Factors that Impede the Formation of Self-Directed work teams in Mexican Organizations</a></u></b>  <b>Author:</b> Martha Patricia Quintero-Fuentes, Montserrat Gómez-Márquez, Alejandra Martínez-Orencia, Jesús Gerardo Llanillo-Navales, Martha Marín-Ramos, Luz del Carmen García-Arroyo, María Isela Eurrieta-Ortiz, Claudia Olivia Carrera-Salazar, Fern Fernando Agustín Romo-Celis2, José Luís Calderón-Palomares, Juan Manuel Méndez-Cervantes, Manuel González-Pérez</p> <p> <b>DOI:</b> <a href="https://doi.org/10.22161/ijaems.4.7.9">10.22161/ijaems.4.7.9</a></p> <p style="text-align: right;"><b>Page No:</b> 557-563</p>
10	<p><b><u><a href="#">Effectiveness of Guided Inquiry Model Student Worksheet to Improve Critical thinking Skill on Heat Material</a></u></b>  <b>Author:</b> Heri Nurdin, Tri Jalmo, Chandra Ertikanto</p> <p> <b>DOI:</b> <a href="https://doi.org/10.22161/ijaems.4.7.10">10.22161/ijaems.4.7.10</a></p> <p style="text-align: right;"><b>Page No:</b> 564-573</p>
11	<p><b><u><a href="#">Facile fabrication and characterizations of nanostructured Fe<sub>2</sub>O<sub>3</sub>-TiO<sub>2</sub> composite from Ilmenite ore</a></u></b>  <b>Author:</b> Chinh Van Tran, Phuong T.H Nguyen, Duy Anh Nguyen, Bac Thanh Le, Tuan Ngoc Truong, Duong Duc La</p> <p> <b>DOI:</b> <a href="https://doi.org/10.22161/ijaems.4.7.11">10.22161/ijaems.4.7.11</a></p> <p style="text-align: right;"><b>Page No:</b> 574-578</p>

# Comprehensive Review of the Investigation of Anthropogenic and Naturally Occurring Radionuclides in Different Parts of Bangladesh

M. N. Islam<sup>1</sup>, H. Akhter<sup>2</sup>, M. Begum<sup>3</sup> and M. Kamal<sup>4</sup>

<sup>1,2,3</sup> Electronics Division, Atomic Energy Centre, Bangladesh Atomic Energy Commission,  
P.O. Box No. 164, Dhaka, Bangladesh.

<sup>4</sup> Radioactivity Testing and Monitoring Laboratory, Atomic Energy Centre, Bangladesh Atomic Energy Commission,  
P.O. Box No. 1352, Chittagong, Bangladesh.  
E-mail: nislam\_baec@yahoo.com

**Abstract**— Authors attempt to depict a survey of anthropogenic  $^{137}\text{Cs}$  and naturally occurring radionuclides ( $^{226}\text{Ra}$ ,  $^{228}\text{Th}$ ,  $^{232}\text{Th}$ ,  $^{214}\text{Bi}$ ,  $^{208}\text{Tl}$ ,  $^{40}\text{K}$ ) in undistributed soil, water, ship scrapped materials such as metal, rubber and foam and tree bark of ship breaking area, cynoglossids i.e. tongue soles and tea leaves collected from different parts of Bangladesh for detecting health hazards, environmental protection and radiation safety of the public. The assessment of such radionuclides in these samples is utmost important due to nuclear test and accident, fallout and disposal of radioactive wastes. These radiotracers have been investigated by using laboratory-based Gamma Spectrometry for Food and Environmental Samples. The observation of activity concentrations for  $^{137}\text{Cs}$ ,  $^{226}\text{Ra}$ ,  $^{228}\text{Th}$ ,  $^{232}\text{Th}$ ,  $^{214}\text{Bi}$ ,  $^{208}\text{Tl}$  and  $^{40}\text{K}$  have been presented in  $\text{Bq.Kg}^{-1}$ . The others radiological parameters such as gamma ray dose rate ( $\text{nGyh}^{-1}$ ), Radium Equivalent Dose ( $R_{\text{eq}}$ )  $\text{Bq.Kg}^{-1}$ , Representative Level Index ( $I_{\text{yr}}$ )  $\text{Bq.Kg}^{-1}$  and Transfer Factor (TF) %. The Radiation Hazard Index ( $H_x$ )  $\text{Bq.Kg}^{-1}$  also has been presented.

**Keywords**—Radionuclides, Radioactivity, Activity Concentration, Radiological Parameters, Gamma Spectrometry.

## I. INTRODUCTION

Assessment of any release of radioactivity to the environment is important the protection of public health, especially if the released radioactivity can enter into the food chain. Assessment demands rapid, reliable and practical techniques for analysis of various radionuclides [1]. In this context, distribution of  $^{137}\text{Cs}$  and naturally occurring radionuclides for soil and water samples in the Terrene of Goainghat and Jaintapur Area of Sylhet district and the same for soil samples at the site of the Rooppur Nuclear Power Plant has been presented [2,3]. In [4], describes the study of the radioactivity in soil and tea leaf and transfer factor of those radionuclides. The

environmental radioactivity levels, both natural and anthropogenic, in the ship scrapped materials such as metal, rubber and foam and tree bark of ship breaking area of Bhatiari, Chittagong in the southern part of Bangladesh have been analyzed [5]. The study on  $^{214}\text{Bi}$ ,  $^{208}\text{Tl}$ ,  $^{40}\text{K}$  and  $^{137}\text{Cs}$  in soil of Chittagong Hills, Bangladesh has been provided to ascertain the baseline data to assess the public exposure of that area [6]. The radionuclides concentration in the cynoglossids i.e. tongue soles collected from the Kutubdia channel of Bangladesh have been estimated. The study consists of the analysis of seasonal occurrence of these radionuclides along with hydrological parameters and biochemical constituents of their living area [7]. In [8], presents the Gamma radiation dose from the naturally occurring radioclides in soil of the Potenga Sea Beach area of Bangladesh. In Potenga Sea Beach soil samples, the activities of  $^{226}\text{Ra}$ ,  $^{232}\text{Th}$  and  $^{40}\text{K}$  have been found to be higher than that of world average values. The radioactivity of naturally occurring radionuclides in water and sediment samples collected from the Meghna-Dakatia River at Chandpur of Bangladesh has been measured. Thus, the external outdoor radiation dose rate, radium equivalent activities,  $R_{\text{eq}}$  and representative level index,  $I_{\text{yr}}$  also have been estimated [9]. Activities of gamma-emitters  $^{238}\text{U}$ ,  $^{226}\text{Ra}$ ,  $^{232}\text{Th}$  and  $^{40}\text{K}$  in tap water samples of Dhaka city have been analyzed by using High-Purity Germanium (HPGe) coaxial detector(EG &ORTEC) coupled with Silena Emcaplus Multichannel Analyzer System. The estimated effective dose and annual effective dose due to intake of different radionuclides for various age groups also have been provided [10]. The current research motivated to the recent trend and development in Radiological Research in Bangladesh. A comprehensive review of the investigation of anthropogenic  $^{137}\text{Cs}$  and naturally occurring radionuclides ( $^{226}\text{Ra}$ ,  $^{228}\text{Th}$ ,  $^{232}\text{Th}$ ,  $^{214}\text{Bi}$ ,  $^{208}\text{Tl}$ ,  $^{40}\text{K}$ ) in undistributed soil, water, ship scrapped materials such as metal, rubber and foam and tree bark of

ship breaking area, cynoglossids i.e. tongue soles and tea leaf collected from different parts of Bangladesh.

## II. MATERIALS AND METHOD

### 2.1: Sample Collection

Double identities should be placed on samples at collection time. It is advisable that a standard form with all relevant information such as date, location, fresh weight, weather, collector's name etc. to be filled up. Care should be taken that the sample is representative and suitable for specific purposes of the monitoring procedures [1].

In this context, M. N. Alam et al [2] study area was in Goainghat and Jaintapur of Sylhet district located at 91° 50' to 92°13' N and 24°56' to 25°12' E. The soil samples have been collected from 17 sites at a depth of 0-10 cm with the help of premeasured steel corer of size 10.5 cm dia and 25 cm height. Water samples have also been collected from 17 sites of natural reservoir corresponding to the location of soils, on the border area at a distance of 500 m to 4 km from each other during the period of September – October, 2000. The collected soils are of sedimentary rock and clay type and believe to be undistributed. Thereafter, N. Absar [4] research area was in Odalia tea Garden which was about 3000 sq. km situated in the hilly region of Fatickchari Chittagong district of Bangladesh. Soil samples have been collected from 5 locations of the garden at a depth upto 20 cm from the surface and tea leaf sample for the same 5 locations [5].

### 2.2: Sample Preparation

Samples received in the laboratory may not in the proper physical form for analysis. They may require reduction in size, evaporating, drying of some form of homogenizing before taken for analysis. Some general consideration for handling and pretreatment of samples are needed. The samples with high levels of activity should be processed in a separate area from low level samples to avoid contamination [1].

All the soil samples M. N. Alam et al [2] have been dried in an oven at 110°C for 48 h, pulverized and passed through sieve, weighed and then packed in cylindrical plastic containers (6.5 cm ×7.5 cm). They have been then sealed tightly with caps, wrapped with thick vinyl tape around their screw necks and stored for 4 weeks to allow secular equilibrium between <sup>226</sup>Ra, <sup>232</sup>Th and their daughter nuclei. Water samples were collected with 5-litre plastic jars from the natural reservoir. Each 5-litre water sample has been boiled to reduce its volume to 500 ml and packed into 500 ml cylindrical containers, sealed tightly and wrapped with thick vinyl tapes around their screw necks. These samples have been stored for 4 weeks too.

### 2.3: Measurement Procedure

The  $\gamma$ -ray activities of all the collected samples for <sup>226</sup>Ra, <sup>232</sup>Th, <sup>214</sup>Bi, <sup>208</sup>Tl, <sup>40</sup>K and <sup>137</sup>Cs have been analyzed by

using a p-type coaxial lead shielded High Purity Germanium (HPGe) detector having relative efficiency of 30%, active volume 132 cm<sup>3</sup>, resolution (FWHM) of 1.85 KeV at 1332 KeV for <sup>60</sup>Co coupled with PCA and other accessories. The calibration of the peak efficiency of the detector was performed using IAEA reference samples <sup>238</sup>U (RGU-1), <sup>232</sup>Th (RGTh-1), <sup>40</sup>K (RGK-1) and <sup>137</sup>Cs (IAEA-152) [11]. The mentioned radiotracers were investigated by using a p-type coaxial lead shielded High Purity Germanium (HPGe) detector with Liquid Nitrogen (LN<sub>2</sub>) cooling having relative efficiency of 20%, resolution (FWHM) of 1.80 KeV at 1332 KeV for <sup>60</sup>Co coupled with DSA-1000, Genie-2000 GAA software and other accessories [3]. The radioactivities of the investigated samples were measured for 10,000s by using the same Gamma Spectrometry configuration as described in N. Absar [4]. The <sup>226</sup>Ra (<sup>238</sup>U) activity was determined individually from the net area of peak at energies of 351.9 keV (<sup>214</sup>Pb), 1120 keV (<sup>214</sup>Bi) and 1764 keV (<sup>214</sup>Bi). <sup>214</sup>Pb and <sup>214</sup>Bi are the decay products of <sup>238</sup>U series. Similarly, the <sup>232</sup>Th activity was determined from the counts at peak energies of 238.6 keV (<sup>212</sup>Pb), 727 keV (<sup>212</sup>Bi), 911 keV (<sup>228</sup>Ac) and 583 keV (<sup>208</sup>Tl) [5]. The <sup>40</sup>K and <sup>137</sup>Cs radionuclides have been measured from their respective  $\gamma$ -ray energies 1460 KeV and 661.66 KeV respectively [1, 12].

### 2.4: Results and Discussion

Radiological parameters are very important for ensuring the public health and safety (reducing environmental radiation exposer), environmental protection and radioecological control. According to N. Alam et al [2], the activity concentration of <sup>137</sup>Cs in soil and water of the sampling area have been observed as 4.12 ± 0.32 to 30.53 ± 0.88 Bq.kg<sup>-1</sup> with an average value of 13.23 ± 6.76 Bq.kg<sup>-1</sup> and 1.0 ± 0.34 to 1.72 ± 0.61 Bq.L<sup>-1</sup>. The activity concentration S. Roy et al [3] of <sup>137</sup>Cs in seven soil samples out of thirty of the Rooppur Nuclear Power Plant (RNPP) sampling area have been observed as 3.46 ± 0.48 to 5.86 ± 0.61 Bq.kg<sup>-1</sup> with an average value of 4.22 ± 0.78 Bq.kg<sup>-1</sup>. In N. Absar [4] research, the average activity concentration of <sup>137</sup>Cs in the soil samples has been obtained as 2.84 ± 0.27 Bq.kg<sup>-1</sup> whereas the <sup>137</sup>Cs for tea samples was not present in all samples, therefore, no uptake has been recorded. Barua, et al [5] obtained the lower limit of detection for <sup>137</sup>Cs was 0.043679 Bq.kg<sup>-1</sup>. In N. Alam et al [6], the activity concentration of <sup>137</sup>Cs in soil of Chittagong Hills varies from 1.08 ± 0.14 to 4.25 ± 0.48 Bq.kg<sup>-1</sup> with an average value of 2.66 Bq.kg<sup>-1</sup>. According to J. Ferdous et al [10], no activity concentration of <sup>137</sup>Cs in tap water of Dhaka City has been detected.

N. Alam et al [2], continued with the activity concentration of naturally occurring radionuclides like  $^{226}\text{Ra}$  in soil and water have been recorded as  $7.2 \pm 1.0 - 57.70 \pm 8.60 \text{ Bq.kg}^{-1}$  and  $5.70 \pm 0.50 - 56.4 \pm 1.20 \text{ mBq.L}^{-1}$  respectively. Similarly, the activity concentration of  $^{232}\text{Th}$  have been given as  $28.80 \pm 3.30 - 66.20 \pm 4.10 \text{ Bq.kg}^{-1}$  and  $36.70 \pm 2.30 - 67.0 \pm 4.20 \text{ mBq.L}^{-1}$  accordingly. Likewise, the activity concentration of  $^{40}\text{K}$  for the same sample have been observed as  $467 \pm 5.0 - 656 \pm 43 \text{ Bq.kg}^{-1}$  and  $7.90 \pm 1.70 - 12.70 \pm 2.0 \text{ mBq.L}^{-1}$  respectively. S. Roy et al [3] furthermore evaluated the minimum and maximum radioactivity level of  $^{226}\text{Ra}$ ,  $^{232}\text{Th}$ , and  $^{40}\text{K}$  of soil samples as  $21.87 \pm 5.87 \text{ Bq.kg}^{-1}$  and  $55.66 \pm 0.74 \text{ Bq.kg}^{-1}$ ,  $31.28 \pm 3.00 \text{ Bq.kg}^{-1}$  and  $78.01 \text{ Bq.kg}^{-1}$  and  $332.86 \pm 48.95 \text{ Bq.kg}^{-1}$  and  $661.96 \pm 63.56 \text{ Bq.kg}^{-1}$  with an average value of  $33.32 \pm 7.96 \text{ Bq.kg}^{-1}$ ,  $46.91 \pm 12.24 \text{ Bq.kg}^{-1}$  and  $448.54 \pm 89.86 \text{ Bq.kg}^{-1}$  respectively. N. Absar [4] research continued with the average activity concentrations of  $^{238}\text{U}$ ,  $^{232}\text{Th}$ , and  $^{40}\text{K}$  of soil samples and the same for tea samples have been obtained as  $44.55 \pm 7.83 \text{ Bq.kg}^{-1}$  and  $5.66 \pm 0.66 \text{ Bq.kg}^{-1}$ ;  $51.08 \pm 10.80 \text{ Bq.kg}^{-1}$  and  $4.38 \pm 0.50 \text{ Bq.kg}^{-1}$  and  $274.81 \pm 78.01 \text{ Bq.kg}^{-1}$  and  $190 \pm 30.50 \text{ Bq.kg}^{-1}$  respectively. Barua, et al [5] measured the radionuclide concentrations of  $^{226}\text{Ra}$  ( $^{238}\text{U}$ ),  $^{232}\text{Th}$  and  $^{40}\text{K}$  in various ship scrapped metal samples and the same from ship engine varied in the range of  $6.89 \pm 0.84 \text{ Bq.kg}^{-1} - 15.27 \pm 1.14 \text{ Bq.kg}^{-1}$  and  $415 \pm 22.25 \text{ Bq.kg}^{-1}$ , which is not comparable to others due the unknown reason;  $6.78 \pm 1.06 \text{ Bq.kg}^{-1} - 238 \pm 8.98 \text{ Bq.kg}^{-1}$  and  $7.40 \pm 0.67 \text{ Bq.kg}^{-1} - 67.32 \pm 7.41 \text{ Bq.kg}^{-1}$  respectively. The levels of the above three radionuclides in the mixture of rubber and foam samples have been observed in the range of  $7.78 \pm 0.66 \text{ Bq.kg}^{-1} - 25.57 \pm 1.53 \text{ Bq.kg}^{-1}$ ;  $8.62 \pm 0.41 \text{ Bq.kg}^{-1} - 31.05 \pm 1.55 \text{ Bq.kg}^{-1}$  and  $12.57 \pm 0.88 \text{ Bq.kg}^{-1} - 312 \pm 34.26 \text{ Bq.kg}^{-1}$  accordingly. Barua, et al [5] also investigated the activity in tree barks (Eucalyptus and Jackfruit) which might helpful for understanding the effect of ship breaking on environmental radioactivity. N. Alam et al [6], the average radionuclide concentrations of  $^{214}\text{Bi}$ ,  $^{208}\text{Tl}$  and  $^{40}\text{K}$  in of Chittagong Hills have been estimated as  $36.33 \pm 15.65 \text{ Bq.kg}^{-1}$ ,  $14.73 \pm 8.54 \text{ Bq.kg}^{-1}$  and  $350.96 \pm 113.34 \text{ Bq.kg}^{-1}$  respectively. According to N. Alam et al [7], the range of  $^{226}\text{Ra}$  activity has been measured as  $9 \pm 2$  to  $20 \pm 5 \text{ Bq.kg}^{-1}$  fresh weight (fw) with maximum in the edible portion of *c. cynoglossus* and minimum in the whole body of *c. lingua*. Seasonal variation of activity of radionuclides in different body parts of cynoglossids also have presented. Afterwards, the activity concentration of  $^{232}\text{Th}$  has been found in the range  $8 \pm 1$  to  $17 \pm 4 \text{ Bq.kg}^{-1}$  fw with highest in the whole body of *c. cynoglossus* and lowest in the whole body of *p. bilineata*. Then, the range of  $^{228}\text{Th}$  activity has been measured as  $4 \pm 1$  to  $14 \pm 4 \text{ Bq.kg}^{-1}$  fw

with maximum in the offal of *c. bilineatus* and minimum in the edible portion of *c. cynoglossus*. At last, the radionuclides concentration of  $^{40}\text{K}$  in the different body parts of cynoglossids i.e. tongue soles on a fw basis also have been detected as  $81 \pm 11 \text{ Bq.kg}^{-1}$  to  $227 \pm 19 \text{ Bq.kg}^{-1}$  fw with highest in the whole body of *c. bilineatus* and lowest in the edible portion of *c. cynoglossus*. Following S. Ghose et al [8], mean the activities of  $^{226}\text{Ra}$ ,  $^{232}\text{Th}$  and  $^{40}\text{K}$  in the Potenga Sea Beach soil samples of high and low tide lines have been determined as 37 and 33; 76 and 54.7 and 424 and 432  $\text{Bq.kg}^{-1}$  respectively. M.I. Chowdhury et al [9], the activity concentrations of  $^{226}\text{Ra}$ ,  $^{228}\text{Th}$ ,  $^{232}\text{Th}$ , and  $^{40}\text{K}$  (average activity concentration) in sediment and water samples of the Meghna and the Dakatia have been measured in the ranges from  $12.0 \pm 2.2$  to  $57.0 \pm 10.0 \text{ Bq.kg}^{-1}$  and  $2.91 \pm 1.7$  to  $14.01 \pm 3.10 \text{ Bq.L}^{-1}$ ;  $27.0 \pm 4.0$  to  $104 \pm 8.5 \text{ Bq.kg}^{-1}$  and  $1.21 \pm 0.51$  to  $6.81 \pm 0.27 \text{ Bq.L}^{-1}$ ;  $25.0 \pm 3.5$  to  $108 \pm 9.70 \text{ Bq.kg}^{-1}$  and  $1.40 \pm 0.50$  to  $7.20 \pm 2.50 \text{ Bq.L}^{-1}$  and  $273 \pm 54 \text{ Bq.kg}^{-1}$  and  $7.90 \pm 1.90 \text{ Bq.L}^{-1}$  respectively. According to J. Ferdous et al [10], the activity concentrations of  $^{238}\text{U}$ ,  $^{226}\text{Ra}$ ,  $^{232}\text{Th}$  and  $^{40}\text{K}$  in tap water samples have been obtained as  $0.82 \pm 0.26$  to  $2.12 \pm 0.32 \text{ Bq.L}^{-1}$ ;  $0.014 \pm 0.0054$  to  $0.040 \pm 0.0055 \text{ Bq.L}^{-1}$ ;  $0.16 \pm 0.003$  to  $0.73 \pm 0.027 \text{ Bq.L}^{-1}$  and  $2.04 \pm 0.0094$  to  $6.40 \pm 0.027 \text{ Bq.L}^{-1}$  respectively. Activity concentration values for radionuclides of artificial ( $^{137}\text{Cs}$ ) and all natural origin for bulk samples have been recommended by IAEA as  $100 \text{ Bq.kg}^{-1}$  and  $1000 \text{ Bq.kg}^{-1}$  respectively; only exception in  $^{40}\text{K}$  which is  $10000 \text{ Bq.kg}^{-1}$  [13].

The absorbed dose rate in air one meter above the ground surface due to the radionuclides  $^{226}\text{Ra}$ ,  $^{232}\text{Th}$ , and  $^{40}\text{K}$  of soil has been estimated using the formula given by

$$D = [0.427C_{RA} + 0.662C_{TH} + 0.0432C_K] \text{ nGyh}^{-1} \quad (1)$$

Where  $C_{RA}$ ,  $C_{TH}$  and  $C_K$  are the average activity concentrations of  $^{226}\text{Ra}$ ,  $^{232}\text{Th}$ , and  $^{40}\text{K}$  of soil samples in  $\text{Bq.kg}^{-1}$  [14]. The dose rate N. Alam et al [2] due to  $^{226}\text{Ra}$ ,  $^{232}\text{Th}$ , and  $^{40}\text{K}$  of soil samples varied in the ranges from  $59.66$  to  $89.84 \text{ nGyh}^{-1}$ , with an average value of  $74.76 \text{ nGyh}^{-1}$ , which is higher than the world average value of  $52 \text{ nGyh}^{-1}$ . The dose rate S. Roy et al [3] due to  $^{226}\text{Ra}$ ,  $^{232}\text{Th}$ , and  $^{40}\text{K}$  of soil samples varied in the ranges from  $50.90$  to  $103.46 \text{ nGyh}^{-1}$ , with an average value of  $69.45 \text{ nGyh}^{-1}$ . According to N. Absar [4] research, the dose rate that has been calculated of  $71.14 \text{ nGyh}^{-1}$  is to be treated as outdoor dose that yielded annual effective dose much below the permissible limit of  $1.0 \text{ mSv.y}^{-1}$  recommended by the International Commission on Radiation Protection (ICRP) for general population [15]. The dose rate in S. Ghose et al

[8] due to  $^{226}\text{Ra}$ ,  $^{232}\text{Th}$ , and  $^{40}\text{K}$  in soil samples of high and low tide lines varied in the ranges from 45.2 – 220 and 51 – 160  $\text{nGyh}^{-1}$  respectively. The average dose rate in M. I. Chowdhury et al [9], of the river sediment has been found as  $0.62 \pm 0.22 \text{ mGy y}^{-1}$ . The indoor dose contribution is assumed to be 1.2 times higher than the outdoor [16].

$$D_{\text{indoor}} = D_{\text{outdoor}} \times 1.2 \text{ (nGyh}^{-1}\text{)} \quad (2)$$

The annual effective dose equivalent  $D_{\text{eff}}$  from outdoor terrestrial gamma radiation is given by

$$D_{\text{eff}} = \text{outdoor dose (nGyh}^{-1}\text{)} \times 0.7(\text{Sv} \cdot \text{Gy}^{-1}) \times 8,760(\text{hy}^{-1}) \times 0.2 \quad (3)$$

Where 0.2 is the outdoor dose occupancy factor and  $0.7 \text{ Sv.Gy}^{-1}$  is the quotient of effective dose equivalent rate to absorbed dose rate in air [17].

The annual effective dose due to intake of  $^{238}\text{U}$ ,  $^{226}\text{Ra}$ ,  $^{232}\text{Th}$  and  $^{40}\text{K}$  in tap water samples of Dhaka city for five age groups are 104.10, 87.90, 75.73, 63.19 and 73.38  $\mu\text{Sv.y}^{-1}$  for 1 year, 5 year, 10 year, 15 year and above 18 year respectively in J. Ferdous et al [10]. These values are significantly lower than both the World Health Organization (WHO) and the International Commission on Radiological Protection (ICRP) limits.

The annual effective dose equivalent  $D_{\text{eff}}$  from indoor exposure is given by:

$$D_{\text{eff}} = \text{indoor dose (nGyh}^{-1}\text{)} \times 0.7(\text{Sv} \cdot \text{Gy}^{-1}) \times 8,760(\text{hy}^{-1}) \times 0.8 \quad (4)$$

Where 0.8 has been used as the occupancy factor [17]. Therefore, the total annual effective dose equivalent from terrestrial radiation is sum of outdoor and indoor annual effective dose equivalent.

The  $\gamma$ -ray radiation hazards due to the radionuclides  $^{226}\text{Ra}$ ,  $^{232}\text{Th}$ , and  $^{40}\text{K}$  of soil samples has been assessed by two different indices. The most widely used radiation hazard index,  $R_{\text{a}_{\text{eq}}}$ , can be derived from the following formula:

$$R_{\text{a}_{\text{eq}}} = C_{\text{RA}} + \left(\frac{10}{7}\right)C_{\text{TH}} + \left(\frac{10}{130}\right)C_{\text{K}} \quad (5)$$

Where  $C_{\text{RA}}$ ,  $C_{\text{TH}}$  and  $C_{\text{K}}$  are the average activity concentrations of  $^{226}\text{Ra}$ ,  $^{232}\text{Th}$ , and  $^{40}\text{K}$  in  $\text{Bq.kg}^{-1}$  respectively [18]. The values of  $R_{\text{a}_{\text{eq}}}$  for N. Alam et al [2] in soils varied from 121.8 to 187.5  $\text{Bq.kg}^{-1}$  with an average value of 153.86  $\text{Bq.kg}^{-1}$ . The values of  $R_{\text{a}_{\text{eq}}}$  for S. Roy et al [3] also in soils varied from 96.68 to 217.04  $\text{Bq.kg}^{-1}$  with an average value of 134.80  $\text{Bq.kg}^{-1}$  which is too low with

respect to allowable limit 370  $\text{Bq.kg}^{-1}$  as recommended by the IAEA but higher than the world average values of 89.25  $\text{Bq.kg}^{-1}$  [1]. The mean value of the radium equivalent activity of the soil samples has been found to be  $150.42 \pm 29.11 \text{ Bq.kg}^{-1}$  with the range of  $175.79 \pm 30.04$  to  $110.26 \pm 29.50 \text{ Bq.kg}^{-1}$  in N. Absar [4]. Barua, et al [5] calculated the  $R_{\text{a}_{\text{eq}}}$  in the range of 21-145  $\text{Bq.kg}^{-1}$  except one scrapped metal from engine (760  $\text{Bq.kg}^{-1}$ ) is of radiological concern indeed. The  $R_{\text{a}_{\text{eq}}}$  for S. Ghose et al [8] due to  $^{226}\text{Ra}$ ,  $^{232}\text{Th}$ , and  $^{40}\text{K}$  in soil samples of high and low tide lines varied in the ranges from 80 – 428 and 93 – 300  $\text{Bq.kg}^{-1}$  respectively. The values of  $R_{\text{a}_{\text{eq}}}$  for M. I. Chowdhury et al [9] in sediments varied from  $114.0 \pm 48.0$  to  $478.0 \pm 89.0 \text{ Bq.kg}^{-1}$  with an average value of  $320.0 \pm 82.0 \text{ Bq.kg}^{-1}$ .

The another radiation hazard index, used to estimate the level of  $\gamma$ -radiation associated with the natural radionuclides in soil, representative level index ( $I_{\gamma\text{r}}$ ) defined as follows

$$I_{\gamma\text{r}} = \left(\frac{C_{\text{RA}}}{150} + \frac{C_{\text{TH}}}{100} + \frac{C_{\text{K}}}{1500}\right) \quad (6)$$

Where  $C_{\text{RA}}$ ,  $C_{\text{TH}}$  and  $C_{\text{K}}$  are the average activity concentrations of  $^{226}\text{Ra}$ ,  $^{232}\text{Th}$ , and  $^{40}\text{K}$  in  $\text{Bq.kg}^{-1}$  respectively [19]. N. Alam et al study calculated the  $I_{\gamma\text{r}}$  for soil samples varied from 0.77 to 1.37  $\text{Bq.kg}^{-1}$  with an average value of 1.08  $\text{Bq.kg}^{-1}$  which is higher than world average values of 0.66  $\text{Bq.kg}^{-1}$  [12]. The mean value of  $I_{\gamma\text{r}}$  for the soil sample has been obtained  $1.22 \pm 0.24 \text{ Bq.kg}^{-1}$  with the range of  $1.46 \pm 0.24$  to  $0.94 \pm 0.23 \text{ Bq.kg}^{-1}$  in N. Absar [4]. The  $I_{\gamma\text{r}}$  for S. Ghose et. Al [8] due to  $^{226}\text{Ra}$ ,  $^{232}\text{Th}$ , and  $^{40}\text{K}$  in soil samples of high and low tide lines varied in the ranges from 0.6 – 3.0 and 0.7 – 2.0  $\text{Bq.kg}^{-1}$  respectively. The value of  $I_{\gamma\text{r}}$  for the sediments sample has been obtained in the range of  $0.70 \pm 0.32$  to  $1.21 \pm 0.46 \text{ Bq.kg}^{-1}$  with mean value of  $0.95 \pm 0.28 \text{ Bq.kg}^{-1}$  in M. I. Chowdhury et al [9].

The Transfer Factor (TF) is defined by the following equation:

$$TF = \frac{\text{Radioactivity in Plant (Bq/kgDW)}}{\text{Radioactivity in Soil (Bq/kgDW)}} \quad (7)$$

The transfer mechanism of radionuclides, represented by TF, is widely used to describe the soil-to-plant transfer of radionuclides through plant roots. The concentration of a nuclide in a plant or plant part (in  $\text{Bq.kg}^{-1}$ , dry weight), is assumed to be linearly related to its concentration in soil within the rooting zone also in  $\text{Bq.kg}^{-1}$ , dry weight) [20].

In N. Absar [4], the average activity concentration of  $^{137}\text{Cs}$  in tea samples  $<0.4 \text{ Bq.kg}^{-1}$ , so no uptake found. The

transfer factor (TF) of  $^{238}\text{U}$ ,  $^{232}\text{Th}$ , and  $^{40}\text{K}$  for soil-to-tea samples have been found as  $0.13 \pm 0.08$ ,  $0.09 \pm 0.05$  and  $0.69 \pm 0.39$  respectively. The average TF of  $^{226}\text{Ra}$ ,  $^{228}\text{Th}$ ,  $^{232}\text{Th}$  and  $^{40}\text{K}$  for sediment-to-water has been recorded as  $0.21 \pm 0.15$ ,  $0.05 \pm 0.02$ ,  $0.06 \pm 0.03$  and  $0.03 \pm 0.01$  respectively in M. I. Chowdhury et al [9].

TF value in excess of unity imply active bioaccumulation of the activity. The values less than unity mean either strong binding of the radionuclides with soil, little or no accumulation in the plant [4].

The external radiation hazard index  $H_{\text{ext}}$  and internal radiation hazard index  $H_{\text{int}}$  has been calculated by using the following formula:

$$H_{\text{ext}} = A_U/370 + A_{Th}/259 + A_K/4810 \quad (8)$$

$$H_{\text{int}} = A_U/185 + A_{Th}/259 + A_K/4810 \quad (9)$$

Where, the numerical quantities of equations (8) and (9) are in units of  $\text{Bq.kg}^{-1}$  and  $A_U$ ,  $A_{Th}$  and  $A_K$  are the activity concentrations of the radionuclides  $^{238}\text{U}$ ,  $^{232}\text{Th}$ , and  $^{40}\text{K}$  respectively [21]. The values of  $H_{\text{ext}}$  and  $H_{\text{int}}$  have been observed in the ranges from  $0.30 \pm 0.08$  to  $0.50 \pm 0.08$  and  $0.62 \pm 0.10$  to  $0.39 \pm 0.10$  with the mean value of  $0.41 \pm 0.08$  and  $0.51 \pm 0.10$  respectively in N. Absar [4]. The  $H_{\text{ext}}$  in Barua, et al [5] varied from 0.06 to 0.39. Since these values are lower than unity, the external radiation hazard in the ship breaking area is low.

The radon mass exhalation rate is calculated by following the equation given below

$$R_m = \lambda_{Rn} C_{\text{soil.Ra}} F_r \quad (10)$$

Where,  $C_{\text{soil.Ra}}$  is the activity mass concentration of  $^{226}\text{Ra}$  ( $\text{Bq.kg}^{-1}$ ) in soil,  $\lambda_{Rn}$  is the decay constant of  $^{222}\text{Rn}$  ( $2.1 \times 10^{-6} \text{ s}^{-1}$ ) and  $F_r$  is the emanation co-efficient [22]. In S. Ghose et. Al [8], the  $^{222}\text{Rn}$  emanation co-efficient ranged from 10-27.5% with a mean value of 15.32% and the  $^{222}\text{Rn}$  exhalation rate ranged from 4.89-20.4  $\mu\text{Bq.kg}^{-1}.\text{s}^{-1}$  with a mean value of 10.63  $\mu\text{Bq.kg}^{-1}.\text{s}^{-1}$ .

### III. CONCLUSION

The recent trend and development in the Radiological Research in Bangladesh has been presented in this study. Firstly, a chronological survey of the investigation of anthropogenic  $^{137}\text{Cs}$  and naturally occurring radionuclides ( $^{226}\text{Ra}$ ,  $^{228}\text{Th}$ ,  $^{232}\text{Th}$ ,  $^{214}\text{Bi}$ ,  $^{208}\text{Tl}$ ,  $^{40}\text{K}$ ) in undistributed soil, water, ship scrapped materials such as metal, rubber and

foam and tree bark of ship breaking area, cynoglossids i.e. tongue soles and tea leaf collected from different parts of Bangladesh has been provided. Afterwards, the matter of sample collection, sample preparation and measurement procedure has been depicted as well. At the end, radioactivity analysis of the samples has been presented for detecting health hazards to ensure public health and safety.

### ACKNOWLEDGEMENTS

Authors wish to express deep gratitude to Mr. Mahbulul Hoq, Chairman (Current-Charge) & Member (Physical Science), Dr. Imtiaz Kamal, Member (Planning and Development), Dr. Md. Sanowar Hossain, Member (Bio-Science) and Engr. Md. Abdus Salam, Member (Engineering), Bangladesh Atomic Energy Commission, Dhaka for their support and cooperation in the research.

### REFERENCES

- [1] IAEA, Measurement of Radionuclides in Food and the Environment, Technical Reports Series 295, 1989.
- [2] M. Nurul Alam, Mantazul Islam Chowdhury, Masud Kamal, Badrun N. Hamid, M. Habibul Ahsan and M. Shamsuzzaman, Distribution of  $^{137}\text{Cs}$  and Naturally Occurring Radionuclides in the Terrene of Goainghat and Jaintapur Area of Sylhet District, Nucl. Sci. and Appl., 10(1 & 2), 21-25, 2001.
- [3] S. Roy, A Hoque and M. Begum, Distribution of  $^{137}\text{Cs}$  and Naturally Occurring Radionuclides in Soil at Site of the Rooppur Nuclear Power Plant, Nucl. Sci. and Appl., 10(1 & 2), 33-38, 2001.
- [4] Nurul Absar "Study of the Radioactivity in Soil and Tea Leaf and Transfer Factor of Radionuclides", M.Phil. Thesis, Chittagong University, Bangladesh, 2012.
- [5] Bijoy Sonker Barua, Md. Shuza Uddin, Md. Asad Shariff, A. K. M. Saiful Islam Bhuian, Masud Kamal and M. A. Rashid, Study on radiological contamination of ship scraps and environmental materials in ship breaking area of Chittagong, Bangladesh, Radiat. Prot. and Envi., 36(2), 52-56, 2013.
- [6] M. N. Alam, M. I. Chowdhury, M. N. Islam et al, Gamma Radioactivity in Soil of Chittagong Hills, Bangladesh, Nucl. Sci. and Appl., 4(1), 1995.
- [7] M. N. Alam, M. I. Chowdhury and M. Kamal, Study of the radionuclide concentrations of Cynoglossids in the Kutubdia Channel, Bangladesh and their seasonal occurrence and biochemical constituents, Nucl. Sci. and Appl., 11(1 & 2), 9-16, 2002.
- [8] S. Ghose, M. Kamal, M. I. Chowdhury, M. N. Alam and M. N. Islam, Gamma radiation dose from the naturally occurring radiocliodes in soil of the Potenga

- Sea Beach area of Bangladesh, Nucl. Sci. and Appl., 12(1 & 2), 31-36, 2003.
- [9] M. I. Chowdhury, M. Kamal and M.D.A. Mojumder et al, Naturally occurring radionuclides in water and sediment of the Meghna-Dakatia Rivers at Chandpur of Bangladesh, Nucl. Sci. and Appl., 16(2),6-10, 2007.
- [10] J. Ferdous, M. Rahman and A. Begum, Radioactivity in tap water of Dhaka city in Bangladesh and consequent dose estimates, Nucl. Sci. and Appl., 20(1 & 2), 25-31, 2011.
- [11] AQCS, Intercomparison Runs Reference Materials, Analytical Quality Control Services, IAEA, Vienna, Austria, 1995.
- [12] ICRP, Radionuclide Transformation, International Commission on Radiological Protection, Oxford: Pergamon Press, 1983.
- [13] Derivation of Activity Concentration Values for Exclusion, Exemption and Clearance, Safety Reports Series, No. 44, Printed by International Atomic Energy Agency (IAEA), Austria, April 2005, Available Online, 2014.
- [14] United Nations Scientific Committee on the Effects of Atomic Radiation (UNSCEAR), Exposures from natural Source of Radiation, Report to the General Assembly, UN, NY, USA, 1988.
- [15] I. Fatima, J.H. Zaidi, M. Arif, M. Daud, S.A. Ahmad and S.N. Tahir, Measurement of natural radioactivity and dose rate assessment of terrestrial Gamma Radiation in the soil of Southern Punjab-Pakistan, Radiat. Prot. Dosimetry, 128(2), 2008.
- [16] Agronne National Laboratory, EVS, Human Health Fact Sheet, 2005.
- [17] Choppin G., Liljenzin J., and Rydberg J., Radiochemistry and Nuclear Chemistry, 3<sup>rd</sup> ed., USA: Butterworth-Heinemann, 2002.
- [18] Beretka, J., & Mathew, P.Y., Natural Radioactivity of Australian Building Materials, Industrial Wastes and By-products, Health Physics, 48(1), 87-95, 1985.
- [19] NEA – OECD, Nuclear Energy Agency, Exposure to Radiation from Natural Radioactivity in Building Materials, Reported by NEA group of Experts, OECD, Paris, 1979.
- [20] Kh. Asaduzzaman, Mayeen Uddin Khandaker, Y.M. Amin, D.A. Bradley, R.H. Mahat and R.M. Nor, Soil-to-root vegetable transfer factors for  $^{226}\text{Ra}$ ,  $^{232}\text{Th}$ ,  $^{40}\text{K}$ , and  $^{88}\text{Y}$  in Malaysia, J. of Envi. Radiat., 135, 120-127, 2014.
- [21] Gilmore G.R., Practical Gamma-ray Spectrometry, 2<sup>nd</sup> ed., Chichester: John Wiley & Sons Ltd., 2008.
- [22] United Nations Scientific Committee on the Effects of Atomic Radiation (UNSCEAR), Sources, Effects and Risks of Ionizing Radiation, Report to the UN General Assembly, 1988.

# Design of charging station for electric vehicle batteries

Kusum<sup>1</sup>, Chetan Parveer<sup>2</sup>

<sup>1</sup>Department of EE, CBS Group of Institution, Jhajjar, Haryana, India

<sup>2</sup>Assistant Professor, Department of EE, CBS Group of Institution, Jhajjar, Haryana, India

**Abstract**— With the increasing requirement in green technologies in transportation, electric vehicles have proven to be the best short-term solution to reduce greenhouse gas emissions. The conventional vehicle drivers are still unwilling in using such a new technology, mainly because of the time duration (4-8 hours) required to charge the electric vehicle batteries with the currently existing Level I and II charging station. For this reason, Level III fast-charging stations capable of reducing the charging duration to 10-15 minutes are being designed and developed. The present thesis focuses on the design of a fast-charging station for electric vehicle, in addition to the electrical grid, two stationary energy storage devices flywheel energy storage and a super capacitor is being used. Power electronic converters used for the interface of the energy sources with the charging stations are designed. The design development also focuses on the energy management that will minimize the battery charging time. For this reason, an algorithm that minimizes durations with its mathematical formulation is required, and its application in fast charging will be illustrated.

**Keywords**— charging station, electric vehicle, batteries.

## I. INTRODUCTION

This chapter gives a background of the thesis topic: **Design for Fast Charging Station for Electric vehicle Batteries** then summarizes the work that has been conducted previously in fast charging technology. The problem is then explained, and the thesis outline is provided.

### Background

This section defines what a PHEV is and describes briefly the equipment involved to charge it.

### PHEV Definition

A Plug-in-Hybrid Electric Vehicle (PHEV) is a hybrid automobile with a higher-capacity battery that can be recharged by connecting the vehicle to the electrical network [1]. When the battery is below 20% capacity, a conventional combustion engine takes over and offers to the driver the same autonomy as a conventional vehicle. The PHEV has been

recognized as the best short-term, economically viable opportunity for significantly reducing oil dependency and CO<sub>2</sub> emissions without altering motorists' driving behaviour [1]. Consequently, nearly all major car makers have invested significant resources in PHEV development, and Toyota and GM delivered their first PHEVs (in small numbers) in 2010.

### Flywheels

Flywheel energy storage (FES) is an electromechanical device that stores energy in kinetic form in a rotating mass [49]. Flywheels are useful when there exists an imbalance between the generated power and the power demanded by the load [56]. In such devices, the charging and discharging processes are done by varying the rotational velocity of the mass: to store some electricity, a motor converts the external electrical energy into mechanical energy (charging), on the other hand to deliver some energy the motor acts as a generator and converts the energy into electrical form (discharging) [56]. Some control strategies have been found to apply flywheels in EVs. One of them has been found in [57], where the charging process is done using fuzzy logic and a PI controller whereas the discharging is done by simply applying the PWM strategy to the interfacing converter (AC/DC) [57].

FESs have been recognized as being the cleanest energy storage devices [59] and find their applications in the following areas:

- Previously, FESs have always been used for short-term energy storage in rotating machines and engines to deliver smooth power [58].
- Recently, they are being used for electrical energy storage [60]. In such case the FES is referred to as a mechanical battery energy storage device: it always stores kinetic energy and releases it in electrical form upon demand. This last advantage will be considered largely in this thesis.
- For the next few years, researches are being conducted in order to design higher specific power density (kW/Kg)

and higher specific energy (kWh/Kg) density. The first one depends completely on the motor/generator that drives it [60].

Any FES is composed of four major parts: a rotor, a rotor bearing, a container, and a power interface [59]. Figure below displays the main flywheel parts.

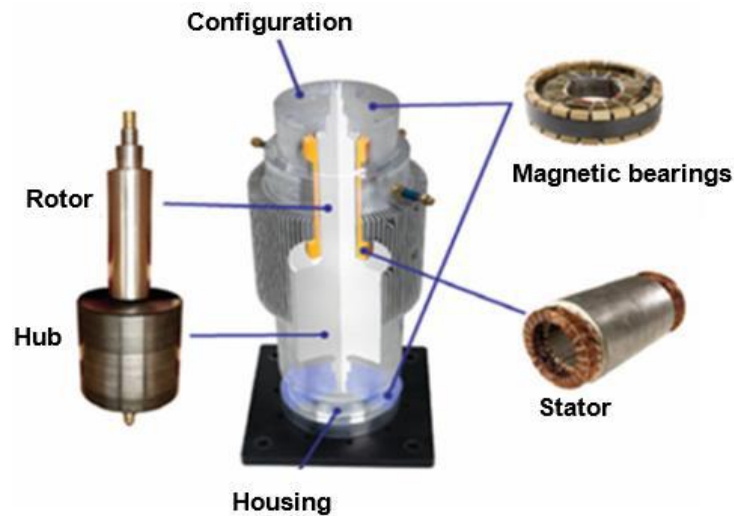


Fig.1: Main FES Components [59]



Fig.1.1: A Typical Supercapacitor [63]

The steady-state energy losses in flywheels are mainly due to the drag force that is induced by the magnetic field of the superconductor magnetic bearing and permanent magnet (PM)-type motor/generator (PMSM/G) [61]. However, the largest losses occur from the PMSM/G, and an acceptable solution would be to simultaneously rotate the PMSM/G and the PM [62].

### Supercapacitors

Also known as electric double layer capacitors (EDLC) or ultracapacitors, such devices behave exactly like any normal capacitor with the differences of having a much higher capacitance (in the order ranging from tens to hundreds of Farads) and a higher power density which lets them charge and discharge rapidly [63] and allows them to be used in applications to replace batteries. A typical supercapacitor is

shown in Figure below.

Such devices store energy using the following mathematical relation that relates the energy stored  $E$  (in J) to the capacitance  $C$  (in F) and the voltage across it  $U$  (in V) [50]:

$$E = C \cdot U^2 \quad (1.8)$$

They are classified into three categories [64]:

- Double-layer capacitors depend on the double electric layer mechanism.
- Electrochemical capacitors rely on the fast Faraday oxide-reduction reactions.
- Hybrid capacitors are a combination of the two previous categories.

A control strategy has been proposed for the supercapacitors

to support current peaks that are momentarily demanded by electrical road vehicles. Such a method is since the supercapacitors must be discharged once the current demanded by the load becomes greater than the reference limit current for battery discharge [65]. Supercapacitors are safe, possess an average light weight, can be recycled, and are environmentally friendly [66], which is what makes them mostly popular in the domain of energy storage for traction applications [67] and elevator systems with a soft commutated interface [64]. Additional applications include the following:

- Diesel-electric locomotives power assistance: supercapacitors are preferred compared to electromechanical accumulators when being used in power assistance [68].
- Recuperation of the braking energy that is wasted in the braking resistors [69].
- Sole energy storage device in hybrid electric cars if they are dimensioned appropriately.

Despite the benefits just mentioned, the energy that can be stored in a supercapacitor is low, which prevents large vehicle autonomy. For this reason, some methods have been found in order to allow fast energy transfer between super capacitors in transport applications, such as the introduction of sequential supply [70].

**II. PROBLEM STATEMENT**

Fast charging of PHEV batteries means that the duration

required to charge such batteries must be minimized, which implies the use of the grid and additional sources of energy that must be managed efficiently and intelligently.

A waiting period is also required to recharge the storage devices once the PHEV leaves the station. Such a period should also be minimized in order to reduce the time that the client needs to wait at the station before charging the battery, and to accelerate the battery swapping process at some charging stations if applicable.

Finally, it is important to look at some aspects of the impacts caused by such charging stations on the grid such as harmonics, THD, phase unbalance, power factor, ground fault and electricity generation.

As mentioned in Section 1.4, the charging station is designed to charge PHEV batteries whose energy capacities do not exceed 15 kWh, from a minimum of 20% of the battery state of charge (SOC) to a maximum of 95% of the battery SOC. This implies that the maximum energy output by the charger will be:

$$E_{O,max} = E_{PHEV,max} \cdot (SOC_{max} - SOC_{min}) = 15 \cdot (0.95 - 0.20)$$

$$E_{O,max} = 11.25 \text{ kWh} \tag{2.3}$$

Using (2.1), (2.2), and (2.3), the maximum energy provided by the charging station storage devices,  $E_{Storage,max}$ , can be found as follow:

$$E_{Storage,max} = E_{O,max} - E_{Grid} = 11.25 - 5$$

$$E_{Storage,max} = 6.25 \text{ kWh} \tag{2.4}$$

The energy management in the designed charging station is summarized in Table 2.3 below.

Table.2.3: PHEV Charging Station Energy Management

Sources	Grid	Storage Devices	Output
Energy (kWh)	5	6.25	11.25

The choice of the charger storage devices is developed in the next section.

**Station Storage Devices Choice**

The present section lists the most popular stationary energy storage devices performance requirements, and then justifies the charging station devices choice.

**Performance Requirements**

The chosen energy storage devices must ideally satisfy all of the following performance criteria in order to maximize the fast charging station efficiency:

- Dynamicity: The charging station is designed to charge

a battery in a maximum 15 minutes (short duration). The storage device must thus be able to charge and discharge in this period.

- High Power Density: The device must be able to deliver a high amount of power in a short period of time.
- High Efficiency: The charging station must meet its maximum possible efficiency. This last criterion depends on the main station parts: converters, storage devices, etc. Therefore, it is a must to consider the storage devices that have the highest efficiency.
- Environmentally Friendly: The device must have no or negligible negative impacts on the environment.

Table 2.4 below displays the most popular stationary storage devices according to the previously mentioned criteria [71, 72].

Table.2.4: Classification by Criterion

Storage Technology	Life time (cycles)	Power Density	Efficiency (%)	Impact on the Environment
Flow Batteries	1500 – 2500	Low	75 – 85	Medium
Metal-Air Batteries	100 – 200	Low	50	Medium
NAS Batteries	2000 – 3000	Low	89	High
Lead-Acid Batteries	200 – 300	Medium	75	High
Li-Ion Batteries	300 – 500	Medium	95	Medium
Supercapacitors	10000 – 100000	High	93 – 98	Low
Flywheels (FES)	$10^5 – 10^7$	High	90	Low

### III. STATIC POWER SWITCHES

This section covers the existing technologies of static power electronic switches and then justifies the use of IGBT as the best option for the design of the converters.

#### i. Existing Technologies

The most popular controllable static switches used in the design of the power electronic converters of Table 1.1 are displayed below in Table 3.1 [19].

Table.3.1: Main Controllable Switches Comparison

Device	Power Capability	Switching Speed
MOSFET	Low	Fast
IGCT	High	Slow
IGBT	Medium	Medium

Furthermore, the grid outputs a real power of 30 kW (see Section 2.2) and has a frequency of 60 Hz; both are in the medium range of operation. In the technologies of Table 3.1, the IGBT tends to be the best option for the design of the charging station is power electronic interfaces. An IGBT converter has an efficiency of typically 90% [58].

#### Converter Design

In order to turn on and off the controllable switches inverters and rectifiers, many types of gating signals can be used, among them are [19]:

- Square wave inverters: DC input must be varied to control the magnitude of the output AC voltage.
- Voltage cancellation: Switches operate at 0.5 duty cycle while the DC input remains fixed.
- Pulse-Width-Modulation (PWM): A modulating signal where the AC side frequency is compared with a carrier having a frequency such that the frequency modulation  $m_f$  (defined below) is a large odd integer:

The most popular gating generation used in inverters is a sinusoidal PWM, where the control signal is a sine wave; it generates harmonic voltages in the range of the switching frequency and higher, which can be easily filtered out [19].

The grid-side converter is shown in Figure 3.1.

Figure Grid-side Converter

#### Flywheel Energy Storage (FES) Converter

When acting as a generator, a FES converts kinetic energy into electrical energy [58]. This can be translated in the following way: when rotating at an angular speed  $\omega$  (rad/s), the energy is converted into AC currents that must be converted to DC currents via an AC/DC converter [81].

#### Supercapacitor Converter

Like any conventional capacitor, a supercapacitor charges and discharges in a DC environment [66]. The interface here is thus between DC quantities, and a bidirectional chopper is required to allow both charging and discharging of the supercapacitor.

#### Charging Station Supercapacitor

The supercapacitor is required to provide the battery with 10% of its required energy during the beginning of the battery charging process (see Chapter 5). Thus, the maximum output energy provided by the supercapacitor is found as follows:

$$E_{Scap,max} = 0.1 \cdot E_{O,max} = 0.1 \times 11.25 = 1.125 \text{ kWh}$$

$$E = \cdot C \cdot U^2$$

However, since the supercapacitor is interfaced with the charging station dc bus via an IGBT converter, the efficiency will play a role:

The relation relating the supercapacitor moment capacitance to its rated voltage (see Section 1.2.10, equation (1.8)) to provide the energy  $E_{Scap,in}$  is reminded below:

Table.3.6: Supercapacitor Options (for  $E_{Scap, in} = 1.25 \text{ kWh}$ )

Capacitance (F)	100	150	200	250	300
Rated Voltage (V)	300	245	212.13	190	173.20

An acceptable option would be a series / parallel combination of supercapacitors whose resulting capacitance and voltage are 150 F and 245 V, respectively.

**Electrical Specifications**

The output converter input current is equal to the sum of the output currents of the three previously mentioned converters:

$$I_{total,DC} = I_{Grid,DC} + I_{FES,DC} + I_{Scap, DC}$$

$$I_{total,DC} = 50 + 51.25 + 22.5 = 123.75 \text{ A} \quad (3.13)$$

The converter input power is calculated as follows:

Table 3.6 below displays the available options for choosing an appropriate capacitance with the required voltage to fulfil condition (3.9):

$$P_{total,in} = V_{DC} \cdot I_{total,DC} = 600 \times 123.75 = 74.25 \text{ kW} \quad (3.14)$$

The converter output power is calculated as follows: The converter output voltage is the maximum PHEV battery voltage, which is 270 V (Table 2.1).

Finally, the converter output current is calculated as follows:

With the information (3.13) -(3.16), the following Table 3.8 which displays the charging station output converter electrical specification can be drawn.

Table.3.8: Charging Station Output Converter Electrical Specifications

	Input Side (DC Value)	Output Side (DC Value)
Voltage (V)	600	270
Current (A)	123.75	248
Power (kW)	74.25	67

**Complete Power Circuit**

The present section describes the combined design of the charging station, and then lists its electrical specifications.

**Circuit Design**

The electrical grid, the supercapacitor, and the FES are all interfaced via their respective power electronic converters

previously designed to a common dc bus. The interface with the PHEV battery is also done via a bidirectional DC/DC converter (see Section 3.5).

**Electrical Specifications**

The energy and power requirements of each current source are summarized in Table 3.9 below:

Table.3.9: Charging Station Electrical Specifications

	Electrical Grid	FES	Supercapacitor
Maximum output energy (kWh)	5.56	5.70	1.25
Converter Efficiency (%)	0.9	0.9	0.9
Maximum output energy (kWh)	5	5.125	1.125
Maximum time of charging operation (min)	10	10	5
Maximum Output power (kW)	30	30.75	13.5

Figure below displays the combined charging station power circuit.

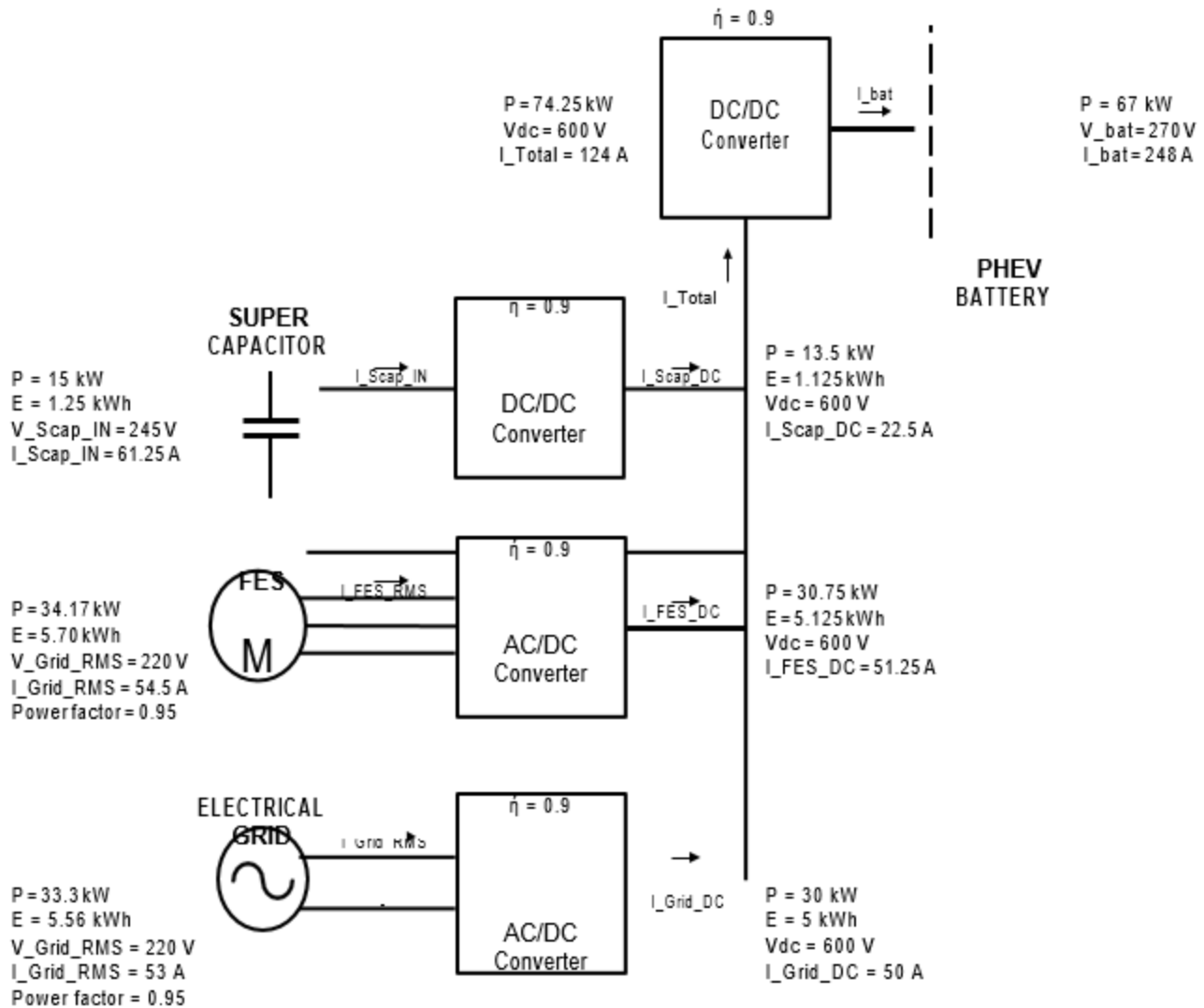


Fig.3: Charging Station Power Circuit

Charging Station Control Circuit

In the previous chapter, the power circuit has been designed along with its electrical specifications. The present chapter explains the control of each individual converter, then the whole charging station control circuit.

IV. CONVERTERS INDIVIDUAL CONTROL

This section elaborates on the individual control schemes of each of the four-charging station power electronic converters.

FES Control

The FES control by itself is difficult.

FES Emulation

It has been demonstrated that a FES could easily be emulated by a PMDC (Permanent Magnet DC Machine) [83]. Such operation would considerably decrease the system size and cost [83]. The FES system model will thus be replaced by a DC machine model as shown in Figure

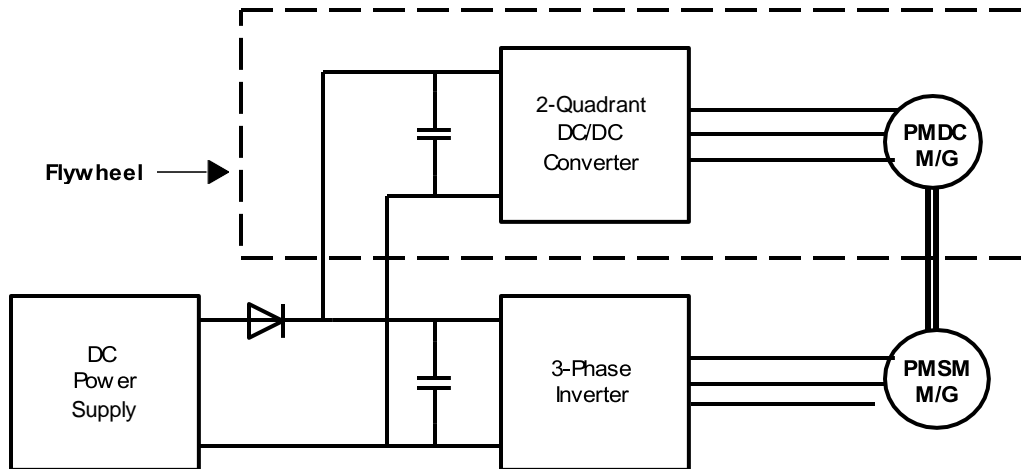


Fig.4: Flywheel Emulation Using a PMDC [Based on 83]

The power flow in the above system is bidirectional. Every power transfer is done through the permanent magnet synchronous machine (PMSM), which can act as motor and generator. The DC power supply not only imposes the dc bus voltage, but it also compensates for the system losses.

It is reminded that the kinetic energy  $dW$  (in J) stored in the above system with moment of inertia  $J_F$  (in  $\text{Kg.m}^2$ ) and rotating from one speed  $\omega_1$  to another speed  $\omega_2$  (in rad/s) is expressed as [83]:

$$dW = -J_F \cdot (\omega_2^2 - \omega_1^2)$$

The above system is designed to operate in three modes based on the stored energy using the above formula: charging, discharging, and no charging [83]. Each model is now explained below.

In the charging mode, the power flows from the dc bus to the PMDC through the PMSM. In such a case the DC machine is accelerated from the speed  $\omega_1$  to a higher speed  $\omega_2$ .

In the discharging mode, the power flows from the PMDC to the dc bus through the PMSM. In such a case, the DC machine is decelerated from the speed  $\omega_2$  to a lower speed  $\omega_1$ .

In the no charging mode, the DC machine runs at a constant at speed, and there is thus no power flow.

### System Control

The amount of energy transferred in or out of the flywheel can be controlled by controlling the PMSM torque by imposing either a positive or negative torque command in the PMSM controller, which is based on field orientated control

(FOC) in a rotor frame.

Under ideal FOC,  $i_r$  is set to 0 and the PMSM electromagnetic torque  $\tau$  can then be written as [84]:

where  $\lambda_{af}$  is the rotor flux linkages,  $i_r$  is the torque component of the stator current in the rotor reference frame, and  $p$  is the number of pole pairs.

The relationship between  $i_r$  and  $i$  (Flywheel transfer current to/from the inverter) is found from the steady-state power balance between the dc power going into the inverter and the ac power going into the PMSM [83]. If we neglect the inverter losses, we have:

$$P_{inv} = P_{SM}$$

$$FW \cdot V_{DC} = \tau E_{SM} \cdot \omega_m \quad (4.2)$$

Substituting the electromagnetic torque expression (4.1) into the power balance relation (4.2) and solving for  $i_r$  we get the following relation (which is also the flywheel control algorithm for both charging and discharging modes):

Figure below displays the FES control loop according to the above relation. At start-up, the control algorithm starts the PMSM using an initiation algorithm. The PI current controller is used to maintain the power flow.

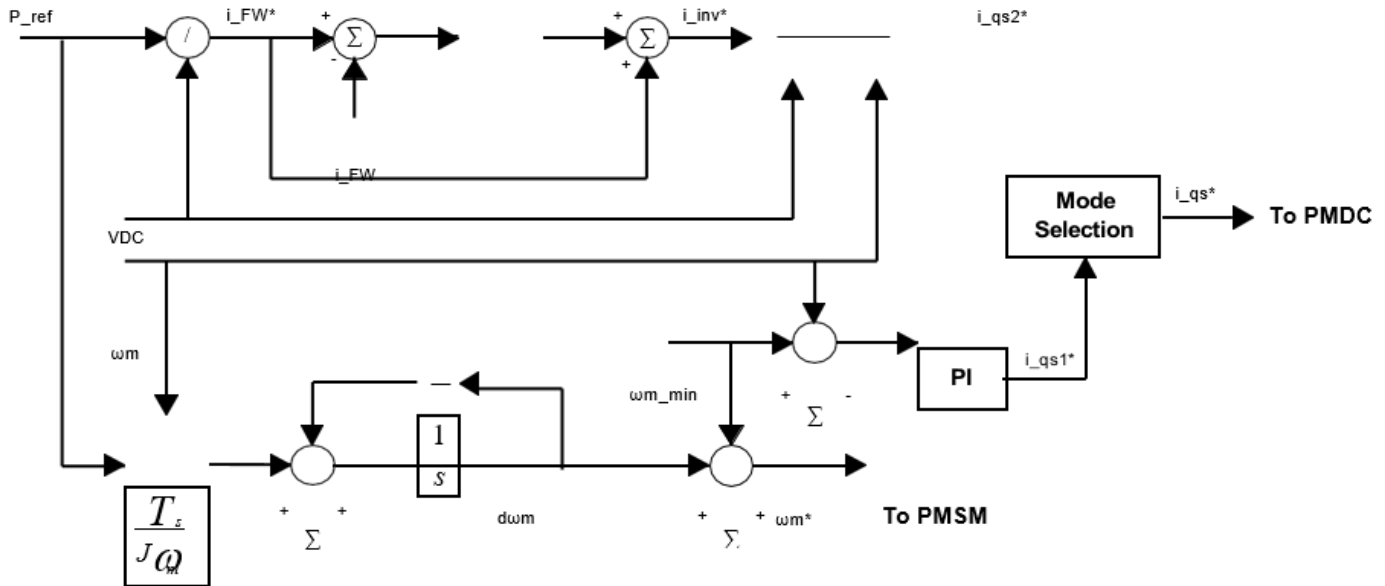


Fig.5: Flywheel Charging and Discharging Control [Based on 83]

**Supercapacitor Converter Control**

The supercapacitor control design is analogous to the flywheel control design shown in Figure 4.3 above and is designed to allow charging and discharging of the super capacitor. The DC/DC converter output current reference is produced by dividing the reference supercapacitor’s required power by the dc bus voltage. The error in current is then fed to a PI current regulator in order to maintain the power flow between the charger dc bus and the supercapacitor. Finally, the regulator output will be directed to the supercapacitor control scheme. The mode of operation (charging or discharging mode) depends on the sign of the supercapacitor’s reference power.

**4.1.4 Charging Station Output Converter Control**

The control scheme of the output converter is very similar to the grid converter control and is presented in Figure below. It is composed of two nested control loops: The outer control loop is designed for voltage regulation. The error between the battery nominal reference voltage and the measured battery charging voltage is fed to a PI controller, whose output is the battery charging current reference. The inner loop regulates the battery charging current. The reference here is the output of the previous outer loop. The error between the reference and the measured current is also fed to a PI controller whose output is sent to the charging station output converter control scheme.

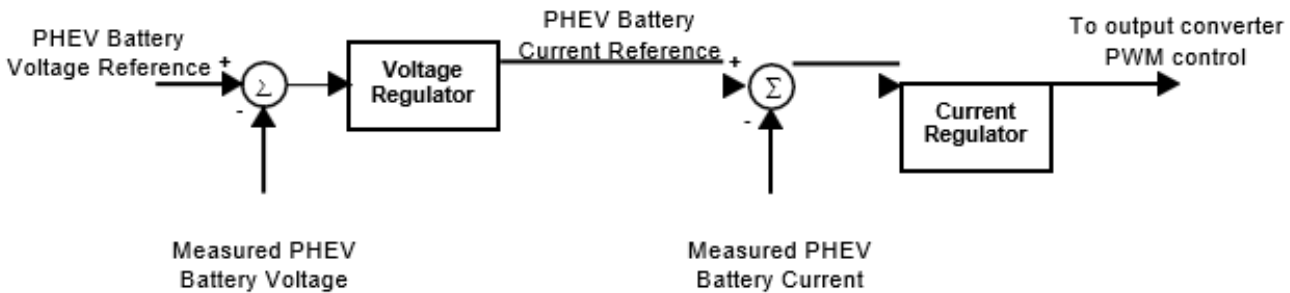


Fig.6: Charging Station Output Converter Control

**Control Circuit Design**

This section presents an algorithm that combines the previous individual controls in such that it minimizes the PHEV battery charging duration.

**Charging Station Central Control**

A charging station cycle is composed of a PHEV battery charging period (two phases) that does not exceed 15 minutes, followed by a period (one phase) during which the storage devices are fully recharged, which lasts a maximum of 7.5 minutes. This is demonstrated in Figure.

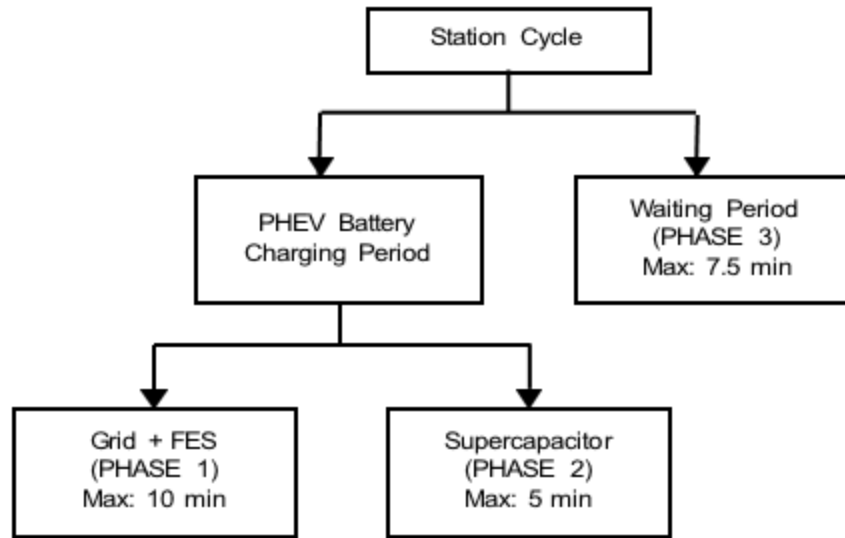


Fig.7: Schematic Diagram of the Charging Station Cycles

More details on the three phases will be provided in the next chapter.

**Central Control Algorithm**

In order to obtain the requirements of Figure, the algorithm of

Figure below is proposed. Table 4.1 displays the abbreviations used in the flowchart in Figure. Blue and red instructions indicate whether energy is being transferred from the charger to the battery, or from the grid to the storage devices (to recharge them), respectively.

Table.4.1: Figure 7 Abbreviations

Abbreviations	SC	FES	C_act	C
Expressions	supercapacitor	flywheel	Actual battery capacity	Total battery capacity

In standby mode, there is no PHEV battery connected to the charging station, and the energy storage devices have been fully recharged. At this moment, the FES rotates at constant speed  $\Omega_o$  (see Section 4.1.2) and thus there is no power transfer

( $dW = 0$ ). The supercapacitor voltage continues to increase asymptotically to its rated voltage, whereas its current tends asymptotically to 0. The charging station remains in this mode until the arrival of a PHEV at the station.

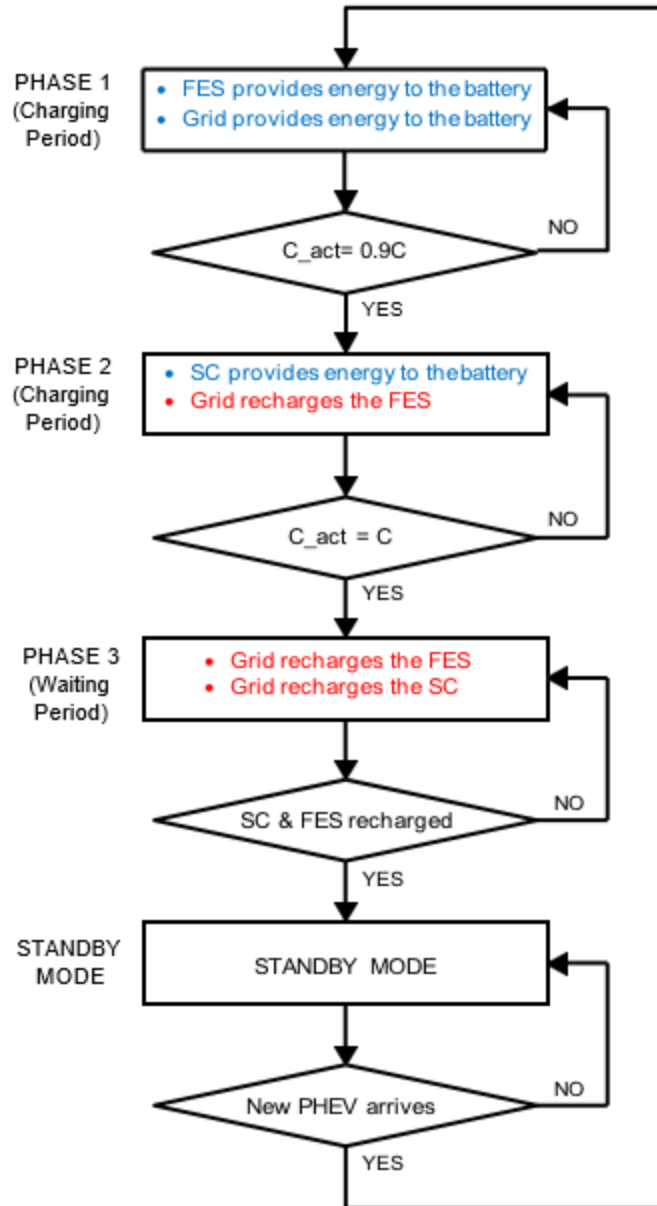


Fig.8: Central Control Algorithm Flowchart

**V. CHARGING STATION OPERATION**

The charging station operates as described in the flowchart shown in Figure. The energy management of the energy sources is done via optimization; the topic of this chapter. Two examples will be used to illustrate such operation.

**Charging Time Minimization**

The charging station is designed to minimize the PHEV battery charging time and required duration to recharge the storage devices. This requires an effective management strategy of the charging stations’ energy sources: grid, supercapacitor, and FES.

**Charging Station Cycle**

As mentioned previously, a charging station cycle is composed of three phases. The order of Phases 1 and 2 has been established by considering the fact that some PHEV users may have a limited amount of time to spend at the charging station; for this reason, most of the PHEV battery charging is done in the beginning of the cycle (Phase 1). The maximum duration of each phase has been determined by optimization (further details on the order of the charging durations of the FES and supercapacitor were provided in section 2.3.2).

- Phase 1: The FES and the electrical grid provide energy

to the PHEV battery until it reaches 90% of its required capacity. The maximum duration of this phase is 10 minutes.

- Phase 2: While the supercapacitor provides energy to the PHEV battery until it reaches its required capacity, the electrical grid is recharging the FES with a capacity determined by optimization (described in Section 5.1.3). The maximum duration of this phase is 5 minutes.
- Phase 3: During this phase, which lasts no more than 7.5 minutes, the electrical grid is recharging the supercapacitor and the FES to their respective full capacities. It is also called the “waiting period” because, during this time, no PHEV battery is allowed to be connected to the charging station.

Once the storage devices are fully recharged, the charging

station enters its standby mode until another PHEV arrives at the charging station to recharge its battery. Examples of the system operation are provided in Section 5.2.

**Problem Formulation**

A charging station cycle is graphically represented in Figure, where:

- Blue and red colours indicate whether energy is being transferred from the charger to the battery, or from the grid to the storage devices (to recharge them), respectively.
- Positive and negative quantities indicate whether energy is being delivered or absorbed by the device, respectively.
- P and C denote the grid power and the PHEV battery capacity, respectively.

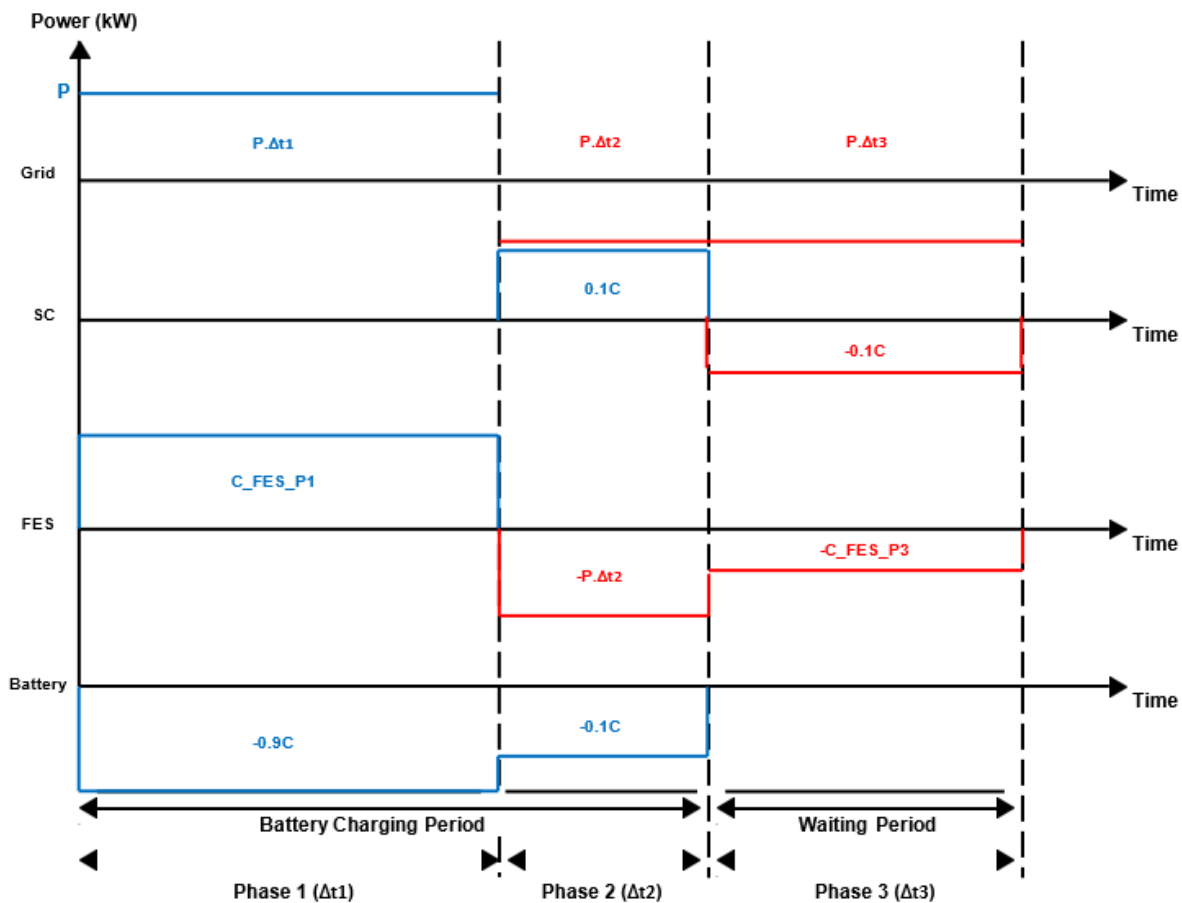


Fig.9: Detailed Charging Station Cycle

While the grid provides 5 kWh of the maximum charging station output energy of 11.25 kWh (see Table 2.3) during

Phase 1, the storage devices provide the remaining 6.25 kWh as follows:

1.125 kWh is provided from the supercapacitor during Phase 2, and 5.125 kWh is provided from the FES during Phase 1.

The choice of such proportions is in accordance with the station’s storage devices characteristics (see Section 2.3.2):

the supercapacitor is in operation for a relatively small period (maximum of 5 minutes) compared to the FES operation duration (maximum 10 minutes).

Once a PHEV arrives at the charging station, the parameters in Figure that need to be computed are listed in Table 5.1 below.

Table.5.1: Optimization Parameters

Parameter Name	Phase 1 Duration (min)	Phase 2 Duration (min)	Phase 3 Duration (min)	FES capacity in phase 1 (kWh)	FES capacity in phase 3 (kWh)
Symbolic Notation	$\Delta t_1$	$\Delta t_2$	$\Delta t_3$	CFES-P1	CFES-P3
Variable Maximum	10	5	7.5	5.125	5.125

- The maximum of each parameter is displayed in table 5.1.
- As already mentioned, in Phase 1, the FES and the grid (who delivers a power,  $p$ , in kW) are recharging the PHEV battery to 90% of its required capacity,  $C$ .

$$p \cdot \Delta t_1 + C_{FES-P1} = 0.9 \cdot C$$

(5.4)

- In Phase 3, the grid is recharging the supercapacitor and the FES:

$$p \cdot \Delta t_3 - C_{FES-P3} - 0.1C = 0$$

(5.5)

- The FES is providing energy to the PHEV battery during Phase 1, and is being recharged by the grid during Phases 2 and 3:

$$C_{FES-P1} - p \cdot \Delta t_2 - C_{FES-P3} = 0$$

(5.6)

**Charging Station Operation**

The charging station operates as shown in the flowchart of Figure Energy management parameters are given in tables 5.3, 5.5A, and 5.5B, where:

- Blue and red numbers indicate whether energy is being transferred from the charger to the battery, or from the grid to the storage devices (to recharge them), respectively.
- Positive and negative quantities indicate whether

energy is being delivered or absorbed by the device, respectively.

The following battery charging characteristics are displayed in Figures:

- Battery SOC (in %)
- Battery current (in A)
- Battery voltage (in V)

The following charger characteristics are displayed in Figures:

- FES speed (in rad/s)
- Grid current (in A)
- FES current (in A)
- Supercapacitor current (in A)
- Total current (in A): The sum of the grid, FES, and supercapacitor currents
- Supercapacitor voltage (in V)

**VI CONCLUSION**

**Summary**

In this thesis, the basic configuration used for the design and analysis of the fast charging station (including energy requirements and storage devices choice) has been described, the different power electronic interfaces have been designed, and the individual control schemes of each converter and the control and proposed algorithm of the whole charging station have been presented.

**Conclusions**

In this thesis, the design and simulation of a fast-charging station for PHEV batteries has been developed. Combination

of a flywheel and a super capacitor as additional stationary storage devices is an excellent option since it inherently has four advantages, high energy density, high power density, charging and discharging times in the order of minutes, and environmentally friendly. The developed algorithm efficiently manages the three-station energy sources and allows the charging of PHEV batteries whose capacities are below 15 kWh in a maximum duration of 15 minutes from 20% to 95% of their state-of-charge and maximizes the waiting time (to recharge the storage devices) to 7.5 minutes when no PHEV is present at the station. Afterwards the station enters the standby mode, where the supercapacitor voltage remains constant and its current tends asymptotically to zero, while the flywheel rotates at constant speed. The reduction of the duration of the charging station operation will accelerate the battery recharging process in a battery swapping scheme.

## VII. RECOMMENDATIONS FOR FUTURE WORK

While a general control algorithm has been developed in this research to minimize the battery charging time and the duration required to charge the storage devices, more research could be conducted on the following topics:

- Optimization of the combination of flywheel and super capacitor in terms of energy and power sizing.
- Impact of the battery charger on the power quality of the electric grid supply.
- Design of more efficient converter systems for the flywheel and super capacitor charging schemes.

## REFERENCES

- [1] Dickerman, L., & Harrison, J. (2010). A New Car, a New Grid. *IEEE Power And Energy Magazine*, 8(2), 55-61. doi: 10.1109/mpe.2009.935553
- [2] Electric Vehicle Chargers Level 3 - Products and Applications - BTCPower (Broadband TelCom Power, Inc.). (2018). Retrieved from <http://www.btcpower.com/products-and-applications/electric-vehicle-chargers-level-3/>
- [3] SAE International. (2001). *Electric vehicle conductive charge coupler*. Warrendale, Pa.
- [4] EV Solutions | Electric Vehicle Charging Products & Services. (2018). Retrieved from <https://www.evsolutions.com/>
- [5] GM to guarantee electric car batteries for eight years. (2010). *Physics Today*. doi: 10.1063/pt.5.024501
- [6] Mengtian, L. (2017). The Electric Car Charging Strategy Based on the User's Intention and Its Optimization. *Journal Of Automation And Control*, 5(1), 16-19. doi: 10.12691/automation-5-1-3
- [7] Oman, H. (1999). Making batteries last longer [for electric vehicles]. *IEEE Aerospace And Electronic Systems Magazine*, 14(9), 19-21. doi: 10.1109/62.793449
- [8] Singh, S., Dhar, A., & Agarwal, A. (2015). Technical feasibility study of butanol-gasoline blends for powering medium-duty transportation spark ignition engine. *Renewable Energy*, 76, 706-716. doi: 10.1016/j.renene.2014.11.095
- [9] Thiringer, T., & Haghbin, S. (2015). Power Quality Issues of a Battery Fast Charging Station for a Fully-Electric Public Transport System in Gothenburg City. *Batteries*, 1(1), 22-33. doi: 10.3390/batteries1010022
- [10] Vorel, P., Cervinka, D., Prochazka, P., Toman, M., & Martis, J. (2016). High Efficiency Fast-Chargers for Lead-Acid Batteries. *ECS Transactions*, 74(1), 23-30. doi: 10.1149/07401.0023ecst
- [11] Wirasingha, S., & Emadi, A. (2011). Pihef: Plug-In Hybrid Electric Factor. *IEEE Transactions On Vehicular Technology*, 60(3), 1279-1284. doi: 10.1109/tvt.2011.2115263
- [12] Zhou, J., & Notten, P. (2008). Studies on the degradation of Li-ion batteries by the use of microreference electrodes. *Journal Of Power Sources*, 177(2), 553-560. doi: 10.1016/j.jpowsour.2007.11.032
- [13] Niresh J, Dr.Neelakrishanan, Muthu C, Sabareesh G, Saravanan P, Tharan Vikram S(2017).Mitigating Instability in Electric Drive Vehicles Due to Time Varying Delays with Optimised Controller. *International Journal of Advanced Engineering Research and Science(ISSN : 2349-6495(P) | 2456-1908(O))*,4(5), 010-017. <http://dx.doi.org/10.22161/ijaers.4.5.3>
- [14] Amjadi, Z., & Williamson, S. (2010). Power-Electronics-Based Solutions for Plug-in Hybrid Electric Vehicle Energy Storage and Management Systems. *IEEE Transactions On Industrial Electronics*, 57(2), 608-616. doi: 10.1109/tie.2009.2032195
- [15] Mizumoto, I., Yoshii, Y., Yamamoto, K., & Oguma, H. (2018). Lead-acid storage battery recovery system using on-off constant current charge and short-large discharge pulses. *Electronics Letters*, 54(12), 777-779. doi: 10.1049/el.2018.1079
- [16] Nicholas, M., & Tal, G. (2013). Dynamics of Workplace Charging for Plug-in Electric Vehicles: How Much is Needed and at What Speed?. *World Electric Vehicle Journal*, 6(4), 819-828. doi: 10.3390/wevj6040819
- [17] Young-Joo Lee, Khaligh, A., & Emadi, A. (2009).

Advanced Integrated Bidirectional AC/DC and DC/DC Converter for Plug-In Hybrid Electric Vehicles. *IEEE Transactions On Vehicular Technology*, 58(8), 3970-3980. doi: 10.1109/tvt.2009.2028070

- [18] P. Divya Sri, P., & Prasad, D. (2011). Single Phase Dual Full Bridge Bi-directional DC-DC Converter for High power applications. *Indian Journal Of Applied Research*, 3(5), 259-265. doi: 10.15373/2249555x/may2013/79

# Identification of Cocoa Pods with Image Processing and Artificial Neural Networks

Sergio A. Veites-Campos<sup>1</sup>, Reymundo Ramírez-Betancour<sup>2</sup>, Manuel González-Pérez<sup>3</sup>

<sup>1</sup>Department of Mechatronic, M. Robotics, Universidad Autónoma de Guadalajara Campus Tabasco, Tabasco, México.

<sup>2</sup>Faculty of Engineering and Architecture, Universidad Juárez Autónoma de Tabasco, Tabasco, México.

<sup>3</sup>Universidad Popular Autónoma del Estado de Puebla, Puebla, México.

\*Corresponding author: [Sergioveites@outlook.com](mailto:Sergioveites@outlook.com)

**Abstract**— *Cocoa pods harvest is a process where peasant makes use of his experience to select the ripe fruit. During harvest, the color of the pods is a ripening indicator and is related to the quality of the cocoa bean. This paper proposes an algorithm capable of identifying ripe cocoa pods through the processing of images and artificial neural networks. The input image pass in a sequence of filters and morphological transformations to obtain the features of objects present in the image. From these features, the artificial neural network identifies ripe pods. The neural network is trained using the scaled conjugate gradient method. The proposed algorithm, developed in MATLAB ®, obtained a 91% of assertiveness in the identification of the pods. Features used to identify the pods were not affected by the capture distance of the image. The criterion for selecting pods can be modified to get similar samples with each other. For correct identification of the pods, it is necessary to take care of illumination and shadows in the images. In the same way, for accurate discrimination, the morphology of the pod was important.*

**Keywords**— *Cocoa pod, Processing of digital images, Artificial Neural Networks.*

## I. INTRODUCTION

Cocoa (*Theobroma cacao* L.) has been cultivated in America for thousands of years. Currently, all types of cultivated cocoa are varieties of numerous natural crosses or human intervention; however, is possible to classify the cocoa into three broad groups: Criollo or native, Forastero or peasant, Trinitario or hybrid [1,2].

The Cocoa Pod is an indehiscent berry. The pods' size oscillates from 10 to 42 cm in variable form (oblong, elliptical, oval, spherical and oblate), the surface of the fruit can be smooth or rough, the colors of the surface can be red or green in the immature state [3]. Some authors consider that the shape of the pod is a reference point for classifying cultivated cocoa trees. The classifying of cocoa by its shape divides among Amelonado, Calabacillo, Angoleta, and Cundeamor [1,4]. A

significant determinant of pod ripening is the outward appearance. The ripening is visible as the colors of the pod's external walls change. Usually, the outer walls turn green or purple changing to shades of red, orange or yellow depending on the genotype [5].

The ideal condition for pods harvest is when they are ripe. It is essential not to let the pods overripening as they can contaminate with some fungal diseases. The state of overripening promotes the germination of seeds and causes quality defects. Green fruits should not be part of the harvest. The seeds of green pods are hard, they cannot be separated easily and do not ferment because the mucilage is not finished forming [6].

For a proper fermentation, it is recommended to separate the pods according to their shape, color, and size to avoid the combination of seeds varieties. Ripeness degree of the pods determines the quality of cocoa beans. No mixtures of pods with different ripen estate should be generated, mainly when it is sold to process fine chocolates. The main chocolate industries look for a unique origin and reject the mixtures of varieties [7].

In food, color is one of the factors considered by the customer at the moment of the purchase of a product. The color is a quality criterion in many classification standards. The color is a parameter used to evaluate the ripening status of fruits [8]. Thus, different technologies have been implemented to harvest fruits in their best conditions.

Artificial vision systems incorporate color information. Within the range of visible wavelengths, some compounds in fruits absorb the light. These compounds are pigments, such as chlorophylls, carotenoids, and anthocyanins [9].

Tools commonly used in graphic design, such as digital cameras, computers and image processing software, can be used to process and analyze images. Image processing can identify the color of food samples during fruit

ripening. The use of vision systems allows replacing the use of color charts, colorimeters and spectrophotometers [8]. Colorimeters has deficiencies to describe perceptual chromatic responses with a multitude of visual parameters [10].

Digital image processing involves methodologies for analyzing and finding quantitative information. The tools and algorithms for the capture of images allow evaluating in a non-destructive way [8]. Since a few years ago, these methodologies were applied. Some examples are listed below: Systems for recognition and localization of quasi-spherical objects by laser telemetry [11], processing of optical images of cherry coffee fruits by acoustic-optical filters [12], Systems to identify the color of the epicarp of tomatoes [13], a mobile platform for the collection of oranges [14], and analysis of fruits such as wheat, Feijoa, Mango, plantain and mandarins [15,16, 17,18].

On the other hand, the use of artificial neural networks (ANNs) and artificial vision has more application in the food industry recently. The ANNs prioritize the classification, the recognition of patterns and the prediction of crops [19]. ANNs try to emulate the behavior of the human brain. The ANNs extract knowledge from a set of data obtained during training. ANNs can be considered as models of calculation that uses very efficient algorithms, which operate in a massively parallel way. These artificial nets allow developing cognitive tasks like learning patterns, classification or optimization [20]. Most applications in ANNs are related to pattern recognition problems and make use of architectures such as multilayer perceptron [21].

The techniques of image processing and ANNs are applied as a methodology for classification of Royal Gala apples. In these techniques, a multilayered neural network was implemented through supervised learning and trained with different algorithms [22].

In this paper, we proposed the processing of images with artificial neuronal networks in the harvest of Cocoa pods using images taken by a photographic camera. Subsequently, from the objects contained in the image, it obtains a matrix of data. Finally, we process the data from the matrix using the data from previous training. This methodology improves the harvest process substituting the handcrafted way. With this methodology, the human perception of the color of the cocoa pod is removed and controls the quality of the harvested fruit.

## II. PROCESSING ALGORITHM

The proposed processing algorithm is divided into four steps (Fig. 1). The algorithm processes an image in JPEG format with dimensions of 1920 x 1080 pixels using the RGB color space (Red, Green, Blue). The image should have good saturation and the least ambient noises. First

three steps remove the colors that are not typical of the ripe cocoa pods and gets the features of the found objects. An ANN evaluates these features. Therefore, the result of the algorithm is the identifier of the ripe cocoa pods on the input image.

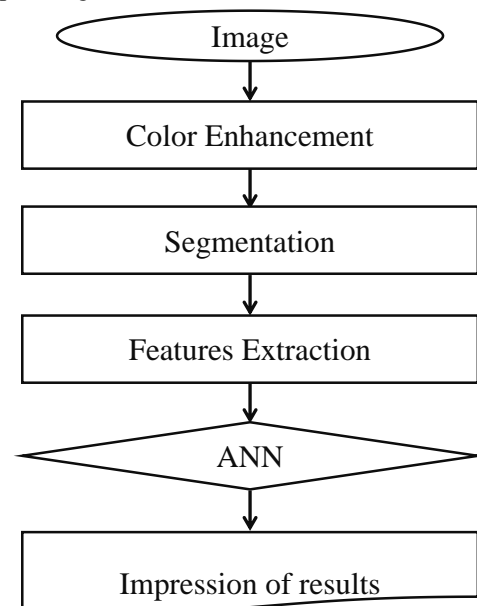


Fig. 1: Processing algorithm

### 2.1 Color Enhancement

The first step of the algorithm is to improve the colors of the input image. The lack of color intensity can be enhanced by adjusting the saturation values. For making it with less computational effort, it is proposed to convert the image in RGB color space to HSV (Hue, Saturation, Value). The three primary components that integrate the HSV color space are hue, saturation, and brightness [23]. The matrices of the HSV space has the same dimension as the RGB image. Assuming that values below 25% characterize obscure colors, the elements of the saturation matrix  $\mathbf{S}$  are modified by,

$$s_{i,j} = \begin{cases} 0.8, & s_{i,j} > 0.25 \\ s_{i,j}, & s_{i,j} \leq 0.25 \end{cases} \quad \dots (1)$$

$$s_{i,j} \in \mathbf{S},$$

$$\mathbf{S} \in \mathcal{M}_{m \times n}(\mathbb{C}),$$

$$\mathbb{C} = \{x \in \mathbb{R}, 0 \leq x \leq 1\},$$

$$\text{Rows } i, 1 \leq i \leq m,$$

$$\text{Columns } j, 1 \leq j \leq n.$$

Consequently, the new saturation matrix holds the dark colors that could represent a flaw in the cocoa pods. To end this stage, the image in the HSV color space converts into the RGB color space. The conversion is done to avoid alterations in the properties of the colors during the following steps of the algorithm [23]. Figure 2 shows the performance of this stage of the algorithm.

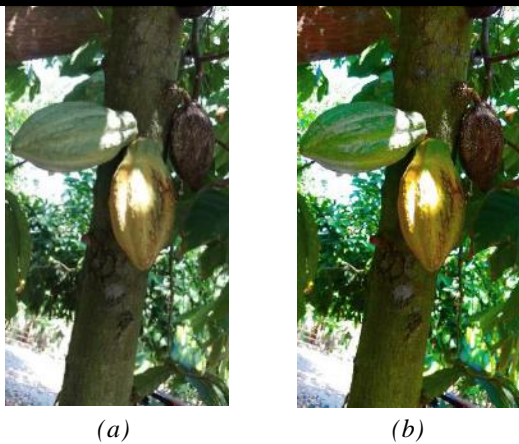


Fig. 2: (a) Original image, (b) Enhanced image

### 2.2 Segmentation

Before the extraction of features, in the segmentation stage of processing, the image is prepared first. Environmental noises and unwanted objects are filtered in the image to acquire reliable features (Fig. 3). At the end of this stage, is get a binary image with smoothed edges.

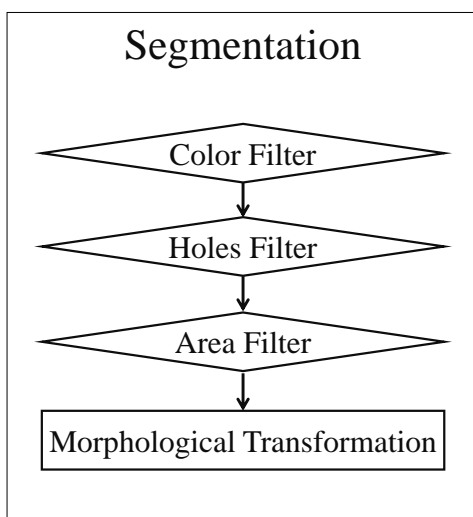


Fig. 3: Segmentation steps

#### 2.2.1 Color Filter

In this segmentation stage, the RGB image is processed to remove several colors ranges through five filters. The colors excluded are white, blue, magenta, green, brown, and some red hues. Relational operators and logical gates form the color filters. The result of the filters is a binary image.

The white filter creates a  $F1$  matrix that meets the conditions of Equation 2. The blue tonalities generate a second  $F2$  matrix that complies with Equation 3. Magenta colors and red hues provide a third  $F3$  matrix that satisfies Equation 4. While the green color, is represented by the  $F4$  matrix created by Equation 5. Finally, Equation 6 represents the filter of yellow colors, brown, and some orange shades. The conditions of the last filter create the

$F5$  matrix. This final filter is calibrated according to the desired ripening of the cocoa pods.

$$f1_{i,j} = (r_{i,j} \geq 235) \&(g_{i,j} \geq 235) \&(b_{i,j} \geq 235), \dots (2)$$

$$f2_{i,j} = (b_{i,j} \geq g_{i,j}) \&(b_{i,j} > r_{i,j}), \dots (3)$$

$$f3_{i,j} = (r_{i,j} \geq b_{i,j}) \&(g_{i,j} \leq b_{i,j}), \dots (4)$$

$$f4_{i,j} = (g_{i,j} > r_{i,j}) \&(g_{i,j} > b_{i,j}), \dots (5)$$

$$f5_{i,j} = ((|g_{i,j} - b_{i,j}|) \leq y) \&((r_{i,j} > g_{i,j}) \&(r_{i,j} > b_{i,j})), \dots (6)$$

$$r_{i,j} \in R, g_{i,j} \in G, b_{i,j} \in B,$$

$$f1_{i,j} \in F1, f2_{i,j} \in F2, f3_{i,j} \in F3,$$

$$f4_{i,j} \in F4, f5_{i,j} \in F5,$$

$$[R, G, B] \in \mathcal{M}_{m \times n}(\mathbb{D}),$$

$$\mathbb{D} = \{x \in \mathbb{N}, 0 \leq x \leq 255\},$$

$$[F1, F2, F3, F4, F5] \in \mathcal{M}_{m \times n}(\mathbb{K}),$$

$$\mathbb{K} = \{0,1\},$$

$$y \in \mathbb{N}, 0 \leq y \leq 255,$$

$$\text{Rows } i, 1 \leq i \leq m,$$

$$\text{Columns } j, 1 \leq j \leq n,$$

where  $R, G,$  and  $B$  represent the RGB matrix color space and,  $y$  represents the filter five setting to calibrate the color hue.

The resulting matrix of filters is added to obtain a matrix containing all the excluded tonalities,

$$FF = F1 + F2 + F3 + F4 + F5. \dots (7)$$

Therefore, the logical negation of  $FF$  provides the binary image with the required tonalities. Color filtering can be seen in Figure 4

$$E1 = \overline{FF} \dots (8)$$



Fig. 4: Filtered and binarized image

#### 2.2.2 Holes Filter

The second segmentation stage removes the holes of the objects found in the binary image. It is proposed to eliminate these holes to improve the results in the morphology stage. Not all holes are covered. Those small holes resulting from reflections on the objects are filled in. Large holes generated by dark spots are not eliminated. Naturally the pods have small dark marks; however, large spots on a cocoa pod are a quality defect.

Identifying the holes consists of finding all the values of 0 in the **E1** matrix that are isolated from the values that make up the background of the binary image. The largest neighborhood group of elements in the **E1** matrix with a value of 0 form the background of the image. Isolated elements are called holes. For identify holes, the "imfill" function of MATLAB ® is applied. The function produces a binary matrix **H**, which contains the holes founded in the input image and represents them with a value of 1 [24].

From **H**, an **H1** matrix containing holes formed by light reflections is obtained,

$$H1 = H \& F1, \quad \dots (9)$$

$$[H, H1] \in \mathcal{M}_{m \times n}(\mathbb{K}).$$

Also, using the methodology described in the following section (Area Filter) the **H2** matrix is generated. This matrix represents the smaller holes. The matrices obtained are added, and a matrix is gotten with the holes to be filled,

$$HF = H1 + H2. \quad \dots (10)$$

Finally, the holes in the original image are filled through **E2 = E1 + HF**,

$$\dots (11)$$

where **E2** represents an image without holes. In Figure 5, the application of the Hole Filter stage can be seen in Figure 4.



Fig. 5: Filtered image without holes

### 2.2.3 Area Filter

There are small objects in the binary image gotten in the previous step. Small groups of pixels and isolated pixels with a value of 1, shape these objects. Removing these pixels from the background of the image makes hold large objects. The third stage of the segmentation, filter the objects by their areas. The methodology removes all neighborhood groups of elements with a value of 1 in the **E2** matrix. For this, the areas of the neighborhood groups are analyzed in the matrix. Using the "Blob Analysis" function of SIMULINK ® is possible to get areas [24]. From this function is obtained the data of the areas and a matrix of Bounding boxes. With the areas of the neighborhood groups found is created a vector column **A**.

The matrix of **BB** contains the coordinates and size of Bounding Boxes. These enclose the neighborhood groups found in the input matrix entered into the function.

In base on vector **A**, is created a reference vector **Q**,

$$q_{k,1} = (a_{k,1} < x), \quad \dots (12)$$

$$q_{k,1} \subset Q, \quad a_{k,1} \subset A,$$

$$A \in \mathcal{M}_{m \times 1}(\mathbb{R}^+),$$

$$Q \in \mathcal{M}_{m \times 1}(\mathbb{K}),$$

$$\text{Rows } k, 1 \leq k \leq z,$$

where  $x$  is the minimum allowed area and  $z$  is the number of neighborhood groups found in the **E2** matrix.

With the values of **Q**, a reference matrix **WW** is generated, which is created from the horizontal concatenation of **Q** with itself four times. The above is done to equal the dimensions of **Q** and **BB**. Based on **WW** the elements of **BB** are conditioned,

$$bb_{k,4} = \begin{cases} bb_{k,4}, & ww_{k,4} = 1 \\ 0, & ww_{k,4} = 0 \end{cases} \quad \dots (13)$$

$$bb_{k,4} \subset BB, \quad ww_{k,4} \subset WW,$$

$$BB \in \mathcal{M}_{m \times 4}(\mathbb{R}),$$

$$W \in \mathcal{M}_{m \times 4}(\mathbb{K}),$$

$$\text{Rows } k, 1 \leq k \leq z.$$

Finally, over the elements of **E2** is drawn with 0 Bounding Boxes of **BB**. The matrix obtained from this procedure is called **E3** and characterizes the binary image filtered by area. This way, smaller objects are removed, and a cleaner image is obtained. Figure 6 shows the performance of this stage.

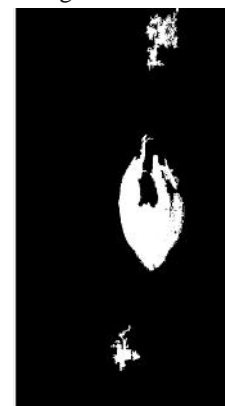


Fig. 6: Image filtered by area

### 2.2.4 Morphological Transformation

The last segmentation stage softens the edges of the objects in the output image. In some cases, the edges of the objects in the image show openings, and in others cases, they have outstanding reliefs. Modifying the edges in objects is known as morphological transformations. The basic morphological operations used here are known as dilation and erosion [25]. Morphological operations apply a structured disk element to objects. The disk structure is the best structuring element that smooth the edges in ovoid shapes. This structured element is subtracted or added to the edges and makes a smoother

perimeter. The modifications do not generate change in the dimension of the binary image.

The first part of the transformation is to apply a dilatation followed by erosion to **E3**. This technique is known as a closing function, and its output is a new binary matrix. This function eliminates small apertures at the edges of objects. Then, an erosion is applied followed by a dilatation. This last technique is known as opening and creates the resulting matrix **E4**. With the opening function, is possible to remove small groups of pixels in the reliefs of the objects [25]. For the transformations mentioned above, the radius of the structuring element in the closing function must be less than the opening function. In Figure 7 the changes are appreciated comparing with Figure 6.



Fig. 7: Image with morphological transformation

### 2.3 Features Extraction

This stage gets the features of the object in the image. These features are used to discriminate objects, which do not have the shapes of cocoa pods. Using "Blob Analysis" from SIMULINK® are gotten these features and the matrix of Bounding Boxes [24]. The features obtained for this processing were: major axis, minor axis, eccentricity, and extent. The extent feature represents a relationship between the area of the found object and the area of its Bounding Box [26]. Features extracted are in the form of column vectors. Features of the major axis and minor axis are joined to represent the following relation:

$$U = \begin{bmatrix} O_{1,1} \\ v_{1,1} \\ O_{2,1} \\ v_{2,1} \\ \vdots \\ O_{k,1} \\ v_{k,1} \end{bmatrix} \dots (14)$$

$$O_{k,1} \in \mathbf{O}, v_{k,1} \in \mathbf{V},$$

$$\mathbf{V} \in \mathcal{M}_{m \times 1}(\mathbb{R}^+),$$

$$\mathbf{O} \in \mathcal{M}_{m \times 1}(\mathbb{R}^+),$$

$$\mathbf{U} \in \mathcal{M}_{m \times 1}(\mathbb{C}),$$

Rows  $k, 1 \leq k \leq z_1,$

where **U** represent the result of dividing the axis vectors, **O** the minor axis, **V** major axis, and  $z_1$  the number of objects in the **E4** image.

There are two significant advantages of the features obtained at this stage. The first is the performance of the three features (relation of axes, eccentricity, and extent) over ovoid objects. Finally, the value of the features tends to be retained with the distance; as shown in Figure 8.

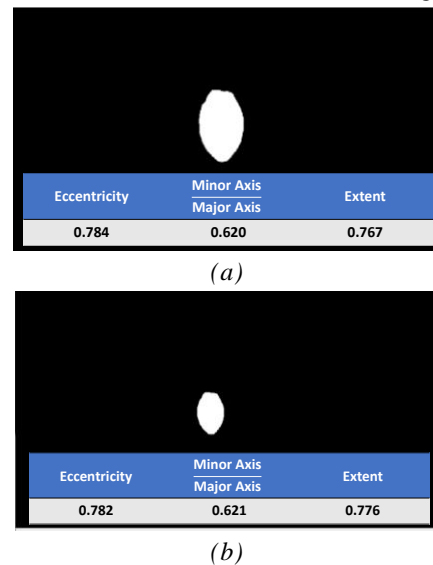


Fig. 8: (a) Pod about a meter away, (b) Pod two meters away.

Finally, in this stage is generated the matrix of **BF** Bounding Boxes that enclose the found objects and the matrix **C** that contains the features of the objects. Matrix **C** come from the horizontal concatenation of the three vectors containing the features separately.

### 2.4 Artificial Neuronal Network (ANN)

In this last stage, the ANN received the features gotten in the previous step. Each feature creates inputs to the Artificial Neuronal Network and, the output relates the inputs by functions [27]. Therefore, the network will be made up of three inputs and a single output. The output is a Real number between 0 and 1. The approximation of the output to 1 indicates that the values of the features come from a cocoa pod.

Within the three fundamental operations of the artificial neuron, the transfer function *f* is related to the type of output (Fig. 9). From the existing transfer functions, the sigmoidal function is selected for this application. This function takes inputs between negative infinity and positive infinity. The output of the sigmoidal function generate values between 0 and 1 [27].

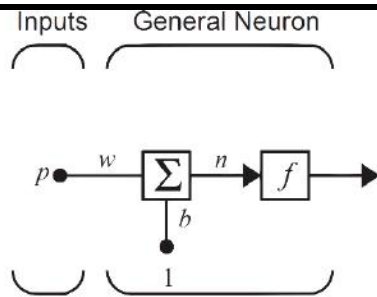


Fig. 9: Single input neuron [27]

The output of a simple artificial neuron with sigmoidal transfer function is described by,

$$t = \text{logsig}(wp + b), \quad \dots (15)$$

$$[w, p, b] \in \mathbb{R},$$

$$t \in \mathbb{C},$$

where  $t$  is the network output,  $p$  is the input variable to the neuron,  $w$  is the net weight and  $b$  is the bias.

A single-layer ANN is deficient for this processing algorithm. Therefore, a multi-layered ANN has been designed. The type of ANN proposed here will be a Feedforward Neuronal Network (FNN). This type of networks behaves with good results in pattern recognition and object classification applications. The number of layers used in this work is two, as recommended by [27]. Finally, the designed network has nine neurons in its first layer and a single neuron in the output layer (Fig. 10).

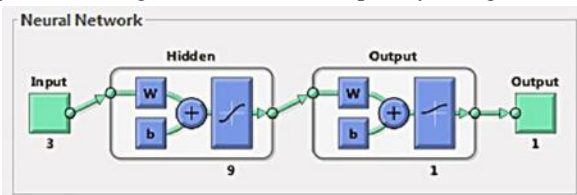


Fig. 10: Feedforward Neuronal Network

Feedforward Neuronal Network can use the scaled conjugate gradient method for training. For large networks, this training algorithm is the most efficient. The pattern recognition problems frequently apply this method [27].

The methodology of the FNN designed is to read the data of  $\mathcal{C}$ . Each row contains the features of an individual object. The single output of the network will be based mainly on the features extracted and weights of the FNN. The result of the network will be a scalar between 0 and 1. This value is conditioned by,

$$t_1 = t \geq l, \quad \dots (16)$$

$$t \in \mathbb{C},$$

$$l \in \mathbb{C},$$

$$t_1 \in \mathbb{K},$$

where  $t$  is the output of the FNN,  $t_1$  is the conditioned output and  $l$  is the criterion that conditions the output. This criterion is in function of the percentage of the output coincidence with the samples in the training.

With the values of  $t_1$  is created the reference column vector  $\mathcal{Q}1$ . This vector comes from the vertical concatenation of the outputs of the FNN.

Based on  $\mathcal{Q}1$ , the  $\mathcal{WF}$  matrix is generated, whose values are gotten from the horizontal concatenation of  $\mathcal{Q}1$  with itself four times. The above is done to equal the dimensions of  $\mathcal{Q}1$  and  $\mathcal{BF}$ . Then, the elements of  $\mathcal{BF}$  are conditioned in the following way,

$$bf_{k,A} = \begin{cases} bf_{k,A}, & wf_{k,A} = 1 \\ 0, & wf_{k,A} = 0 \end{cases} \quad \dots (17)$$

$$bf_{k,A} \subset \mathcal{BF}, \quad wf_{k,A} \subset \mathcal{WF},$$

$$\mathcal{BF} \in \mathcal{M}_{m \times 4}(\mathbb{R}),$$

$$\mathcal{W} \in \mathcal{M}_{m \times 4}(\mathbb{K}),$$

$$\text{Rows } k, 1 \leq k \leq z_1.$$

Finally, the image processing algorithm takes the  $\mathcal{BF}$  data to draw the Bounding Boxes that point out to the cocoa pods on the RGB input image that this algorithm received. Using the SIMULINK® "Draw Shapes" block, draw the Bounding Boxes over the RGB image.

### III. RESULTS AND DISCUSSION

The methodology proposed in this research was developed in MATLAB® R2018A using the Visual Programming Environment SIMULINK®. The simulation was done on a computer with Microsoft® Windows® 7 Home Premium, Intel® Core™ i7-2630QM 2.00 GHz processor and 8 Gb DDR3 1333Mhz RAM.

The images used for the development of the investigation were obtained from cacao farms of the village Cucuyulapa. This locality is part of the municipality of Cunduacán, Tabasco, Mexico. In the locality, images were taken with the natural daylight of midday. All the images taken had the same illumination and focal aperture. The images capture was taken at distances between 1 and 2 meters.

The types of pods used in this experiment were hybrids of criollo cocoa with an amelonada shape. The observed color changes in these pods were from green to yellow. Some variations in the length of the pod were observed in the same cocoa genotype.

An FNN of nine neurons in their hidden layer and a single neuron in the output layer process the images. The training following an algorithm that trains, validates and tests the results. The training algorithm uses, 175 images of cocoa pods, of which 70% were used for training, 15% for validation and another 15% for testing. Training algorithm got a gradient of 0.294 final at 39 iterations. The results obtained are shown in Table 1. Consequently, minimizing cross-entropy in training results in accurate pod identification, while decreased percent error reduces mistakes relate with pods and erroneously identified objects.

Table 1: Training results

	Cross-Entropy	Percent Error
Training	5.77386e-1	6.50406e-0
Validation	9.35257e-1	0
Testing	9.95469e-1	0

The identification of the objects leads us to create a confusion matrix. This matrix has the erroneous or successful percentages of the FNN to obtain its targets. Figure 11 represents the total confusion matrix of the training algorithm processes. The percentage of total assertiveness towards to the wanted Targets is 95.4%.

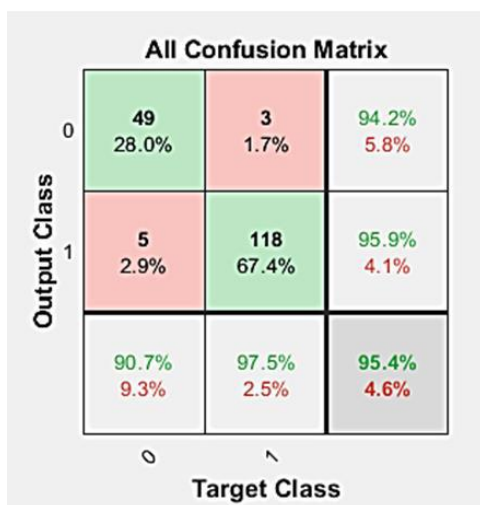


Fig. 11: All confusion matrix from FNN

The processing algorithm was tested using 23 images of cocoa pods different from those used in the training algorithm. The tests are in charge of evaluating the performance of the algorithm for each image at different values of the *l* match criterion (Equation 16). Value of *l* evaluates the image more stringent. A high value in *l* allows making a homogeneous selection of pods in good shape and with proper ripening. According to the ripening of the pods, Table 2 shows the most appropriate values of *l* for the algorithm.

Table 2: Test results

<i>l</i>	Percent Assertiveness
0.7	89%
0.8	91%
0.9	91%
0.95	83%

The values of *l* between 0.8 and 0.9 gets the best performance of the algorithm. Criterion of 0.95 presents a lower percentage of assertiveness because it penalizes the shape of the pod. The criterion of 0.95 is suitable if it is looking for pods that have the proper ripening and the average shape that characterizes the selected cocoa genotype. Finally, the criterion of 0.7 shows good results

to select ripe cocoa pods, but with the disadvantage of confusing some pods with some green hue. Then, in Figure 12, the result of the algorithm can be seen using 0.9 as the criterion for evaluating the sample.

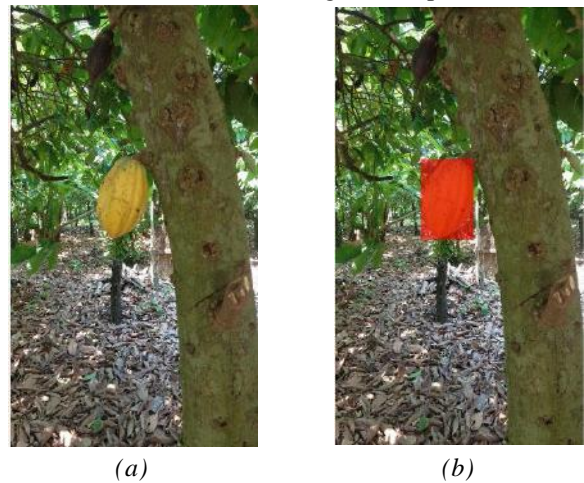


Fig. 12: (a) Image inputted, (b) Image result

The errors generated in the tests came from the values of the features in the pods. These values are affected by the length of long pods and pods with green color or spots at its ends. At the time of evaluating the features of these types of pods with considerable deviations in their form, the algorithm can recognize the samples as morphologically correct pods.

#### IV. CONCLUSION

In this work, a methodology was proposed to identify ripe criollo cocoa pods type amelonado. It could be observed that these fruits tend to change from green to yellow. The overripening make color changes on the pod to yellow to orange hues. Therefore, it was proposed to use a filter in which the desired tonality of the fruit could be adjusted. Also, the measurements of the features of the pods were essential to identifying if the pod presents damage for some disease.

The images taken for this algorithm were carried out taking care of lighting and light reflections. These factors cause noises that impair the calibration of the camera's colors and the adjustment of the desired hue of a pod. The modification of the saturation of the image helped to improve noises that derive from these factors; however, excessive shadows and reflections cause problems in digital image processing.

The use of the area filter helps the shapes in the images do not have so many morphological changes and to be able to eliminate objects that cause noises in the binary image. The previous methodology proposes to maintain as much as possible the original size of the forms and despite this eliminate noises by a group of pixels.

Features used to evaluate the objects in the images, gave optimal results to discriminate between pods and different

shapes. It could be seen that the features retained their value, regardless of the distance of the photograph. The performance of features represents an advantage, allowing selecting similar shapes without the need for a reference distance.

The technique of modifying the criterion of selection of samples in the processing algorithm behaved in the manner expected. In this way, it is possible to adjust the criterion making it more critical and having homogeneous samples. Getting good results within 80% and 90% of coincidence criterion with training samples. If the study objects have many variations in their shape, setting the selection criterion may not be the most appropriate.

It is expected in future work to study the variations of pods of different genotypes. This study could select ripe cocoa pods from all types of shapes. The selection of these pods could be made without being confused with other objects. In the same way, the features should be improved or complemented, to avoid confusion between ripe pods and pods with possible morphological diseases.

#### REFERENCES

- [1] Reyes Vayssade, M. (1992). *Cacao: Historia, Economía y Cultura*. Mexico City: Nestlé
- [2] CacaoMexico.org (2010). *Cacao México*. Retrieved from <https://www.cacaomexico.org/>
- [3] Avendaño, C. H., Villarreal, J. M., Campos, E., Gallardo, R.A, Mendoza, A., Aguirre, J. F., ... Zaragoza, S. E. (2011). *Diagnóstico del cacao en México*. Mexico City: Universidad Autónoma Chapingo.
- [4] Lépidio Batista. (2009). *Morfología de la planta de cacao*. Retrieved from <http://www.fundes yram.info/biblioteca.php?id=3096>
- [5] Afoakwa, E. O. (2016). *Chocolate science and technology*. Oxford: John Wiley & Sons.
- [6] Cubillos, G., Merizalde, G., & Correa, E. (2008). *Manual de beneficio del cacao*. Antioquia: Secretaria de Agricultura de Antioquia.
- [7] Lutheran Word Relief (2013). *Cosecha, Fermentación y Secado del cacao (Guía 8)*. Retrieved from <http://cacaomovil.com/>
- [8] Padrón, C. A., León, M. G., Montes, A. I., & Oropeza, R. A. (2016). *Procesamiento Digital de Imágenes: Determinación del color en muestras de alimentos y durante la maduración de frutos*. Retrieved from [https://www.amazon.com/dp/B01MU1K0OF/ref=rd\\_r\\_kindle\\_ext\\_tmb](https://www.amazon.com/dp/B01MU1K0OF/ref=rd_r_kindle_ext_tmb)
- [9] Viñas, M. I., Usall, J., Echeverria, G., Graell, J., Lara, I., & Recasens, D. I. (2013). *Poscosecha de pera, manzana y melocotón*. Madrid: Mundi-Prensa Libros.
- [10] Martínez Verdú, F. M. (2001). *Diseño de un colorímetro triestímulo a partir de una cámara CCD-RGB*. (Doctoral Thesis). Universidad Politécnica de Catalunya, Department of Optica and Optometry, Barcelona. Retrieved from <http://hdl.handle.net/2117/94055>
- [11] Ruiz, A. R. J. (1998). *Sistema de reconocimiento y localización de objetos cuasi-esféricos por telemetría láser. Aplicación a la detección automática de frutos para robot Agribot*. (Doctoral Thesis). Universidad Complutense de Madrid, Department of computer architecture and Automation, Madrid.
- [12] Mosquera, J. C., Sepúlveda, A., & Isaza, C. A. (2007). Procesamiento de imágenes ópticas de frutos de café en cereza por medio de filtros acusto-ópticos. *Ingeniería y Desarrollo*, (21), 93-102.
- [13] Padrón Pereira, C. A., León, P., Marié, G., Montes Hernández, A. I., & Oropeza González, R. A. (2012). Determinación del color en epicarpio de tomates (*Lycopersicon esculentum* Mill.) con sistema de visión computarizada durante la maduración. *Agronomía Costarricense*, 36(1), 97-111.
- [14] Tovar Yate, C. G. (2014). *Desarrollo e implementación de una plataforma móvil para recolección de naranjas*. (Bachelor's Thesis). Universidad Católica de Colombia, Faculty of Engineering, Colombia.
- [15] Acosta, C. P. S., Mir, H. E. V., García, G. A. L., Ruvalcaba, L. P., Hernández, V. A. G., & Olivas, A. R. (2017). Tamaño y número de granos de trigo analizados mediante procesamiento de imagen digital. *Revista Mexicana de Ciencias Agrícolas*, 8(3), 517-529.
- [16] Bonilla-González, J. P., & Prieto-Ortiz, F. A. (2016). Determinación del estado de maduración de frutos de feijoa mediante un sistema de visión por computador utilizando información de color. *Revista de Investigación, Desarrollo e Innovación*, 7(1), 111-126. doi: 10.19053/20278306.v7.n1.2016.5603
- [17] Alberto, C., Pereira, P., León, P., & Valencia, M. (2012). Determinación del color en epicarpios de mango (*Mangifera* sp.) y plátano (*Musa* AAB) en maduración mediante sistema de visión computarizada. *Revista Venezolana de Ciencia y Tecnología de Alimentos*, 3(2), 302-318.
- [18] Padrón-Pereira, C. A. (2013). Utilización de imágenes digitales para medición del diámetro de frutos de mandarina (*Citrus reticulata*) en crecimiento / Using digital images for measurement of mandarin (*Citrus reticulata*) Fruits Diameter During Growth. *Ciencia y Tecnología*, 6(1), 1-9.
- [19] Ávila, G. A. F., & Ricaurte, J. A. B. (2016). Identificación del estado de madurez de las frutas con redes neuronales artificiales, una revisión. *Revista Ciencia y Agricultura*, 13(1), 117-132.

- [20] López, R. F., & Fernández, J. M. F. (2008). *Las redes neuronales artificiales*. La Coruña: Netbiblo.
- [21] Bishop, C., & Bishop, C. M. (1995). *Neural networks for pattern recognition*. New York: Oxford University Press.
- [22] Avila, G. A. F. (2016). Clasificación de la manzana royal gala usando visión artificial y redes neuronales artificiales. *Research in Computing Science*, 114, 23-32.
- [23] Gil, P., Torres, F., & Ortiz Zamora, F. G. (2004). *Detección de objetos por segmentación multinivel combinada de espacios de color*. Universidad de Alicante, Department of Physics, Systems Engineering and Signal Theory, Alicante. Retrieved from <http://hdl.handle.net/10045/2179>
- [24] Matlab, Mathworks (2018). *Image processing Toolbox™ User's Guide*. Retrieved from [https://la.mathworks.com/help/pdf\\_doc/images/index.html](https://la.mathworks.com/help/pdf_doc/images/index.html)
- [25] Ortiz Zamora, F. G. (2002). *Procesamiento morfológico de imágenes en color: aplicación a la reconstrucción geodésica*. (Doctoral Thesis). Universidad de Alicante, Department of Physics, Systems Engineering and Signal Theory, Alicante. Retrieved from <http://hdl.handle.net/10045/10053>
- [26] Matlab, Mathworks (2018). *Computer Vision System Toolbox™ User's Guide*. Retrieved from [https://la.mathworks.com/help/pdf\\_doc/vision/index.html](https://la.mathworks.com/help/pdf_doc/vision/index.html)
- [27] Demuth, H. B., Beale, M. H., De Jess, O., & Hagan, M. T. (2014). *Neural network design*. Oklahoma: Martin Hagan.

# Intellectual Capital Impact on Organizations' Performance

Sayed Khawar Abbas<sup>1</sup>, Hafiz Ali Hassan<sup>1</sup>, Zair Mahmood Hashmi<sup>2</sup>, Hafiz Muhammad Junaid<sup>3</sup>, Sikandar Majid<sup>2</sup>, Tanzila Ijaz<sup>2</sup>

<sup>1</sup>Hailey College of Commerce, University of the Punjab, Pakistan

<sup>2</sup>University of Lahore, Chenab Campus, Gujrat, Pakistan

<sup>3</sup>Institute of Administrative Sciences, University of the Punjab, Pakistan

**Abstract**— *The abundance of traditional financial evaluation methods reflects historical performances. It is necessary to consider such elements which add value off-balance sheet towards growth. It is argued that there is the difference between book value and market value of a firm, and that difference could be explained by intellectual capital profile. The study is proposed to investigate the impact of six intellectual capital elements human capital, structural capital, customer capital, technology capital, social capital and spiritual capital on the overall performance of the firms. The impact is diagnosed. A developed questionnaire is used to conduct the study. Correlation analysis depicts the data, OLS is used to conduct the analysis.*

**Keywords** – *Intellectual capital, firms' performance, service sector, Pakistan.*

## I. INTRODUCTION

In the current century, people will tend to do more brainwork, and the tendency of physical activities will reduce. The process of economic growth will be more driven by knowledge and information rather than the production process. The knowledge and information referred to intellectual capital never appears on financial reports but have a significant impact on firms' performance as compare to physical assets (Akpınar & Akdemir, 1999).

The globalization phenomenon has increased the interaction of individuals for their common benefits and the quest for better living standards (Hassan, Abbas, & Zainab, 2018). Sharia screening process in a country like Pakistan having similarities and differences with other countries (Waris, Hassan, Abbas, Mohsin, & Waqar, 2018). Financial Deficit has widened the importance of equity capital raising (Asif, Abbas, & Hassan, 2018). In the current scenario, intangible resources, knowledge-based economies, and various competencies have become crucial elements in the growth

and progress of firms (Wang, Wang, & Liang, 2014). According to Abbas et al. (2018), to meet the growing financial challenges in the current atmosphere, credit risk analysis along with remodeling of current practices and advancement of procedures have become pivotal for sustained progress. Intellectual Capital is one of the key determinants of financial performance of banking sector of Pakistan (Shehzadi, Abbas, & Hassan, 2018). Economic development has seen different phases in which, Developing country like Pakistan is being engaged in the formulation of different tools to boost the economy (Hassan, Abbas, & Shehzadi, 2008). Even investment avenues which pool the short investment and makes an idle sector of economy active are becoming part of the economy of Pakistan (Abbas S., 2017).

According to Hashim, Adeyemi, & Alhabshi, (2018), intellectual capital refers to knowledge and expertise which adds value to the performance of the organization. The definition also referred to the knowledge management process is intellectual capital. Abbas et al. (2018), validated through their research findings that cognitive, emotional and behavioral determinants affect consumer approach. Similarly, intellectual capital indulgence significantly approaches the stakeholder's interest towards the organization. Bayburina & Golovko (2009), explained intellectual capital consists of human capital, network capital, process capital, innovation capital and client capital. All these characteristics lead to the development of competitive advantage within the organization. The induction of innovation in the current practices surely helps to achieve competitive advantage (Abbas S. K., Hassan, Asif, Junaid, & Zainab, 2018); (Abbas S., Hassan, Iftikhar, & Waris, 2018) & (Abbas S., et al., 2018). Alike, survival and competitive earnings are highly depending on the strategic management of intellectual capital resources compared to financial ones.

In the current economic structure, the quality human capital structure favors to become a developed nation and to maintain that status is everyone priority (Berzkalne & Zelgalve, 2014). Furthermore, the competitiveness can be increased if the available workforce is knowledgeable, proficient and adaptable. Therefore, many nations are continuously making efforts to develop human capital and enhancing mental skills and intellectual capacity of the people (Hashim, Adeyemi, & Alhabshi, 2018).

## II. LITERATURE REVIEW

Wang & Liang (2014), explained intellectual capital is a sum of knowledge competencies which help organizations to achieve growth and sustainable competitive advantage. Steward (1994), explained the intellectual capital concept was introduced to differentiate firms' book value and market value. While defining the concept of intellectual capital, there is a great deal of convergence in opinion. Meanwhile, most scholars generally agree that intellectual capital contributes towards value creation and value extraction of organizations through knowledge not only held by employees but also stored within organizations database, systems, processes and relationships (Wang, Wang, & Liang, 2014).

Several studies have enriched the extant literature regarding interconnections between knowledge management processes and intellectual capital phenomenon (Ramadan, Dahiyat, Bontis, & Al-Dalahmeh, 2017). The firms' ability to manage its intellectual capital is directly depending on its knowledge capability (Rajesh, Pugazhendhi, & Ganesh, 2011). Similarly, Roos (2017), contended the process through which a firm creates, develop and manage its knowledge resources and intellectual capital is critical for the attainment of competitive performance.

Chen & Wang (2018) found that the role of knowledge management and intellectual capital has become crucial in the information technology sector. Likewise, Kianto (2018), argued intellectual capital resources have a significant impact on firms' financial performance. A no of similar studies explored the relationship of intellectual capital and firms' performance and concluded it has a significant impact over firms' overall performance (Bontis, Chua Chong Keow, & Richardson, 2000; Berzkalne & Zelgalve,

2014; Wang, Wang, & Liang, 2014; & Ramadan, Dahiyat, Bontis, & Al-Dalahmeh, 2017).

Intellectual capital consists of three main elements including human capital, customer capital and structural capital (Bontis, Chua Chong Keow, & Richardson, 2000). Additionally, Hashim, Adeyemi, & Alhabshi (2018), further extended the research framework with the inclusion of three additional variables such as technological capital, social and spiritual capital. Human capital referred to skills, expertise and experience employees share within the organization (Baron, 2011). The customer capital is organizations' relationships with customers, suppliers, and other people and structural capital consists of organizations' processes, methods, concepts, and overall system owned by the organization (Akpınar & Akdemir, 1999).

The extended use of information technology, innovation, research and development in organization termed as technological capital whereas, social capital consists of norms and relationships resulted from organizational behavior which shapes the quality of social interactions among stakeholders contributing to the growth of the economy (Hashim, Adeyemi, & Alhabshi, 2018). Spiritual capital emerges from ethical, spiritual and religious practices individuals adhere to the workplace. Marques (2008), found spiritual behavior within organizational conduct leads to better corporate performance. Subsequently, the study is focused on determining the impact of human capital, structural capital, social capital, customer capital, technological capital and spiritual capital on the overall performance of firms.

## III. RESEARCH METHODOLOGY

Study adhere to a nature in which primary data was required, so primary data collected through developed questionnaire. The questionnaire was adopted from (Khalique, Bontis, Shaari, & Isa, 2015) (Amrizah & Rashidah, 2013) (Ngah & Ibrahim, 2009). A questionnaire distributed to 950 individuals by using non-probability judgmental and convenient samplings. Only 755 responses were useable and complete. Data collected through questionnaire analyzed through reliability test. All the variables reliability around 0.70. It depicts that data is normal to conduct the analysis. Study model adheres following the schematic diagram.



So the following hypothesis can be constructed

Hypothesis	Details
1	HC → OP
2	STC → OP
3	CC → OP
4	SOC → OP
5	TC → OP
6	SPC → OP

HC stands for Human Capital, STC stands for Structural Capital, CC stands for Customer Capital, SOC stands for Social Capital, TC stands for Technological Capital, SPC stands for Spiritual Capital, and OP stands for Organizational performance.

**Research Findings**

Correlation analysis conducted to check the association between variables. The table below shows the data results of correlation analysis.

**Correlation Analysis**

	A	B	C	D	E	F	G
A. OP	1						
B. HC	.691**	1					
C. STC	.856**	.129**	1				
D. CC	.566*	.014	.143**	1			
E. SOC	.728**	.021	.641**	.028	1		
F. TC	.860**	.114*	.724*	.058*	.622**	1	
G. SPC	.518**	.033	.412**	.049	.310**	.408**	1

Note: \*\*. Correlation is significant at the 0.01 level (2-tailed).

\*. Correlation is significant at the 0.05 level (2-tailed).

It can be observed through table OP having a strong positive association with HC, STC, SOC, TC, and SPC at 1

% level of significance whereas, it has a strong positive association with CC at 5 % level of significance. Now

observe HC, it has a strong positive association with STC at 1 % level of significance and with TC at 5% level of significance. But it does not have a significant association with CC, SOC, and SPC. STC has a strong positive association with CC, SOC, SPC at 1% level of significance whereas with TC at 5 % level of significance. CC has a strong positive association with TC at 5 % of the level of significance. Whereas, it does not have a significant association with SOC and SPC. SOC has strong association at 1 % level of significance with TC and SPC. TC has a strong positive association with SPC at 1 % level of significance.

#### Reliability Analysis

Reliability analysis shows below that internal consistency of variables are very good as it above 0.70 in all variables. So, Data could bear the analysis.

Variables	Cronbach's Alpha
OP	0.87
HC	0.91
STC	0.73
CC	0.76
SOC	0.79
TC	0.88
SPC	0.90

#### Multicollinearity Analysis

Thumb rule for Multicollinearity is Tolerance less than 0.1 and VIF more than 10 show multicollinearity exist. It is to check the viability and usefulness of data, Multicollinearity analysis conducted.

Variables	Multicollinearity Statistics	
	VIF	Tolerance
HC	3.237	.242
STC	4.381	.341
CC	5.901	.176
SOC	3.503	.235
TC	4.536	.281
SPC	3.473	.311

From the table results, it can be observed almost all variables fulfills the rule of thumb. Only CC contains the mild multicollinearity, but it does not require any working on it.

#### Regression Analysis

The model was significant, and R square shows that independent variables collectively explains to organizational performance 67.6%. Following Table shows the results of OLS regression.

Variables	Coefficients	Sig.
HC	3.627*	.051
STC	2.921**	.025
CC	3.418***	.003
SOC	2.811***	.006
TC	1.940**	.036
SPC	3.202***	.009

\*\*\*1% = P<.01, \*\*5%= P<.05, \*10%=P<0.10

It can be observed from the regression table that CC, SOC, and SPC are having a strong positive relationship at 1% level of significance. Whereas, STC and TC have a strong positive relationship at 5% level of significance. Only HC is having a significant positive relationship with Organizational behavior at 10% level of significance.

#### IV. CONCLUSION

Intellectual Capital importance has raised with the performance evaluation for organizations in today's era. Furthermore, the low-income level has become the reason to develop the importance of intellectual capital, especially in underdeveloped nations (Abbas S. K., Hassan, Asif, & Zainab, 2018). It also has seen that Human capital relationship with organization performance is not only the key determinants of performance. As, Quality Education in Pakistan has become a challenging part ever (Maryam, Amen, Safdar, Shehzadi, & Abbas, 2018). So, Human Capital impacts but not much significant. Moreover, Information sharing effects broadly to employees working behavior (Hassan, Asif, Waqar, Khalid, & Abbas, 2018) and employee engagement based on services environment of an organization (Hassan et al., 2018). It has seen that green consumption is much important now in Pakistan (Hassan H., Abbas, Zainab, Waqar, & Hashmi, 2018). So study comprehend that Structural Capital, and technological capital having a significant impact at organization performance more than Human capital but still this effect not much stronger. The Strongest effect upon Organizational performance measured in the model is of customer, social and spiritual capital. Results are consistent with (Bontis, Chua Chong Keow, & Richardson, 2000) in the nature of variables. Intellectual Capital is a very important and emerging area of research. The study is implying top management of organizations and regularity authorities mainly. Future researchers could check the effect of intellectual capital with mediating role of motivation or dissatisfaction upon organizational performance. Even they

could specify the population up to specific types of originations.

### REFERENCES

- [1] Abbas, S. (2017). *Determinants of Investment Behavior of Investors towards Mutual Funds*. Beau Bassin, Mauritius: Lap Lambert Academic Publishing.
- [2] Abbas, S. K., Hassan, H. A., Asif, J., & Zainab, F. (2018). HOW INCOME LEVEL DISTRIBUTION RESPONDS TO POVERTY: EMPIRICAL EVIDENCE FROM PAKISTAN. *Global Scientific Journals*, 6(3), 131-142.
- [3] Abbas, S. K., Hassan, H. A., Asif, J., Junaid, H. M., & Zainab, F. (2018). What are the key determinants of mobile banking Adoption in Pakistan? *International Journal of Scientific & Engineering Research*, 9(2), 841-848.
- [4] Abbas, S. K., Hassan, H. A., Hashmi, Z. M., & Waqar, N. (2018). HOW COGNITIVE, EMOTIONAL AND BEHAVIORAL DETERMINANTS AFFECT CONSUMER CREDIT APPROACH? *Global Scientific Journals*, 6(3), 164-171.
- [5] Abbas, S., Haider, S., Zainab, F., Hassan, H., & Fazal, A. (2018). Why remodeling of risk management Practices in banking is required? Evidence from Pakistan. *International Journal of Scientific & Engineering Research*, 9(2), 686-691.
- [6] Abbas, S., Hassan, H., Asif, J., Ahmed, B., Hassan, F., & Haider, S. (2018). Integration of TTF, UTAUT, and ITM for mobile Banking Adoption. *Integration of TTF, UTAUT, and ITM for mobile Banking Adoption*, 4(5), 375-379.
- [7] Abbas, S., Hassan, H., Iftikhar, S., & Waris, A. (2018). Assimilation of TTF and UTAUT for Mobile Banking Usage. *International Journal of Advanced Engineering, Management and Science*, 4(4), 305-308.
- [8] Akpinar, A. T., & Akdemir, A. (1999). Intellectual capital. In *Third European Conference*, (pp. 332-340).
- [9] Amrizah, K., & Rashidah, A. R. (2013). Intellectual capital profiles: Empirical evidence of Malaysian companies Kamaluddin & Rahman. *International Review of Business Research Papers*, 9(6), 83-101.
- [10] Asif, J., Abbas, S., & Hassan, H. (2018). Valuation Based Test of Market Timing Theory. *International Journal of Academic Multidisciplinary Research*, 2(4), 28-30.
- [11] Baron, A. (2011). Measuring human capital. *Strategic HR Review*, 10(2), 30-35.
- [12] Bayburina, E., & Golovko, T. (2009). Design of Sustainable Development: Intellectual Value of Large BRIC Companies and Factors of their Growth. *Electronic Journal of Knowledge Management*, 7(5), 535-558.
- [13] Berzkalne, I., & Zelgalve, E. (2014). Intellectual capital and company value. *Procedia - Social and Behavioral Sciences*, 110, 887-896.
- [14] Bontis, N., Chua Chong Keow, W., & Richardson, S. (2000). Intellectual capital and business performance in Malaysian industries. *Journal of Intellectual Capital*, 1(1), 85-100.
- [15] Chen, M. H., Wang, H. Y., & Wang, M. C. (2018). Knowledge sharing, social capital, and financial performance: the perspectives of innovation strategy in technological clusters. *Knowledge Management Research & Practice*, 1-16.
- [16] Hashim, M. J., Adeyemi, A. A., & Alhabshi, S. M. (2018). *Effects of Intellectual Capital on Microfinance Institutions' Performance*. In *Proceedings of the 2nd Advances in Business Research International Conference*. (pp. 187-196). Springer, Singapore.
- [17] Hassan, H. A., Abbas, S. K., & Zainab, F. (2018). ANATOMY OF TAKAFUL. *Global Scientific Journals*, 6(3), 143-155.
- [18] Hassan, H., Abbas, S., & Shehzadi, A. (2008). *Takafuls' Anatomy and Potential in Pakistan*. Beau Bassin, Mauritius: Lap Lambert Academic Publishing.
- [19] Hassan, H., Abbas, S., Zainab, F., Waqar, N., & Hashmi, Z. (2018). Motivations for Green Consumption in an Emerging Market. *Asian Journal of Multidisciplinary Studies*, 6(5), 7-12.
- [20] Hassan, H., Asif, J., Waqar, N., Khalid, S., & Abbas, S. (2018). The Impact of Knowledge Sharing On Innovative Work Behavior. *Asian Journal of Multidisciplinary Studies*, 6(5), 22-25.
- [21] Khalique, M., Bontis, N., Shaari, J. A., & Isa, A. H. (2015). Intellectual capital in small and medium enterprises in Pakistan. *Journal of Intellectual Capital*, 16(1), 224-238.
- [22] Kianto, A. (2018). Intellectual capital profiles and financial performance of the firm. *The Routledge Companion to Intellectual Capital*, 1-16.
- [23] Marques, J. F. (2008). Spiritual performance from an organizational perspective: the Starbucks way. *Corporate Governance*, 8(3), 248-257.

- [24] Maryam, S., Amen, U.-e., Safdar, A., Shehzadi, A., & Abbas, S. (2018). Education to Educate: A Case of Punjab Education Foundation. *International Journal of Advanced Engineering, Management and Science*, 4(6), 460-465.
- [25] Ngah, R., & Ibrahim, A. R. (2009). The relationship of intellectual capital, innovation and organizational performance: A preliminary study in Malaysian SMEs. *International Journal of Management Innovation Systems*, 1(1), 1-13.
- [26] Rajesh, R., Pugazhendhi, S., & Ganesh, K. (2011). Towards taxonomy architecture of knowledge management for third-party logistics service provider. *Benchmarking: An International Journal*, 18(1), 42-68.
- [27] Ramadan, B. M., Dahiyat, S. E., Bontis, N., & Al-Dalhmeh, M. A. (2017). Intellectual capital, knowledge management and social capital within the ICT sector in Jordan. *Journal of Intellectual Capital*, 18(2), 437-462.
- [28] Roos, G. (2017). Knowledge management, intellectual capital, structural holes, economic complexity and national prosperity. *Journal of Intellectual Capital*, 18(4), 745-770.
- [29] Shehzadi, A., Abbas, S., & Hassan, H. (2018). *Determinants affecting the financial performance of the banking sector of Pakistan*. Beau bassin, Mauritius: Lap Lambert Academic Publishing.
- [30] Stewart, T. (1994). "Your company's most valuable asset: intellectual capital", . *Fortune*, 130(7), 68-74.
- [31] Wang, Z., Wang, N., & Liang, H. (2014). Knowledge sharing, intellectual capital and firm performance. *Management decision*, 52(2), 230-258.
- [32] Waris, A., Hassan, H., Abbas, S., Mohsin, M., & Waqar, N. (2018). Sharia Screening Process: A Comparison of Pakistan and Malaysia. *Asian Journal of Multidisciplinary Studies*, 6(5), 13-21.

# Optimization of Cutting Rate for EN 1010 Low Alloy Steel on WEDM Using Response Surface Methodology

Munish Giri<sup>1</sup>, Manjeet Bohat<sup>2</sup>, Ravinder Chaudhary<sup>3</sup>, Anish Taneja<sup>4</sup>

<sup>1</sup>Research Scholar, Department of Mechanical Engineering, UIET, Kurukshetra University Kurukshetra, India

<sup>2</sup>Asst. Professor, Department of Mechanical Engineering, UIET, Kurukshetra University Kurukshetra, India

<sup>3</sup>Asst. Professor, Department of Mechanical Engineering, UIET, Kurukshetra University Kurukshetra, India

<sup>4</sup>Asst. Professor, Department of Mechanical Engineering, SKIET, Kurukshetra, India

**Abstract**— EN 1010 is a low-carbon steel alloy with 0.10% carbon content. It is known for its fairly low strength and low ductility; however, it can be tempered to increase strength. Machinability of EN 1010 carbon steel is measured to be fairly good. EN 1010 is commonly used for cold headed fasteners, rivets and bolts, in addition to structural, construction and automotive applications such as fenders, pans, nails and transmission covers. Wire Electric Discharge Machine (WEDM) seems to be a good option for machining the complicated profiles. This paper, find effects of various process parameters of Wire EDM such as pulse on time (Ton), pulse off time (Toff), peak current (Ip) and servo voltage (Sv) for analysis of cutting rate (CR) while machining EN 1010. Central Composite Design is used to plan the design of experiment. The output response variable being cutting rate will be measured for all number of experiments conducted. The optimal parameter level combination would be analysed which gives desired cutting rate. These optimized values of different parameters would then be used in execution the machining operation in order to obtain the necessary outputs.

**Keywords**— CCD, Cutting Rate, EN 1010, Process Parameters, RSM, Wire EDM.

## I. INTRODUCTION

The main objective of this paper is to study different parameters like (Ton, Toff, Sv, Wt) of WEDM operations using response surface methodology, in particular central composite design (CCD), to develop empirical relationships between different process parameters and output response namely CR. The mathematical models so developed are analysed and optimised to yield values of process parameters producing optimal values of output response.

## II. LITERATURE REVIEW

Puri A.B. and B. Bhattacharyya [1] (2001) study was considered all the control parameters for the machining

operation which comprised the rough cut followed by the trim cut. The objective of the study has been carried out experimental investigation based on Taguchi method involving thirteen control factors with three levels for orthogonal array L<sub>27</sub>. The main factors are finding for given machine were average cutting speed, surface finish and geometrical inaccuracy were caused due to wire lag and also considered the optimum parametric settings for different machining situations have been found and selected the most appropriate cutting parameter combination for Wire Electrical Discharge Machining process to get the required surface roughness value of machined work pieces.

Hewidy MS et al. [2] (2005) study the development of the mathematical models for relating the relationships of the various Wire EDM machining parameters of Inconel 601 material i.e. Peak Current, Water Pressure and Wire Tension on the Wear Ratio, Material Removal Rate and Surface Roughness. This work was used as Response Surface Methodology. Wire EDM process has shown its competence to machine Inconel 601 material under the acceptable condition of volumetric material Removal Rate which reached to 8mm<sup>3</sup>/min and Surface Finish less than 1µm.

Jinyuang et al. [3] (2007) discuss the development of reliable /multi objective optimization based on Gaussian process regression (GPR) to optimize the parameters of WIRE EDM. The process parameters were mean rate, pulse on time, pulse off time and the output parameters are MRR and surface roughness. The objective function was determined by the predictive reliability with a multi objectives were made by probabilistic variance of the predictive response used as empirical reliability measurement and responses of GPR models. The experiment result shows that GPR models advantage over other regression models in terms of model accuracy. The experimental optimization shows that the effectiveness of

controlling optimization process to produce more reliable solution.

**Andromeda T. A et al. [4](2011)** studied to finding the Material Removal Rate in the Electrical Discharge Machining using the Artificial Neural Network technique. The result of 18 experimental runs to find out the cutting velocity and surface finish collected from the Die Sinking EDM process for the copper electrode and the steel work piece. It was targeted to develop a behavioural model making use of input-output pattern of the raw data from the EDM process experiment. The use was made of behavioural model to predict the MRR and then the predicted value of MRR was compared to the actual value of MRR. The results showed a good harmony of predicting the MRR between them.

**Jaganjeet Singh and Sanjeev Sharma [5] (2013)** investigate the effects of various WEDM process parameters on the machining quality and to optimize the response variables of WEDM. The work related to effects of various process parameters of WEDM like  $T_{on}$ ,  $T_{off}$ , Servo voltage ( $S_v$ ),  $I_p$ , Wire feed ( $W_f$ ) and Wire tension ( $W_t$ ) have been investigated to demonstrate the influence on material removal rate of P20 Tool Steel by using Elektra Sprint cut 736 WEDM machine. Where the surface roughness was measured by Mar Surf PS5 roughness measuring instrument. The experiments were used by Taguchi methodology (L18) Orthogonal Array and results of the experimentation were analysed by MINITAB software.

**H.V.Ravindra et al. [6] (2014)** study outlines the development of model to optimize the WEDM machining parameters using the Taguchi's technique which was based on the robust design. Experimentation was performed as per Taguchi's L16 orthogonal array. Each experiment has been performed under different cutting conditions of pulse-on, pulse-off, current, and bed speed. Molybdenum wire having diameter of 0.18 mm was used as an electrode. Three responses have been considered for each experiment namely accuracy, surface roughness, volumetric material removal rate. Based on this analysis,

process parameters were optimized. ANOVA was performed to determine the relative magnitude of each factor and responses was done using artificial neural network.

**F. Klocke et al. [7] (2016)** paper study the effect of different annealing and heat treatment processes of 42CrMo4 (AISI 4140) on the S-EDM process. Hence, changes of state variables depending on different machining parameters and were considered. Therefore, the resulting microstructures were analyzed by scanning electron microscope (SEM). Additionally, residual stress was determined and compared to the initial state. The identified changes of investigated state variables were the described modifications.

**Amit. R Choudhary and P Shende [8] (2017)** objective of this research was to investigate and predict the impact of the electrical parameters: peak current ( $I$ ), pulse duration ( $T_{on}$ ) and pulse off ( $T_{off}$ ) on the surface roughness (SR), Cutting time (CT). Adaptive Neuro-Fuzzy Inference System (ANFIS) as one of the active methods and also a set of new data was obtained with different levels. The results indicate that even with the complexity of the EDM process, the Adaptive Neuro-Fuzzy Inference System (ANFIS) was found to be adequate in forecasting response variable with high accuracy

### III. EXPERIMENT METHODOLOGY

#### 3.1 Machine tool

In this research work, CR is Output characteristics. This output characteristic is studied under varying conditions of input process parameters, which are namely pulse on time ( $T_{on}$ ), pulse off time ( $T_{off}$ ), peak current ( $I_p$ ) and servo voltage ( $S_v$ ). The experiments were performed on Electronica Sprintcut 734 CNC Wirecut machine as shown in figure 3.1. Electronica Sprintcut 734 provides full freedom to operator in choosing the parameter values with in a wide range. A brass wire of 0.25 mm diameter is used as the cutting tool material. Deionized water is used as dielectric, which flush away metal particle from the workpiece.



Fig.3.1: Electronica Sprintcut 734 CNC wire cut machine and its parts

### 3.2 Material

EN 1010 is a low-carbon steel alloy with 0.10% carbon content. It is known for its fairly low strength and low ductility; however, it can be quenched to increase strength. Machineability of EN 1010 carbon steel is

measured to be equally good. EN 1010 is commonly used for cold headed fasteners, rivets and bolts, in addition to structural, construction and automotive applications such as fenders, pans, nails and transmission covers. Table 3.1 gives the chemical composition of the work material.

Table.3.1: Chemical composition of EN 1010

Element	C	Si	Mn	P	S
% age by Weight	0.1144	0.0908	0.3843	0.04255	0.02170

The work material used is in rectangular form of dimensions as given below. Figure 3.2 shows the workpiece material used for experiment purpose.

Length = 200mm, Breadth = 100mm, Height = 10mm

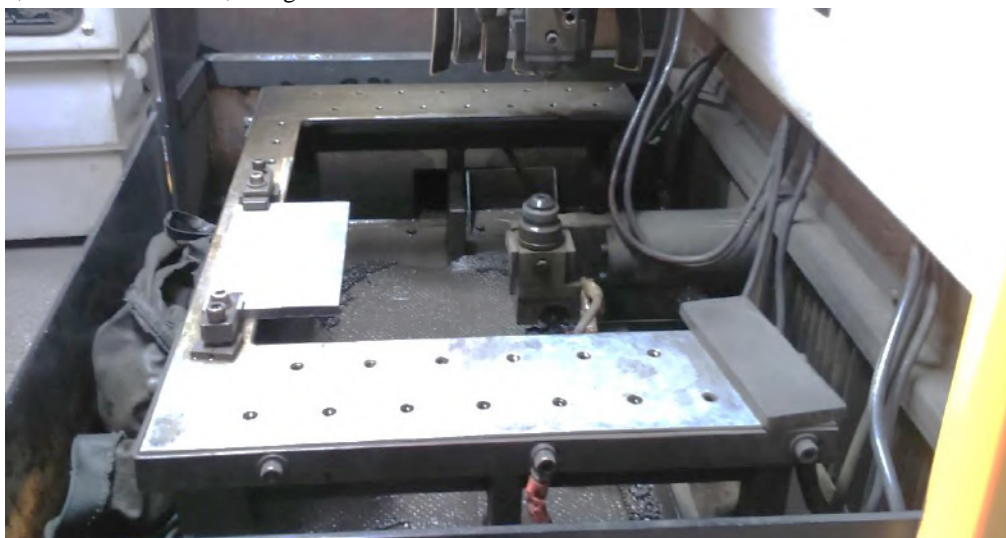


Fig.3.2: EN 1010 workpiece material

3.2 RSM and Design of Experiment

Response surface methodology is a collection of the statistical and mathematical methods which are useful for the modelling and optimization of engineering science problems. Response surface methodology discovers the

relationships between controllable input parameters and obtained Outputs. There are in total 21 experiments carried out according to design of experiments. The average values of CR (mm/min) are shown in Table 3.2.

Table.3.2: Design of Experiment and CR

Run	Ton	Toff	Ip	Sv	CR
1	130	50	80	10	3.68
2	120	30	155	30	3.63
3	110	40	80	10	2.64
4	130	50	230	10	4.99
5	120	40	155	30	3.69
6	120	50	155	30	3.40
7	120	40	230	30	3.67
8	130	30	80	50	4.63
9	120	40	90	30	2.65
10	130	40	155	30	4.26
11	110	30	80	50	2.16
12	120	30	155	50	3.60
13	120	40	155	30	3.65
14	110	40	155	30	2.86
15	120	40	155	10	3.60
16	120	40	155	30	3.85
17	120	40	155	30	3.84
18	110	40	230	10	2.90
19	110	50	230	50	2.86
20	130	30	230	50	3.64
21	120	40	155	30	3.86

IV. RESULT AND DISCUSSIONS

4.1 Analysis of Cutting rate

According to fit summary obtained from analysis, it is found that the quadratic model is statistically significant for CR. The results of quadratic model for CR in the form of ANOVA are presented in Table 4.1. If F value is more corresponding, p value must be less and corresponding resulting in a more significant coefficient. Non-significant terms are removed by the backward elimination for fitting of CR in the model. Alpha out value is taken as 0.05 (i.e., 95 % confidence level). It is found from the Table 4.1 that F value of model is 27.05 and related p value is <0.0001 results in a significant model. The lack of fit is a measure of failure of model to represent data in experimental field at which the points are not included in regression differences in model that cannot be accounted for by the random error. If there is the significant lack off it, as indicated by the low probability value, response predictor is discarded. Lack of fit is non-significant and its value is 5.80. From Table 4.1 it is found that R<sup>2</sup> of

model is 0.970641, which is very close to 1. It means that 97.06 % variation can be explained by the model and only 0.02% of the total variation cannot be explained, which is the indication of good accuracy. The predicted R<sup>2</sup> is in the logical concurrence with adjusted R<sup>2</sup> of 0.238569. Figure 4.1 shows normal probability plot of residuals for CR. Most of residuals are found around straight line, which means that the errors are normally distributed. Adequate precision compares significant factors to non-significant factors, i.e., signal to noise ratio. According to results obtained from software, ratio greater than 4 is desirable. In this, adequate precision is 22.943. So, signal to noise ratio is significant. By applying multiple regression analysis on experimental data, empirical relation in terms of actual factors obtained as follows, equation 4.1

$$CR = -4.27428 + 0.09818 * Ton - 0.1317 * Toff + 0.00868 * Ip + 0.02138 * Sv - 0.000254033 * Ton^2 - 0.001275 * Toff^2 - 0.0000877977 * Ip^2 -$$

$$0.0014*Sv^2 - 0.0005Ton*Ip + 0.00134 Ton$$

$$*Sv+0.00171*Toff*Ip -$$

$$0.0049*Toff*Sv+0.00046Ip*Sv;(4.1)$$

Table.4.1: ANOVA of Response Surface for cutting rate

Pooled ANOVA for Response Surface Reduced Quadratic Model Analysis of variance table						
[Partial sum of squares]						
Source	Sum of Squares	DF	Mean Square	F Value	P-value Prob> F	
Model	8.805163	11	0.800469	27.04977	< 0.0001	Significant
A-Ton	1.532993	1	1.532993	51.80349	< 0.0001	
B-Toff	0.041116	1	0.041116	1.389393	0.2687	
C-Ip	1.033738	1	1.033738	34.93246	0.0002	
D-Sv	0.666173	1	0.666173	22.51156	0.0011	
AC	0.450635	1	0.450635	15.22804	0.0036	
AD	0.281203	1	0.281203	9.502527	0.0131	
BC	1.192385	1	1.192385	40.29354	0.0001	
BD	0.483252	1	0.483252	16.33023	0.0029	
CD	0.465452	1	0.465452	15.72873	0.0033	
A <sup>2</sup>	0.105407	1	0.105407	26.34125	0.0009	
B <sup>2</sup>	0.423345	1	0.423345	16.8713	< 0.0001	
C <sup>2</sup>	0.619743	1	0.619743	20.94259	0.0013	
D <sup>2</sup>	0.300854	1	0.300854	10.16659	0.0110	
Residual	0.266332	9	0.029592			
Lack of Fit	0.234052	5	0.04681	5.80055	0.0567	Not significant
Pure Error	0.03228	4	0.00807			
Cor Total	9.071495	20				
Std. Dev.	0.172025			R-Squared		0.970641
Mean	3.529524			Adj R-Squared		0.934757
C.V. %	4.873876			Pred R-Squared		0.238569
PRESS	6.907321			Adeq Precision		22.94323

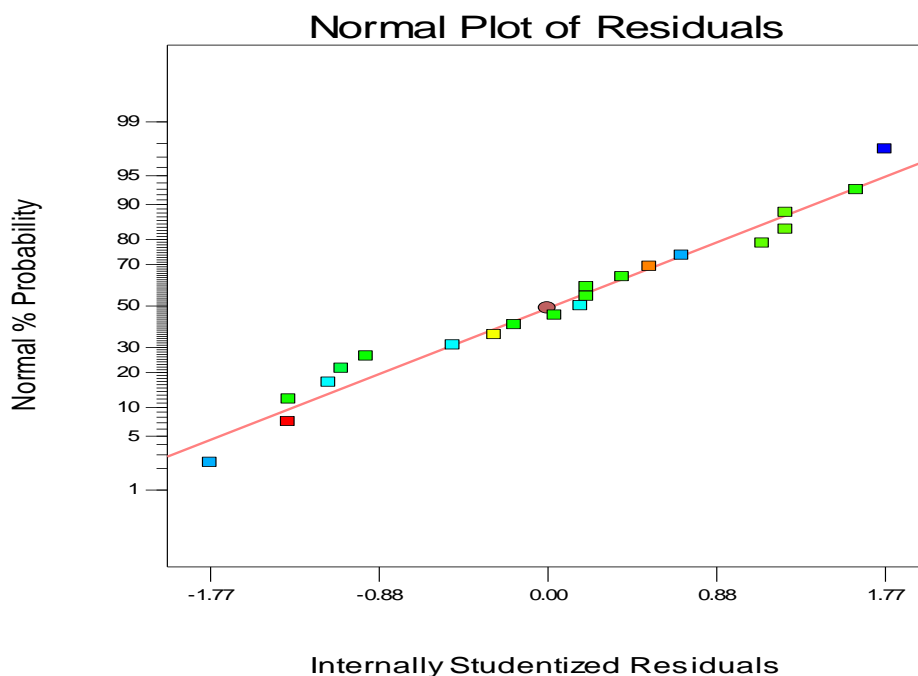


Fig.4.1: Normal plot of residual for cutting rate

4.2 Effect of Process parameters on Cutting rate

The combined effect of two Process Parameters on Output variables is called interaction effect. For interaction plot, two parameters vary keeping the other two process parameters constant at their central value and observe effect on Output characteristics. This plot is called three-dimensional surface plot. So, the significant interactions are shown in figures 4.2-4.7.

The interaction effect of pulse on time (Ton) and pulse off time (Toff) on cutting rate (CR) is shown graphically in figure 4.2. According to this, cutting rate (CR) attains a peak value of 4.5 mm/min; when Ton is increased from

110 to 130µs with Toff remain unchanged at 30µs. This is because at high value of Ton and corresponding lower value of Toff result in longer duration of spark occur which leads to higher discharge energy subjected on work piece causing faster and greater erosion of material. It also shows that CR attains a minimum value of 2.8 mm/min; when Toff is increased from 30 to 50µs with Ton remain unchanged at 110µs. This is due to the fact that lower value of Ton with a higher value of Toff results in a smaller duration of spark to occur that leads to less amount of release of spark energy causing slower erosion of material.

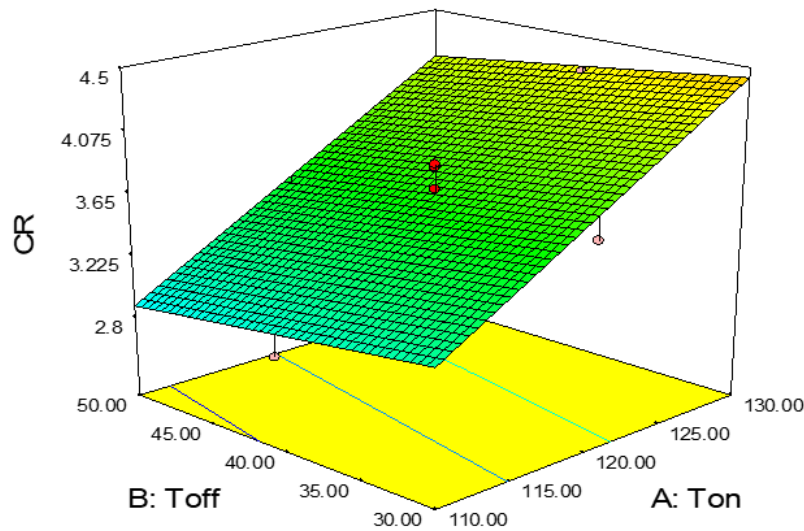


Fig.4.2: Interaction effect of Ton and Toff on cutting rate (CR)

Figure 4.3 shows the interaction effects of pulse on time (Ton) and peak current (Ip) on cutting rate (CR). The cutting rate is increased from 1.3 to 3.65 mm/min when peak current is increased from 80A to 230A with pulse on time remain unchanged at 110 µs.

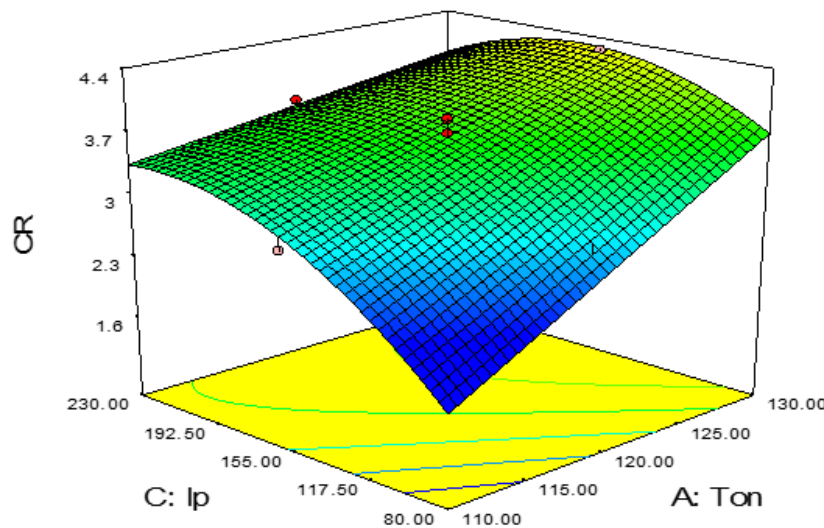


Fig.4.3: Interaction effect of Ton and Ip on cutting rate (CR)

On the other hand, on increasing the pulse on time value from 110 to 130µs the cutting rate increased from 1.3 to 3.65 mm/min with peak current remain unchanged 80A.

On setting the pulse on time and peak current to the highest level 130µs and 230A respectively the cutting rate increases to the maximum value of 4.3 mm/min. Increase

in peak current leads to the increase of the cutting rate. This can be explained by the fact that at higher peak current the pulse energy increases resulting in higher melting and evaporation of the work piece. By increasing the peak current value, the temperature around the spark increases which leads to fast melting of the material at a high rate that increases the cutting rate of the process.

Interaction effect of pulse off time (Toff) and peak current (Ip) on cutting rate (CR) is shown in figure 4.4. When pulse off time is varied from 30 to 50µs, with a constant peak current of 80 A, the cutting rate decreased from 2.58 to 1.2 mm/min.

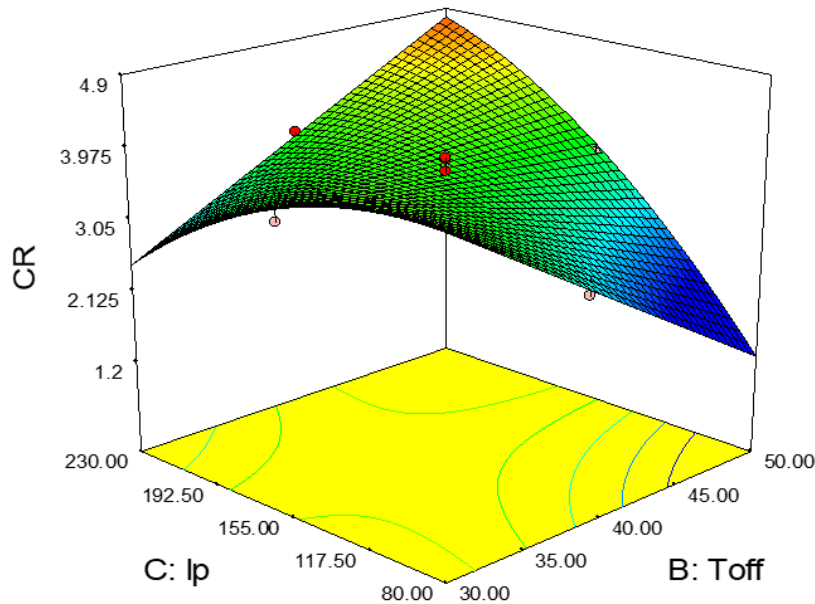


Fig.4.4: Interaction effect of Toff and Ip on cutting rate (CR)

It is due to the fact that on increasing the time gap between the two consecutive sparks the process of erosion of material becomes slow. By increasing the peak current from 80 to 230 A, the cutting rate increased from 2.58 to 4.5 mm/min as on increasing the peak current the pulse energy increases resulting in higher melting and erosion of work piece material.

rate of 4.5 mm/min is obtained at lower values of Toff (30µs) and Sv (10V) owing to the reasons mentioned earlier. On increasing the values of pulse off time from 30 to 50µs and servo voltage from 10 to 50V the cutting rate decreased to 1.4 mm/min. Sv is the reference voltage in the gap. Higher is the Sv, larger the gap between wire and work piece. It takes a large time for discharge to build up and hence cutting rate need to be reduced by the control system.

The interaction effect of pulse off time (Toff) and servo voltage (Sv) (figure 4.5) depicts that a larger cutting

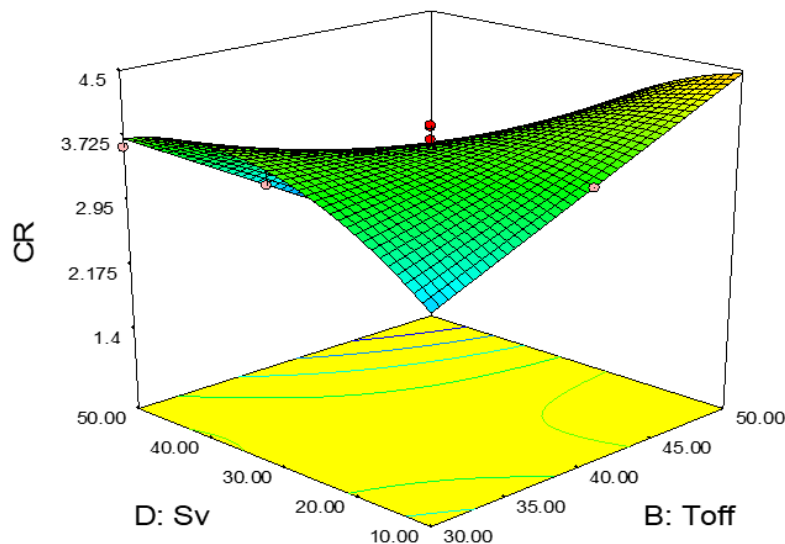


Fig.4.5: Interaction effect of Toff and Sv on cutting rate (CR)

The interaction effect of pulse off time (Ton) and servo voltage (Sv) (figure 4.6) depicts that a larger cutting rate of 4.3 mm/min is obtained at maximum values of Ton (130µs) On increasing the values of pulse on time from 110 to 130 µs so the cutting rate is increased up to 4.3 mm/min. This is because at high value of Ton result in longer duration of spark occur which leads to higher discharge energy subjected on work piece causing faster

and greater erosion of material. It also shows that CR attains a minimum value of 1.5 mm/min; when Sv is increased from 10 to 50V. Sv is the reference voltage in the gap. Higher is the Sv, larger the gap between wire and work piece. It takes a large time for discharge to build up and hence cutting rate need to be reduced by the control system.

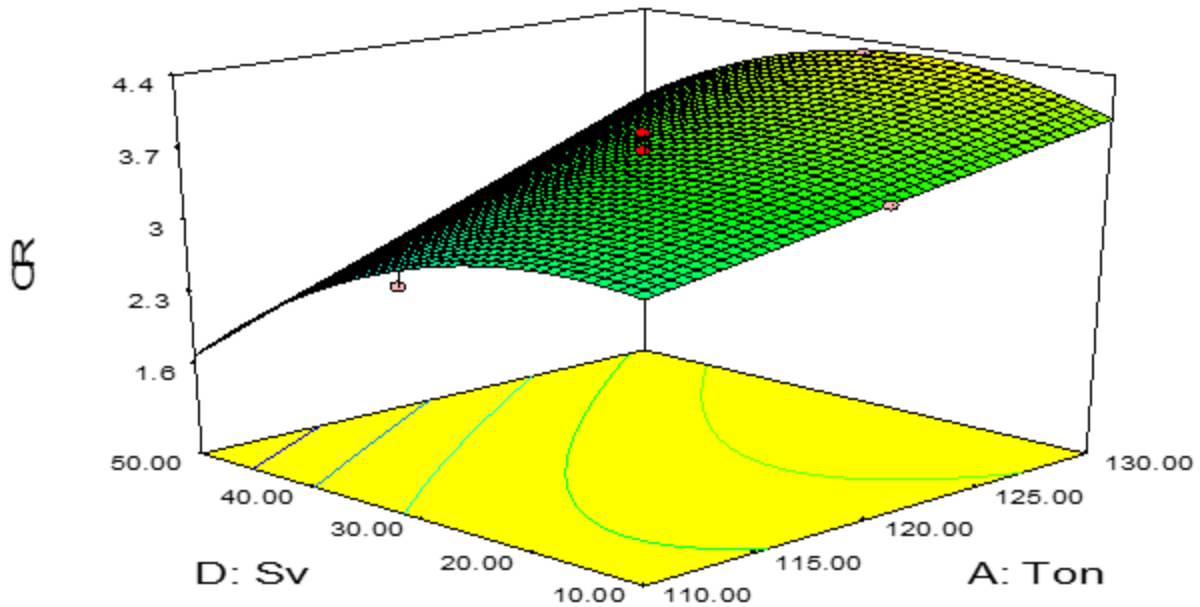


Fig.4.6: Interaction effect of Ton and Sv on cutting rate (CR)

Interaction effect of peak current (Ip) and Servo Voltage (Sv) on cutting rate (CR) is shown in figure 4.7. When Peak current is varied from 80 to 230A. so the cutting rate is increased from 1.3 to 3.8 mm/min. On increasing the peak current, the pulse energy increases resulting in higher melting and erosion of work piece

material and the Servo voltage is increased from 10 to 50 v with cutting rate is decreased from 3.8 to 1.3 mm/min. It is due to the fact that on increasing the time gap between the two consecutive sparks the process of erosion of material becomes slow.

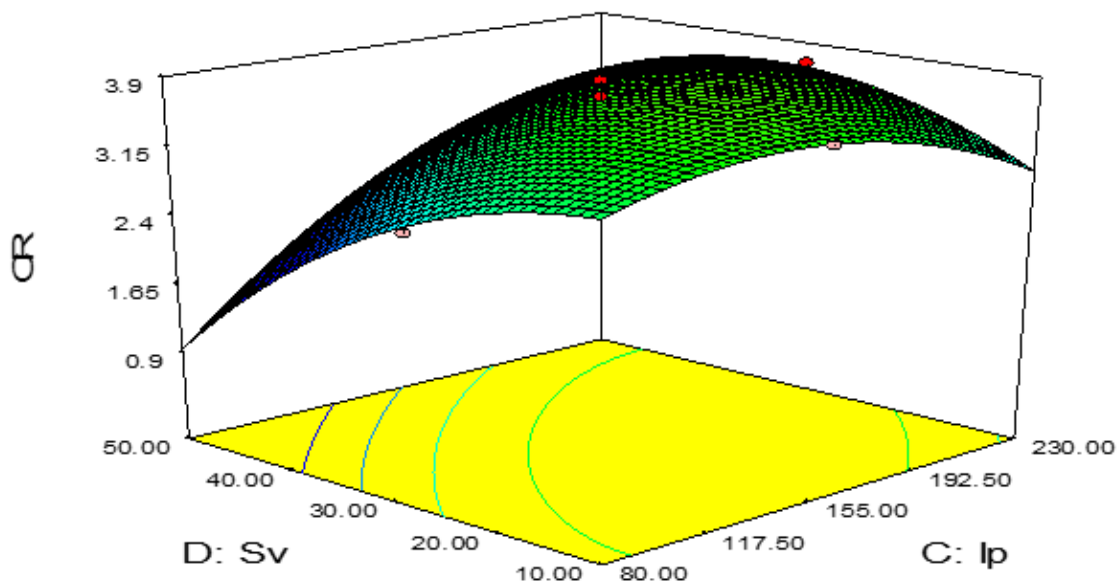


Fig.4.7: Interaction effect of Ip and Sv on cutting rate

## V. CONCLUSION

In this paper the effect of Process Parameters on Cutting Rate is optimized, it is concluded that:

1. Main effect of pulse on time, pulse off time, peak current and servo voltage and interaction effect of pulse on time and pulse off time, pulse on time and peak current, pulse off time and peak current, pulse on time and servo voltage, pulse off time and servo voltage, peak current and servo voltage and second order of pulse on time, pulse off time, peak current and servo voltage found to be important from the ANOVA of cutting rate.
2. It was found experimentally and by successive analysis that on increasing the pulse on time and peak current, the cutting rate increases, whereas increasing the pulse off time and servo voltage decreases the cutting rate. The higher discharge energy associated with the increase of pulse on time leads to a more controlling explosion and thus increases cutting rate.
3. For Output parameter, the predicted values of the response are in close agreement with experimental results.

## REFERENCES

- [1] Puri, A.B; and Bhattacharyya,B; 2001, "An analysis and optimisation of the geometrical inaccuracy due to wire lag phenomenon in WEDM,"*International Journal of Machine Tools & Manufacture* 43, pp.151-159
- [2] Hewidy, M.S., El-Taweel, T.A. and El-Safty, M.F., 2005, "Modelling the machining parameters of wire electrical discharge machining of Inconel 601 using RSM", *Journal of Materials Processing Technology*, pp. 328-336
- [3] Yuan, Jin; Wang, Kesheng; Yua, Tao and Fanga, Minglun;2007, "Reliable multi-objective optimization of high-speed WEDM process based on Gaussian process regression",*International Journal of Machine Tools & Manufacture* 48, pp.47-60.
- [4] Andromeda, T., Yahya, A., Hisham, N., Khalil, K. and Erawan, A., 2011, "Predicting Material Removal Rate of Electrical Discharge Machining (EDM) using Artificial Neural Network for High gap current", *IEEE*, pp. 259-262.
- [5] Singh, Jaganjeet and Sharma, Sanjeev;2013, "Effects of Process Parameters on Material Removal Rate and Surface Roughness in WEDM of P20 Tool Steel", *International Journal of Multidisciplinary and Current Research*.
- [6] Ugrasena, G; Ravindra; Naveen Prakash, G.V and Keshavamurthy, R; 2014, "Process optimization and estimation of machining performances using artificial neural network in wire EDM", *International Journal of Material Science*, pp. 1645-1648.
- [7] Klocke, F; Schneider, S; Ehle, L; Hensgen, L and Klink, A; 2016, "Investigation on Surface Integrity of Heat Treated 42CrMo4 (AISI 4140) Processed by Sinking EDM", *International Journal of Elsevier Engineering Research*, pp 580-585.
- [8] R Choudhary, Amit and Shende, P; 2017, "To Improve Process Parameters of Wire EDM", *International Journal of Engineering Science & technology*, vol.2, pp 170-175.

# Optimization of Surface Roughness for EN 1010 Low Alloy Steel on WEDM Using Response Surface Methodology

Munish Giri<sup>1</sup>, Manjeet Bohat<sup>2</sup>, Ravinder Chaudhary<sup>3</sup>, Anish Taneja<sup>4</sup>

<sup>1</sup>Research Scholar, Department of Mechanical Engineering, UIET, Kurukshetra University Kurukshetra, India

<sup>2</sup>Asst. Professor, Department of Mechanical Engineering, UIET, Kurukshetra University Kurukshetra, India

<sup>3</sup>Asst. Professor, Department of Mechanical Engineering, UIET, Kurukshetra University Kurukshetra, India

<sup>4</sup>Asst. Professor, Department of Mechanical Engineering, SKIET, Kurukshetra, India

**Abstract**— The term steel is used for many different alloys of iron. All steels cover small amounts of carbon and manganese. There do exist many types of steels which are (among others) plain carbon steel, stainless steel, alloy steel and tool steel. Carbon steel is the most extensively used kind of steel. The properties of carbon steel depend mainly on the amount of carbon it contains. Maximum carbon steel has a carbon content of less than 1%. Carbon steel is made into an extensive range of products, including structural beams, car bodies. In fact, there are 3 types of plain carbon steel namely low carbon steel, medium carbon steel, high carbon steel. It is good to exact that plain carbon steel is a type of steel having a maximum carbon content of 1.5% along with small percentages of silica, Sulphur, phosphorus and manganese. EN 1010 is a lowest amount of carbon alloy steel with carbon content of 0.10%. Machineability of EN 1010 carbon steel is measured to be fairly good. EN 1010 is usually used for rivets and bolts, construction and automotive applications such as pans, nails and transmission cover. The objective of paper is to study the effect of process parameters namely pulse on time, pulse off time, peak current and servo voltage on surface roughness (SR). The effect of process parameters on productivity and accuracy facts is material dependent. To study parametric effect on Surface Roughness a Central Composite design approach of response surface methodology (RSM) is used to plan and study the experiments. The mathematical relationships between WEDM input process parameters and response parameter namely surface roughness is established to determine optimal values of surface roughness mathematically and graphically. The Analysis of variance (ANOVA) is performed to find statistically significant process parameters. Interaction effects of process parameters on surface roughness are analysed using statistical and graphical representations.

**Keywords**— ANOVA, CCD, EN 1010, RSM, Surface Roughness, Wire EDM.

## I. INTRODUCTION

The objective of this paper is to analyse the effect of different input process parameters like pulse on time (Ton), pulse off time (Toff), peak current (Ip) and servo voltage (Sv) of Wire EDM on output response namely surface roughness using response surface methodology (RSM), in particular the central composite design (CCD). The mathematical models so produced have been analysed and optimized to give the values of process parameters producing the optimal values of the Surface Roughness

## II. LITERATURE REVIEW

**HoK. H et al. [1] (2004)** reviewed the large array of research work done from inception of the EDM process to its development. It suggested on the Wire EDM research work involving optimization of the process parameters, influence of different factors affecting the productivity and machining performance. The paper also showed the adaptive monitor and control of process investigating the possibility of different control strategies to obtain the optimum machining conditions

**Ramakrishnan R. and Karuna Moorthy L. [2] (2008)** described the growth of Artificial Neural Network (ANN) models and the Multi Response optimization technique to envisage and select the best cutting parameters of Wire Electrical Discharge Machining (WEDM) process. To envisage the performance characteristics viz. Surface Roughness, Material Removal Rate Artificial Neural Network models were formed using the Back-Propagation algorithms. Inconel 718 was selected as the work material to conduct the experiments. Experiments were done as per the Taguchi's L9 Orthogonal Array. The responses were optimized using the Multi Response Signal-To-Noise (MRSN) ratio in addition to the Taguchi's parametric design approach

**Pa Jagannathan et al. [3] (2012)** This paper studied of EN31 used material as a workpiece. It is done in Taguchi L27 orthogonal array (OA) by Design of experiments (DOE) table. In this paper a WEDM process rough machining gives lesser accuracy and finish machining gives fine surface finish, but it reduces the machining speed. Hence the result was obtained by improve the MRR and reduce the Ra as the objective, which was done by Taguchi method.

**Noor khan et al. [4] (2013)** investigation the parameters of wire electric discharge machining of high strength and low alloy (HSLA) steels has been carried out. HSLA steels provide greater resistance to atmospheric corrosion. The work has been done using Taguchi L9 orthogonal array. Each experiment was conducted under different parameters combinations of pulse on time, pulse off time and peak current. The machining parameter was optimized combination by using the ANOVA for determine the level of the machining parameters on micro-hardness. The study was used as Taguchi technique for minimum number of marks on the surface S.

**Sivanaga et al. [5] (2014)** This work deals with the effect of thickness of the job on discharge current, cutting speed, spark gap/over cut, metal removal rate and surface roughness value of high carbon high chromium steel (HC-HCr). In this work a die steel cut by wire-electrical discharge machining (WEDM) was used. To obtain a good quality workpiece the machine was experimentally optimized. The mathematical relation developed for estimated thickness of workpiece for an output criterion.

**Kumar Jitender and Rupesh [6] (2015)** study that multi response optimization technique has been undertaken by using traditional method in finish cut WEDM. In this paper pure titanium used as a work material. The effect of process parameters on response variables i.e. MRR, surface roughness. Two different types of electrodes were used in this work to predict the MRR over a wide range of parameters. Result was obtained using ANOVA.

**Abhijit Sahal and Himadri Majumder [7] (2016)** this paper process capability study was performed for turning

operation. Three process input like spindle speed, feed and depth of cut has been chosen for process capability study in plain turning operation by Taguchi's L27 orthogonal array. Process Capability Index was estimated for two machining characteristics frequency of tool vibration and average surface roughness. Single response optimization was affected for these two machining qualities to travel the input settings, which could optimize turning process ability. Optimum limit settings for frequency of tool vibration and average surface roughness were found to be spindle speed: 240 rpm, feed: 0.16 mm/rev, depth of cut 0.2 mm and spindle speed: 240 rpm, feed: 0.16 mm/rev, depth of cut: 0.1 mm. respectively.

**Kumar Sujeet Chaubey and Kumar Neelesh Jain[8] (2017)** paper presents review of the past research work accepted out on manufacturing of micro spur and helical gears highlighting their material, specifications, type of manufacturing processes used, their capabilities and limitations. It exposes most of the past work has attentive on manufacturing of meso and micro spur gear using various micro-manufacturing processes which yield poor quality. The optimization of input parameters of the micro manufacturing processes distressing quality of the meso and micro gears. Based upon these exposures, it also categorizes the commands and possibility for future research in this significant area of micro-manufacturing.

### III. EXPERIMENT METHODOLOGY

#### 3.1 Machine tool

In this research work, SR is Output characteristics. This output characteristic is studied under varying conditions of input process parameters, which are namely pulse on time (Ton), pulse off time (Toff), peak current (Ip) and servo voltage (Sv). The experiments were performed on Electronica Sprintcut 734 CNC Wirecut machine as shown in figure 3.1. Electronica Sprintcut734 provides full freedom to operator in choosing the parameter values with in a wide range. A brass wire of 0.25 mm diameter is used as the cutting tool material. Deionized water is used as dielectric, which flush away metal particle from the workpiece.



Fig.3.1: Electronica Sprintcut 734 CNC wire cut machine and its parts

3.2 Material

EN 1010 is a low-carbon steel alloy with 0.10% carbon content. It is known for its fairly low strength and low ductility; however, it can be quenched to increase strength. Machineability of EN 1010 carbon steel is

measured to be equally good. EN 1010 is commonly used for cold headed fasteners, rivets and bolts, in addition to structural, construction and automotive applications such as fenders, pans, nails and transmission covers. Table 3.1 gives the chemical composition of the work material.

Table.3.1: Chemical composition of EN 1010

Element	C	Si	Mn	P	S
% age by Weight	0.1144	0.0908	0.3843	0.04255	0.02170

The work material used is in rectangular form of dimensions as given below. Figure 3.2 shows the workpiece material used for experiment purpose.

Length = 200mm, Breadth = 100mm, Height = 10mm

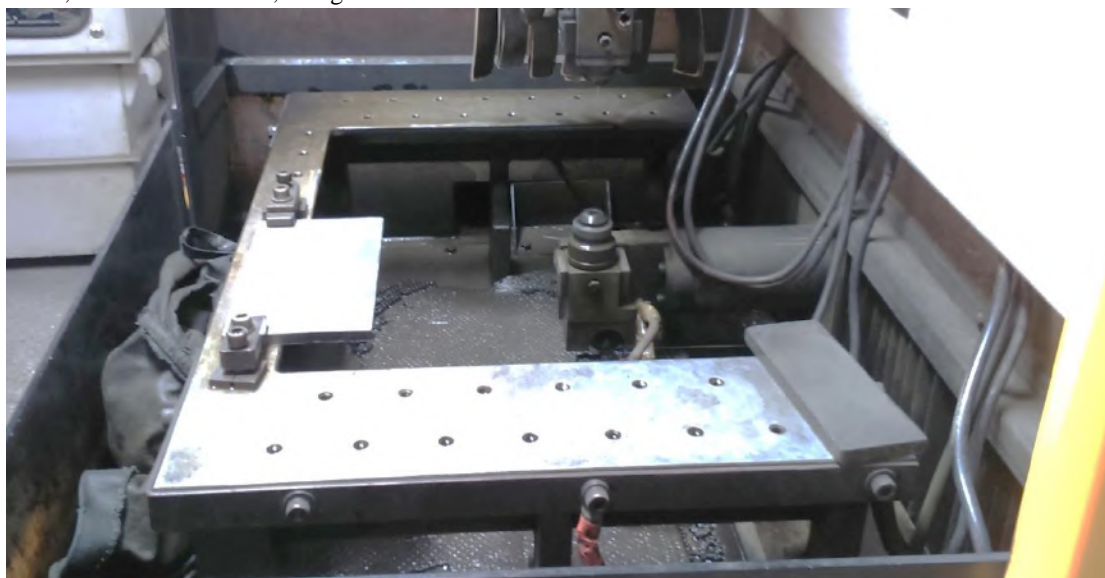


Fig.3.2: EN 1010 workpiece material

### 3.2 RSM and Design of Experiment

Response surface methodology is a collection of the statistical and mathematical methods which are useful for the modelling and optimization of engineering science problems. Response surface methodology discovers the

relationships between controllable input parameters and obtained outputs. There are in total 21 experiments carried out according to design of experiments. The average values of SR ( $\mu\text{m}$ ) are shown in Table 3.2.

Table.3.2: Design of Experiment and SR

Run	Ton	Toff	Ip	Sv	SR
1	130	50	80	10	2.69
2	120	30	155	30	2.68
3	110	40	80	10	2.49
4	130	50	230	10	2.98
5	120	40	155	30	2.7
6	120	50	155	30	2.60
7	120	40	230	30	2.99
8	130	30	80	50	2.80
9	120	40	90	30	2.50
10	130	40	155	30	2.8
11	110	30	80	50	2.4
12	120	30	155	50	2.62
13	120	40	155	30	2.7
14	110	40	155	30	2.58
15	120	40	155	10	2.61
16	120	40	155	30	2.78
17	120	40	155	30	2.76
18	110	40	230	10	2.59
19	110	50	230	50	2.56
20	130	30	230	50	2.70
21	120	40	155	30	2.79

## IV. RESULT AND DISCUSSIONS

### 4.1 Analysis of Surface Roughness

According to fit summary obtained from analysis, it is found that the quadratic model is statistically significant for SR. The results of quadratic model for SR in the form of ANOVA are presented in Table 4.1. If F value is more corresponding, p value must be less and corresponding resulting in a more significant coefficient. Non-significant terms are removed by the backward elimination for fitting of SR in the model. Alpha out value is taken as 0.05 (i.e., 95 % confidence level). It is found from the Table 4.1 that F value of model is 12.35 and related p value is  $<0.0001$  results in a significant model. The lack of fit is a measure of failure of model to represent data in experimental field at which the points are not included in regression differences in model that cannot be accounted for by the random error. If there is the significant lack of fit, as indicated by the low probability value, response predictor is discarded. Lack of fit is non-significant and

its value is 2.55. From Table 4.1 it is found that  $R^2$  of model is 0.9851, which is very close to 1. It means that 98.51 % variation can be explained by the model and only 0.02% of the total variation cannot be explained, which is the indication of good accuracy. The predicted  $R^2$  is in theological concurrence with adjusted  $R^2$  of 0.9071. Figure 4.1 shows normal probability plot of residuals for SR. Most of residuals are found around straight line, which means that the errors are normally distributed. Adequate precision compares significant factors to non-significant factors, i.e., signal to noise ratio. According to results obtained from software, ratio greater than 4 is desirable. In this, adequate precision is 15.724. So, signal to noise ratio is significant. By applying multiple regression analysis on experimental data, empirical relation in terms of actual factors obtained as follows, equation 4.1

$$\begin{aligned}
 SR = & -1.8576415 + 0.0317377 * Ton + 0.061463 * Toff - 0.0006304 * Sv^2 - 0.0001514 * Ton * Ip + \\
 & 0.015994 * Ip + 0.759481 * Sv - 0.00085794 * Ton^2 - 0.0004403 * Toff * Ip - 0.0017092 * Toff * Sv + 0.0001524 \\
 & 0.0010708 * Toff^2 + 0.000839373 * Ip^2 - *Ip * Sv \quad ;(4.1)
 \end{aligned}$$

Table.4.1: ANOVA of Response surface for surface roughness

ANOVA for Response Surface Reduced Quadratic Model						
Analysis of variance table [Partial sum of squares]						
Source	Sum of Squares	DF	Mean Square	F Value	p-value	
Model	0.400373	10	0.04004	12.354	0.0002	Significant
A-Ton	0.0277652	1	0.02777	8.5674	0.0151	
B-Toff	0.0145212	1	0.01452	4.4807	0.0604	
C-Ip	0.1523956	1	0.1524	47.024	< 0.0001	
D-Sv	0.0411476	1	0.04115	12.697	0.0052	
AC	0.0439432	1	0.04394	13.559	0.0042	
BC	0.0859131	1	0.08591	26.51	0.0004	
BD	0.0599051	1	0.05991	18.485	0.0016	
CD	0.0523508	1	0.05235	16.154	0.0024	
A <sup>2</sup>	0.086463	1	0.086463	648.0429	< 0.0001	
B <sup>2</sup>	0.0205861	1	0.02059	6.3522	0.0304	
C <sup>2</sup>	0.002992	1	0.002992	22.42587	0.0021	
D <sup>2</sup>	0.0710337	1	0.07103	21.919	0.0009	
Residual	0.032408	10	0.00324			
Lack of Fit	0.025688	6	0.00428	2.5484	0.1922	Not significant
Pure Error	0.00672	4	0.00168			
Cor Total	0.432781	20				
Std. Dev.	0.056928			R-Squared		0.9251
Mean	2.682381			Adj R-Squared		0.8502
C.V. %	2.1222938			Pred R-Squared		0.9071
PRESS	0.8124115			Adeq Precision		15.724

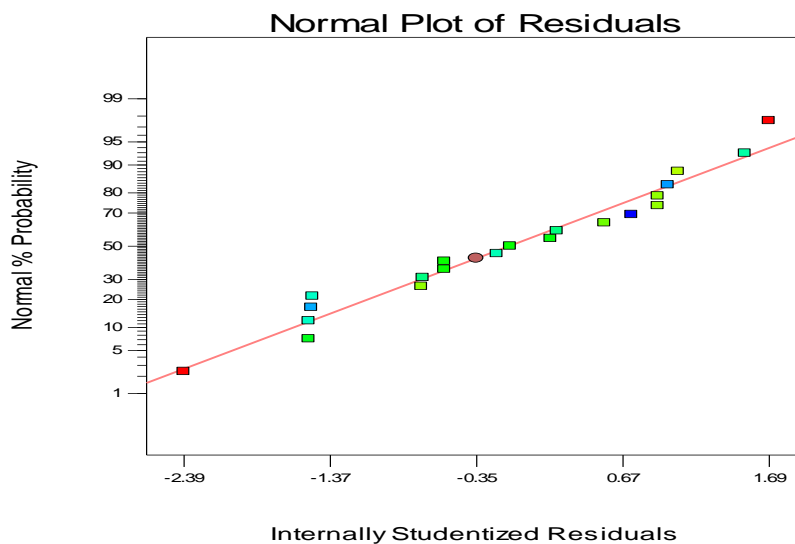


Fig.4.1: Normal plot of residual for surface roughness

#### 4.2 Effect of Process parameters on Surface Roughness

The combined effect of two Process Parameters on Output variables is called interaction effect. For interaction plot, two parameters vary keeping the other two process parameters constant at their central value and observe effect on Output characteristics. This plot is called three-dimensional surface plot. So, the significant interactions are shown in figures 4.2-4.7

The interaction effect of pulse on time ( $T_{on}$ ) and pulse off time ( $T_{off}$ ) on surface roughness (SR) is shown in the figure 4.2. From the figure it is observed that as the value of  $T_{on}$  is increased from 110 to 130 $\mu$ s and  $T_{off}$  constant at 30  $\mu$ s the surface roughness value increased from 2.68 to 2.832  $\mu$ m. When the value of  $T_{off}$  is increased from 30 to 50  $\mu$ s and  $T_{on}$  constant at 110  $\mu$ s the surface roughness value decreased from 2.695 to 2.5475  $\mu$ m.

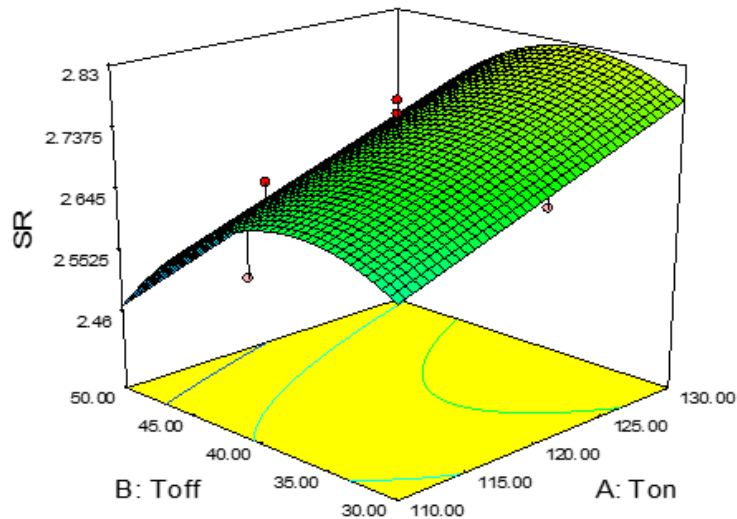


Fig.4.2: Interaction effect of  $T_{on}$  and  $T_{off}$  on surface roughness (SR)

The increase in surface roughness due to increase in pulse on time is due to the fact that a high value of  $T_{on}$  causes longer duration of spark to occur which leads to higher discharge energy which enters deep inside the material. This removes large amounts of material from the work piece producing large hollows. Large hollows are clear indicator of large surface roughness. The decrease in surface roughness due to increase in pulse off time is due to the fact that larger value of pulse off time increases the gap between the two successive sparks which results in impingement of lower discharge energy leading to the

removal of fine particles of materials from work piece surface, hollows obtained are light. Hence, lower surface roughness is obtained.

The interaction effect of pulse on time ( $T_{on}$ ) and peak current ( $I_p$ ) on surface roughness (SR) is shown in the figure 4.3. From the figure it is observed that as the value of  $T_{on}$  is increased from 110 to 130 $\mu$ s and  $I_p$  constant at 80A the surface roughness value increased from 2.5475 to 2.90m. When the value of  $I_p$  is increased from 80 to 230A and  $T_{on}$  constant at 110  $\mu$ s the surface roughness value increased from 2.68 to 2.832 $\mu$ m.

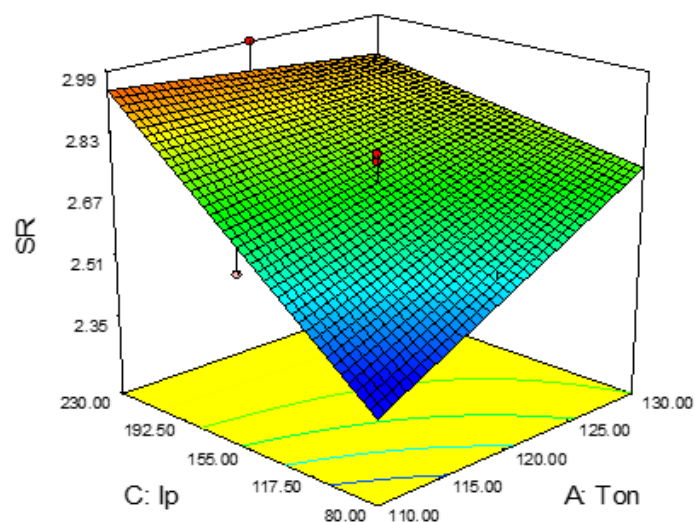


Fig.4.3: Interaction effect of  $T_{on}$  and  $I_p$  on surface roughness (SR)

The increase in surface roughness due to increase in pulse on time is due to the reason mentioned earlier. The increase in surface roughness due to increase in peak current is due to the fact that a larger value of peak current increases the temperature of discharge channel. The energy obtained at large level of  $I_p$  has larger heat energy that enter deep inside the material and larger piece of material are removed, which produces larger hollow on work piece surface. Hence, surface roughness increases. The interaction effect of pulse off time (Toff) and peak current ( $I_p$ ) on surface roughness (SR) is shown in the figure 4.4. From the figure it is observed that as the value of Toff is increased from 30 to  $50\mu s$  and  $I_p$  constant at

80A the surface roughness value decreased from 2.695 to  $2.5475\mu m$ . When the value of  $I_p$  is increased from 80 to 230A and Toff constant at  $30\mu s$  the surface roughness value increased from 2.68 to  $2.832\mu m$ . The decreased in surface roughness due to increase in pulse off time is due to the reason mentioned earlier. The increase in surface roughness due to increase in peak current is due to the fact that a larger value of peak current increases the temperature of discharge channel. The energy obtained at large level of  $I_p$  has larger heat energy that enter deep inside the material and larger piece of material are removed, which produces larger hollow on work piece surface. Hence, surface roughness increases.

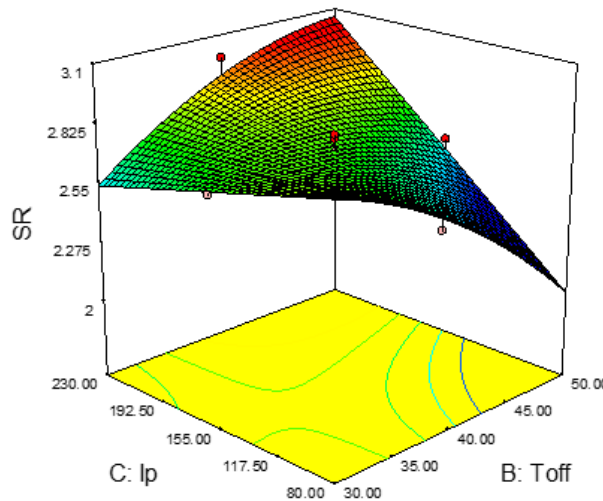


Fig.4.4: Interaction effect of Toff and Ip on surface roughness (SR)

The interaction effect of pulse off time (Toff) and servo voltage (Sv) on surface roughness (SR) is shown in the figure 4.5. From the figure it is observed that as the value of Toff is increased from 30 to  $50\mu s$  and Sv constant at 10V the surface roughness value decreased from 2.695 to  $2.5475\mu m$ . When the value of Sv is increased from 10 to 50V and Toff constant at  $30\mu s$  the surface roughness value decreased from 2.695 to  $1.5\mu m$ . The decrease in surface roughness due to increase in pulse off time due to

the reasons mentioned earlier. The decrease in surface roughness due to increase in servo voltage is due to the reason that a high value of servo voltage increases the gap between two successive sparks. Higher the servo voltage longer is the discharge waiting time which results in lower discharge energy, which produces thin hollow on work piece and hence lower surface roughness is obtained.

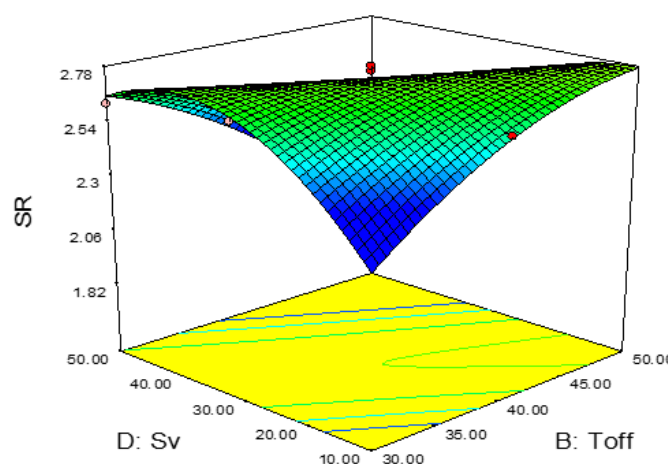


Fig.4.5: Interaction effect of Toff and Sv on surface roughness (SR)

The interaction effect of pulse on time (Ton) and servo voltage (Sv) on surface roughness (SR) is shown in the figure 4.6. From the figure it is observed that as the value of Ton is increased from 110 to 130 V and Sv constant at 10V the surface roughness value is increased from 2.5495 to 3.0 $\mu$ m. When the value of Sv is increased from 10 to 50V and Ton constant at 110  $\mu$ s the surface roughness value decreased from 2.695 to 1.5 $\mu$ m. The increase in surface roughness due to increase in pulse on time due to

the reasons mentioned earlier. The decrease in surface roughness due to increase in servo voltage is due to the reason that a high value of servo voltage increases the gap between two successive sparks. Higher the servo voltage longer is the discharge waiting time which results in lower discharge energy, which produces thin hollow on work piece and hence lower surface roughness is obtained.

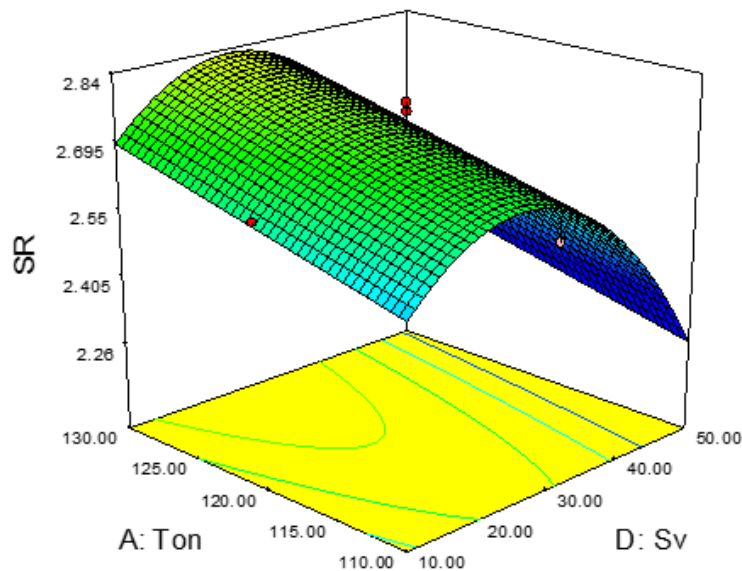


Fig.4.6: Interaction effect of Ton and Sv on surface roughness

The interaction effect of peak current (Ip) and servo voltage (Sv) on surface roughness (SR) is shown in the figure 4.7. From the figure it is observed that as the value of Ip is increased from 80 to 230A and Sv constant at 10V the surface roughness value increased from 2.45 to 3.0  $\mu$ m. When the value of Sv is increased from 10 to 50V

and Ip constant at 80A the surface roughness value decreased from 2.500 to 1.591  $\mu$ m. The increase in surface roughness due to increase in peak current and decrease in surface roughness due to increase in servo voltage is due to the reasons mentioned earlier.

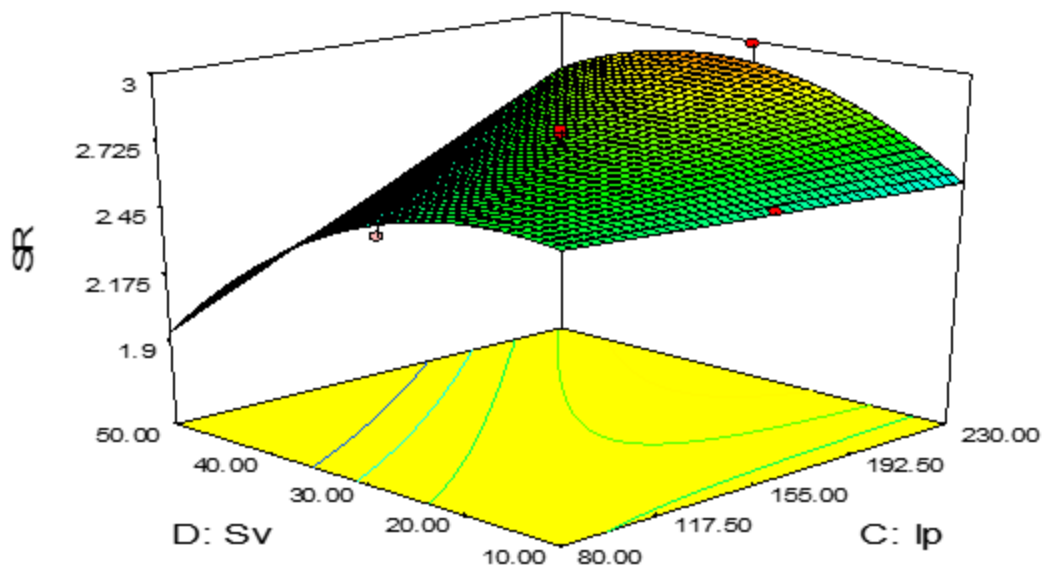


Fig.4.7: Interaction effect of Ip and Sv on surface roughness (SR)

## V. CONCLUSION

In this paper the effect of Process Parameters on Surface Roughness is optimized, it is concluded that:

1. Main effect of pulse on time, pulse off time, peak current and servo voltage and interaction effect of pulse on time and pulse off time, pulse on time and peak current, pulse off time and peak current, pulse on time and servo voltage, pulse off time and servo voltage, peak current and servo voltage and second order of pulse on time, pulse off time, peak current and servo voltage found to be important from the ANOVA of surface roughness
2. Surface Roughness (SR) of the machined surface increased with increase in pulse on time because the discharge energy becomes more controlling with increasing pulse on time, whereas with increase in pulse off time and servo voltage surface finish increases. On increasing the value of peak current, surface roughness of the machined surface increases whereas on decreasing the peak current surface roughness decreases.
3. For Output parameter, the predicted values of the response are in close agreement with experimental results.

## REFERENCES

- [1] Ho, K.H., Newman, S.T., Rahimifards, S. and Allen, R.D., 2004, "State of the art in wire electrical discharge machining (WEDM)", *International Journal of Machine Tools & Manufacture*, pp. 1247-1259.
- [2] Ramakrishnan, R. and Karunamoorthy, L.;2008, "Modeling and multi-response optimization of Inconel 718 on machining of CNC WEDM process", *Journal of Materials Processing Technology*, pp. 343-349.
- [3] P, Jaganathan; Kumar Naveen.T; Dr.R. Siva Subramanian; 2012, "Machining Parameters optimization of WEDM Process using Taguchi method", *International Journal of Scientific and Research*, Vol.2
- [4] Zaman Khan, Noor; Wahid, Mohd. Atif; Singh, Stayover; Sidiquee, Arshad noor; A. khan, Zahid., 2013, "A study of Microhardness on WEDM using Taguchi Method", *International Journal of Mechanical and Production Engineering*, vol. 1.
- [5] Malleswara Rao, S. Sivanaga and Parameswara Rao, Ch. V.S; 2014, "Parametric Evaluation for machining Die steel with WEDM", *International Journal of Scientific and Research Publications*, vol. 3 (3), pp. 2250-3153.
- [6] Chalisgaonkar, Rupesh and Kumar, Jatinder; 2015, "Multi-response optimization and modelling of trim cut WEDM operation of commercially pure titanium (CPTi) considering multipleuser's preferences", *International Journal of Engineering Science and Technology*, pp. 125-134
- [7] Saha, Abhijit and Majumder, Himadri; 2016, "Performance Analysis and Optimization in Turning of ASTM 36 through Process Capability Index" *Journal of King Saud University - Engineering Sciences*.
- [8] Chaubey, Sujeet Kumar and Jain, Neelesh Kumar; 2017, "State-of-art review of past research on manufacturing of meso and microcylindrical gears", *International Journal of Precision Engineering Research*.

# Development of Interactive E-Module for Global Warming to Grow of Critical Thinking Skills

Wayan Suwatra<sup>1</sup>, Agus Suyatna<sup>2\*</sup>, Undang Rosidin<sup>2</sup>

<sup>1</sup>SMAN 9 Bandar Lampung, Indonesia

<sup>2</sup>Physics Education Department, Lampung University, Bandar Lampung, Indonesia

\*Corresponding author: asuyatna@yahoo.com

**Abstract**— *Critical thinking skills are important for solving global warming problems. This critical thinking skill is grown through learning with an interactive e-module for global warming designed to cultivate critical thinking skills. The purpose of this research is to develop an interactive e-module for critical thinking skills on global warming. This research was designed with Research and Development (R&D). The product has been validated by the design of the learning expert through the assessment and qualitatively analyzed descriptive. The product was tested with a quasi experiments Non-equivalent control group pretest-posttest. Classroom experimental learning using an interactive e-module, but control class learning using conventional books. The test subjects are students from one high school in Bandar Lampung. The result is that the average of N-gain of experiment class is higher than control class, that is 0.77 for the experimental class and 0.55 for the control class. The ability of critical thinking skills on global warming for the experimental class increased significantly by 95%. In conclusion e-module interactive global warming can cultivate critical thinking skills.*

**Keywords**— *interactive e-Module, critical thinking, global warming.*

## I. INTRODUCTION

Global warming is one of the environmental issues of rising earth temperatures due to rising greenhouse gas emissions in the atmosphere caused by human attitudes. Shepardson et al (2011) states that temperature changes impact climate change, rainfall patterns and bad weather. Climate change in Indonesia such as changes in the rainy season, the length of the dry season, floods, whirlwinds, and others.

The impact of global warming can be reduced by understanding the effects of global warming. Students are expected to have a critical attitude on the behavior of greenhouse gas donations. Therefore, the Government of Indonesia is making global warming a part of the curriculum of junior and senior secondary schools (Curriculum Developing Team, 2014). The government's move is positive and relevant to current conditions.

Rosidin and Suyatna (2017) showed that the understanding of Indonesian students about global warming is very low. This not only happens in Indonesia, according to Yazdanparast et al, (2013) students do not have enough information about the phenomenon of globalization. Shepardson et al (2011) says there are still middle school students from the Midwest who are confused about the greenhouse effect and the type of radiation in the greenhouse effect. Efforts to grow critical thinking skills have been done, such as by Susanto, et al (2016) by developing interactive multimedia. Maria et al. (2016) by developing the Learning Cycle 7E student worksheet. Novrizawati, et al. (2017) by developing TRAPI learning model, but has not obtained optimal results. This problem will be tackled by providing an interactive e-module that can cultivate critical thinking skills on global warming, especially in the formation of greenhouse gases in the atmosphere caused by human behavior. Communication information technology (ICT) as a learning resource an innovative learning process where the learning process becomes more varied, not limited by space, time and age. One of the real forms of ICT as a learning resource is the interactive electronic module. According to Susanto et al (2015) the use of interactive multimedia global warming is more effective than conventional learning. Provision of stimulus can train students' critical thinking skills, which can be done in learning (Snyder & Snyder, 2008). Critical thinking skills can be achieved through investigation-based learning (Ching and Fong, 2013). Students can acquire knowledge, behavior, and skills by learning materials (Dimiyati and Mudjiono, 2013).

Learning is the process by which a person undertakes to obtain a whole new change of behavior as a result of his own experience in interaction with his environment (Slameto, 2013). Related to that, one of the ways that can be taken is to optimize the use of technological development in the preparation of teaching materials. Available teaching materials are generally static, so less able to cultivate the power of critical thinking, creative, innovative and care about the environment. If in the study of physical matter displayed natural phenomena in the form of animation and video, then learners as if

experiencing phenomena observed. The concept of global warming can be easily understood and long-lasting when learning is related to everyday life and packed interesting so as to motivate students to learn. Teaching materials can be packaged in the form of conventional books or electronic modules. Innovations in electronic modules, can be designed interactively and incorporate technologies that develop in time. The contents of the interactive electronic module of the students are more varied by incorporating moving images (video), animation, simulation, and materials in an integrated manner.

In learning physics students not only hear, record and remember from the subject matter presented by the teacher, but more emphasis on the ability of students to be able to solve problems and act (make observations, experiment, discuss a problem, answer questions and apply concepts and laws to solve the problem) to the learned, then communicate the results. The interactive electronic module for students can be a guideline in the learning process, as well as a means of evaluating the achievement of learning outcomes. Student learning outcomes can be formulated through a well-structured learning process using appropriate models, instructional materials, and assessments. TRAPI learning model can improve critical thinking ability (Novrizawati, et al., 2017) and Authentic assessment of global warming materials in the learning process can improve student's critical thinking ability (Damayanti, et al., 2017). According to Ennis, (1996) that the sub-ability of critical thinking is deciding what action should be trusted or

done. These measures accommodate what needs to be done to achieve the learning objectives that have been formulated. The result of observation at high school in Bandar Lampung is from 30 students who were questioned in 80% of students did not know the cause of global mobilization, 73% of students can not mention the effect of global warming properly and 50% of students do not understand the action to be done related to reducing global warming and 75% of teachers have not used student-centered teaching materials and 75% of teachers do not have special teaching materials to teach students. One of the causes of the incompleteness of understanding concept in learning caused special teaching materials supporting learning global warming. This study aims to develop interactive electronic module of global warming that can be used to cultivate critical thinking skills of high school students.

The concept of global warming can be easily understood and long lasting when learning related to everyday life and packed interesting, according to Duron et al., (2006) student's critical thinking ability can be optimized through 5 steps that is determining the purpose of learning, experiments before drawing conclusions, providing feedback and assessment of learning, so that critical thinking skills and student learning outcomes can be improved, these 5 steps are written on an interactive e-module. The developed interactive module incorporates video elements, images, graphics, sound, animation and simulations that support to achieve maximum learning and can grow critical thinking skills.

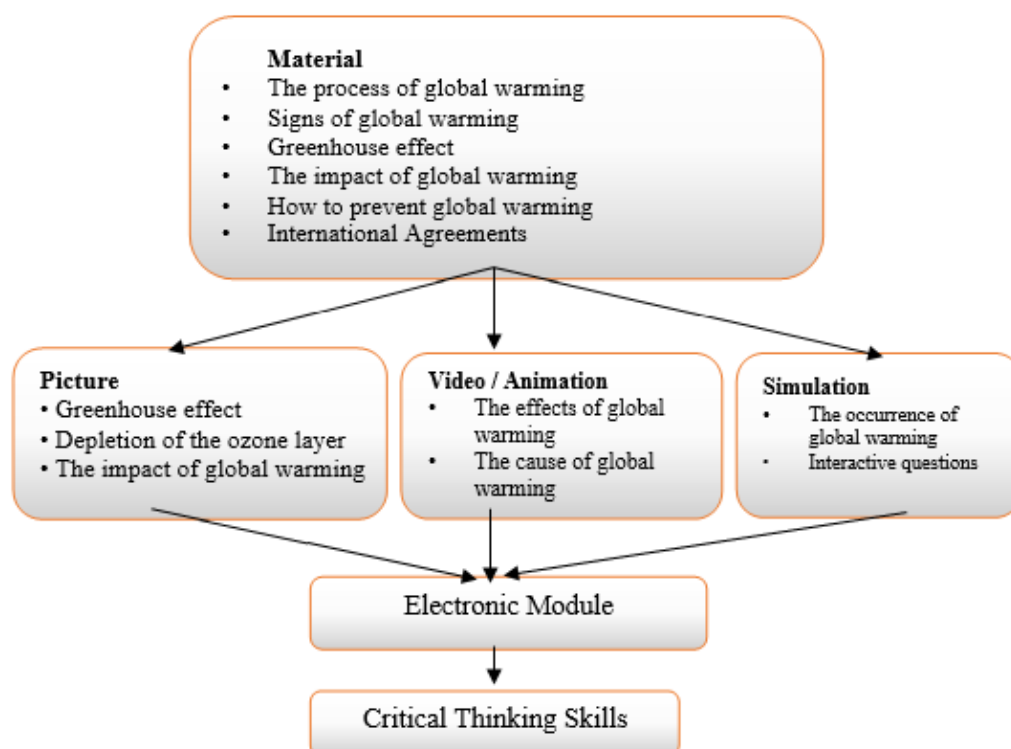


Fig.1: The flow of Electronic Subject Materials

**II. METHOD**

The development model used is research and development (R & D) according to Borg & Gall (2003). The implementation of this research is limited to the seventh step, ie 1) preliminary research, 2) planning, 3) initial product development, 4) initial product testing, 5) product revision, 6) revision test, 7) final product. Validation of teaching material product is done by 3 experts and 4 practitioners in physics lesson. Intrumen validation test of e-module experts using questionnaires. Data analysis of validation test result was done using descriptive quantitative analysis. The effectiveness of e-modules is determined by comparing student learning outcomes using e-modules with students learning using printed modules and by comparing pre-test with posttest results. The e-module implementation test is carried out at high school in Bandar Lampung. The experimental design of the product used was a quasi experiment with pre-test post-test control group design. The subject of the e-module usage test is the student of class XI IPA1 as the experimental class and XI IPA2 as the control class using the printed module. The test subject is determined by purposive sampling taking into account the equivalence of the experimental class with the control class. The data were analyzed using statistical test ie normality test, homogeneity test, test of n-gain average difference of control class with experiment class (independent sample t-test), test the average difference pretest with posttest (paired sample t- test). N-gain is calculated using the Hake (1999) formula as follows.

$$N\text{-gain } (< g >) = \frac{(\%<Sf> - \%<Si>)}{(100 - \%<Si>)}$$

Information:

$g \geq 0.7$  high category

$0.3 \leq g < 0.7$  medium category

$g < 0.3$  low category

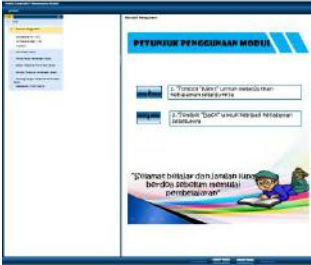
**III. RESULTS AND DISCUSSION**

In the early stages of the study, preliminary research was conducted to find out how the initial concept of global warming materials of students and how the need of teaching materials of students/teachers. The results of a questionnaire distributed by one of the high schools in Bandar Lampung are 80% of students can not answer the question about the causes of global warming in detail and 75% of teachers have not used special teaching materials global pemorientan material. According to Situmorang et al, (2005) that instructional innovation is needed especially to produce learning that can give better learning result toward renewal, innovation on teaching materials can be done by adopting technology. By utilizing technological progress, electronic textbook development can be maximized to convey material on learning according to Djamarah, (2000). Interactive electronic modules can make it easier to include sound, video, animation and simulation elements (Dwiyoga, 2013). Development of interactive electronic module after the preliminary research subsequently design and develop interactive e-module consisting of:

a) Introduction

The introductory section consists of cover, usage instructions and core competency (CC) analysis, basic competency (BC), indicator. The introductory section of the design is as interesting as possible in terms of colors, images, and animations so as to keep learners interested and motivated to learn.

Table.1: Opening / Introduction Section

Cover	Instructions	Analysis of CC, BC, indicators
		
The front cover of the interactive e-module	The instructions contain navigation instructions for using interactive modules.	Introduction contains of KI, KD, and indicator.

b) Content / material section  
The content section displays the stages of the activities of each material to be conveyed. Learning stages use TRAPI

learning model on global warming materials to improve students' critical thinking skills (Novrizawati, et al., 2017).

Table.2: Part Content of interactive e-module

Global Warming Opening Matter	Signs and Causes of Global Warming	Global warming impacts and mitigation	International Agreements Global warming
			
Contains material delivering signs of global warming and there are animated and video phenomenon and contains material about the causes of the occurrence of global warming	Contains introductory materials on the global warming process and animation as well as video phenomena of global warming.	Contains about a volt meter animation that can be used for demonstration of volt meter and contains about how to cope with global warming.	Contains material on the International Agreement relating to global warming

a) Final part of e-module interactive  
The cover section of the student's counseling test contains interactive questions that can test the level of students' understanding of global warming materials.

After the interactive electronic module planning is completed then the product validation test is done by content / material experts, constructors, and linguists.

Table.3: Results of Expert Validation Test

No.	type of test	Validator	Category
1	Validation contents	3.40	Very good
2	construct Validation	3.29	Very good
3	Validation language	3.40	Very good

The interactive e-module effectiveness test is performed by analyzing the pretest and posttest results of students' critical thinking skills on the causes and impacts of

global warming as well as ideas for addressing the effects of global warming. The results of the effectiveness analysis are presented in Table 4.

Table.4: Test the average difference between pretest and posttest critical thinking skills

Treatment	The average value of pretest	Value On average posttest	N-gain	p
interactive e-module (experimental group)	34.40	81.06	0.57	0,00
Textbooks available (Control group)	34.80	71.20	0.72	0,00
p	0.859	0,00	-	-

The pretest giving based on table 4 obtained the average pretest result of the class using the electronic material is 34.40 and the average pretest for the class using the available book 34.80. The results of independent sample t-test showed the students' average early ability in the class using interactive e-learning module and the class using the book no difference ( $p = 0.859 > 0.05$ ). After the learning process where the experimental class using electronic module and control class using printed book done post-test. The average class posttest uses an 81.06 interactive electronic module and a pretest average value for a class that uses printed books 71,20.

The post-test analysis concludes that there is an experimental N-gain class that uses an interactive electronic module with a control class that uses textbooks.

The critical thinking skills of students acquiring learning using interactive electronic modules increased significantly at the 95% confidence level ( $P = 0.000 < 0.05$ ) from 34.40 to 81.06. The average increase in classes using the interactive e-module obtained N-gain of 0.76 with the high category, while the class using textbook material printed printed obtained N-gain of 0.57 with medium category. It appears that the use of e-modules is more effective in improving students' critical thinking skills about global warming. To further examine the effect of e-module utilization, data analysis is based on each indicator of critical thinking skill. The results are shown in Table 5. It appears that all the indicators of critical thinking skills of the experimental class are significantly higher than the control class.

Table.5: Average N-Gain of Critical Thinking Skills Each Indicator

No. Question	Critical Thinking Indicators	Class				P
		Experiment	Criteria	Control	Criteria	
1	Analyzing arguments.	0.72	High	0.56	moderate	0.00
2	Defining the term and consider a definition.	0.87	High	0.60	moderate	0.00
3	Consider whether the source is reliable or not.	0.87	High	0.53	moderate	0.00
4	Ask and answer questions of clarification and critical questions.	0.81	High	0.61	moderate	0.00
5	Induce and consider the results of the induction.	0.65	moderate	0.60	moderate	0.00
6	Decide a course of action.	0.81	High	0.45	moderate	0.00
7	Making and reviewing the results of consideration of values.	0.62	moderate	0.55	moderate	0.00
8	Deducing and consider the results of deduction.	0.87	High	0.56	moderate	0.00
9	Analyzing arguments.	0.72	High	0.56	moderate	0.00
Average		0.76	High	0.56	moderate	0.00

According to Anori et al (2013) that the use of e-book in direct learning model has a positive and significant impact on student learning outcomes. It also uses technology to create and combine text, graphics, audio, video by using tools that enable users to interact, create, and communicate (Rosida, 2015). Multimedia-assisted learning can be designed to turn learning into an active process. Learning media can represent what teachers are less able to say through a particular speech or sentence, with technological innovation can also increase students' interest in learning the material to be taught (Djamarah, 2000). Factors that influence the learning outcomes in this study are media and teaching materials as a source of learning. Learning innovation is needed especially to produce new learning that can give better learning result toward renewal, as well as one of the must possess of

teaching material that is interesting appearance in teaching materials so that can motivate student to learn (Holliday, 2002). Innovation in teaching materials can be done by adopting new technologies to improve content, illustrations, presentations and graphics (Situmorang and Saragih, 2012).

In table 5 the critical thinking indicator that obtains high category results is the definition of terms and define a definition, consider whether the source is reliable or not, ask questions and answer clarification questions and critical questions, decide an action, and deduce and consider the outcome deduction. Of the nine indicators of critical thinking, seven indicators experienced a high category increase, while the two indicators were induced and considered induced results and assessed the values of the considerations increased in the medium category. This

can be caused by the design of interactive electronic modules still can not lead students in inducing and considering induced results, as well as creating and reviewing the values of the results of consideration. Snyder & Snyder (2008) reveals that critical thinking embodies training, practice, and patience. This interactive electronic module that is produced enables students to systematically study the problem so that critical thinking ability can be grown (Kartimi and Permanasari, 2012). It also supports the existence of integrated multimedia in module enabling the module to be an effective learning resource, as the research results Susanto et al (2017) by using interactive multimedia of global warming can cultivated critical thinking skills of students.

### CONCLUSION

Global warming interactive e-module that integrates global warming images/phenomena, videos on the causes of global warming, global warming simulations, animated impacts of global warming for life on earth, and interactive practice exercises can foster critical thinking skills of high school students. The interactive e-module of global warming development results assessed by students to have appeal, usefulness, and easy to operate.

### REFERENCES

- [1] Anori, S., A. Putra, &Asrizal. (2013). The Influence of Electronic Textbook Usage in the Direct Learning Model of Student Results of Class X SMAN 1 LubukAlung. *Pillar of PhysicsEducation* 1 (1): 104-111.
- [2] Borg, W. R, & Gall, M. D., Gall, J. P. (2003). *Educational Research: An Introduction* (Seventh Edition ed.). United States: Pearson Education, Inc.
- [3] Ching, H. S., & Fong, S. F., (2013). Effects of multimedia-based graphic novels presentation on critical thinking among students of different learning approaches. *TOJET: The Turkish Online Journal of Education*, 12 (4).
- [4] Damayanti, R. S., Suyatna, A., Warsono, W., &Rosidin, U. (2017), Development of Authentic Assessment instruments for Critical Thinking skills in Global Warming with a Scientific Approach. *International Journal of Science and Applied Science: Conference Series*, 2 (1), 289-299.
- [5] Djamarah, S.B., (2000), *Teachers and Students in Educational Interaction*, Publisher RinekaCipta, Jakarta.
- [6] Dimiyati and Mudjiono (2013). *Learning and Learning*. PT RinekaCipta, Jakarta
- [7] Duron, R., Limbach, B., & Waugh, W. (2006). Critical thinking framework for any discipline. *International Journal of Teaching and Learning in Higher Education*, 17 (2), 160-166.
- [8] Ennis, H Robert. (1996). *Critical Thinking*. University of Illinois: Prentice Hall, Upper Saddle River, New Jersey 07458.
- [9] Hake, R.R. (1999). Interactive-engagement vs traditional methods: A six thousand student survey of mechanics test data for introductory physics courses. *American Journal of Physics*, 66, 64-74, from <http://aapt.scitation.org/doi/abs/10.1119/1.18809>
- [10] Holliday, W. G., (2002), *Selecting A science Textbook*, Science Scope, 25 (4): 16
- [11] Kartimi, L., &Permanasari, A. (2012). Development of Critical Thinking Measures on Concepts of Hydrocarbon Compounds for High School Students in Kuningan District. *Journal of MIPA Education*, 13 (1), 18-25.
- [12] Maria, L., Suyatna, A. and Warsito. (2016). Development of Learning Students Worksheet (LKPD) Learning Cycle 7E Global Warming Materials to Cultivate Student Critical Thinking Skills. *Journal of Physics Learning*. 4 (5)
- [13] Novrizawati, F., Suyatna, A., &Fadiawati, N. (2017). Effectiveness of the Application of Tradis' Learning Model to Cultivate Critical Thinking Skills. *Journal of Physics Learning*, 5 (1), 97-106
- [14] Rosida, Imran. (2015). Development of Scientific Approach-Based Module as a Supporting Material for Implementation of Curriculum 2013 On Special Journal Material. *Journal of Accounting Education*, 3 (2). (<http://ejournal.unesa.ac.id/index.php/jmpt/article/view/12561>, accessed April 08, 2017).
- [15] Rosidin, U &Suyatna, A. (2017). Teachers and Students Knowledge about Global Warming: a Study in the Smoke Disaster Area of Indonesia. *International Journal Of Environmental Science & Education*, 12 (4), 777-785
- [16] Situmorang, M. &Saragih, N., (2012), Development of High School Chemical Learning Module Through Innovation and Integration Character Education To Prepare Characteristic Resource Facing Global Competition, *Journal Litjak* (In Press).
- [17] Slameto (2013). *Learning and Influencing Factors*. RinekaCipta, Jakarta
- [18] Shepardson, D. P., Niyogi, D., Choi, S., &Charusombat, U, (2011). Students' Conceptions About The Greenhouse Effect, Global Warming, And Climate Change. *Climatic Change*, 104 (3), 481-507
- [19] Susanto, B., Suyatna, A. &Warsito (2015). Design Learning Media of Global Warming Based On Interactive Multimedia With Scientific Approach To Improve Critical Thinking Skills. In *Proceeding of*

The Third South East Asia Design / Development Research International Conference.

- [20] Susanto, B., Suyatna, A. & Warsito. (2016). Multimedia Interaktif Global Warming with Scientific Approach to Improve Student's Critical Skills. *Journal of Physics Learning*, 4 (5), 113-122
- [21] Snyder, L. G., & Snyder, M. J. (2008). Teaching critical thinking and problem solving skills *The Journal of Research in Business Education*, 50 (2)
- [22] Yazdanparast, T., Salehpour, S., Masjedi, M. R., Seyedmehdi, S. M., Boyes, E., Stanisstreet, M. & Attarchi, M. (2013). Global warming: knowledge and views of Iranian students. *Acta Medica Iranica*, 51 (3), 178-184.

# Multi-Index Bi-Criterion Transportation Problem: A Fuzzy Approach

Dr. Samiran Senapati

Department of Mathematics, Nabadwip Vidyasagar College, Nadia, West Bengal, India  
samiransenapati@yahoo.co.in

**Abstract**—This paper represents a non linear bi-criterion generalized multi-index transportation problem (BGMTP) is considered. The generalized transportation problem (GTP) arises in many real-life applications. It has the form of a classical transportation problem, with the additional assumption that the quantities of goods change during the transportation process. Here the fuzzy constraints are used in the demand and in the budget. An efficient new solution procedure is developed keeping the budget as the first priority. All efficient time-cost trade-off pairs are obtained.  $D_1$ -distance is calculated to each trade-off pair from the ideal solution. Finally optimum solution is reached by using  $D_1$ -distance.

**Keywords**— Time-cost trade-off pair,  $D_1$ -distance, ideal solution, membership function, priority.

## I. INTRODUCTION

The cost minimizing classical multi-index transportation problems play important rule in practical problems. The cost minimizing classical multi-index transportation problems have been studied by several authors [14, 15, 16, 17] etc. Some times there may exist emergency situation eg police services, time services, hospital management etc. where time of transportation is of greater importance than cost of transportation. In this situation, it is to be noted that the cost as well as time play prominent roles to obtain the best decision. Here the two aspects (ie cost and time) are conflicting in nature. In general one can not simultaneously minimize both of them. Bi-criterion transportation problem have been studied by several authors [3, 4, 8, 17, 11] etc.

There are many business problems, industrial problems, machine assignment problems, routing problems, etc. that have the characteristic in common with generalized transportation problem that have been studied by several authors [1, 2, 4, 5, 9, 10, 14] etc.

In real world situation, most of the intimations are imprecise in nature involving vagueness or to say fuzziness. Precise mathematical model are not enough to tackle all

practical problems. Fuzzy set theory was developed for solving the imprecise problems in the field of artificial intelligence. To tackle this situation fuzzy set theory are used. In this field area pioneer work came from Bellman and Zadeh [6]. Fuzzy transportation problem have been studied by several authors [12, 18, 19, 20, 21, 23, 24] etc.

The importance of fuzzy generalized multi-index transportation problem is increasing in a great deal but the method for finding time-cost trade-off pair in a bi-criterion fuzzy generalized multi-index transportation problem has been paid less attention. In this paper, we have developed a new algorithm to find time-cost trade-off pair of bi-criterion fuzzy generalized multi-index transportation problem. Thereafter an optimum time-cost trade-off pair has been obtained.

## Problem Formulation:

Let there be  $m$ -origins,  $n$ -destinations and  $q$ -products in a bi-criterion generalized multi-index fuzzy transportation problem.

Let,

$x_{ijk}$  = the amount of the  $k$ -th type of product transported from the  $i$ -th origin to the  $j$ -th destination,

$t_{ijk}$  = the time of transporting the  $k$ -th type of product from the  $i$ -th origin to the  $j$ -th destination which is independent of amount of commodity transported so long as  $x_{ijk} > 0$ ,

$r_{ijk}$  = the cost involved in transporting per unit of the  $k$ -th type of product from the  $i$ -th origin to the  $j$ -th destination,

$a_i$  = number of units available at origin  $i$ ,

$b_j$  = number of units required at the destination  $j$ ,

$c_k$  = requirements of the number of units of the  $k$ -th type of product and

$d_{ijk}^1, d_{ijk}^2$  = positive constants rather than unity, due to

generalized multi-index transportation problem (GMTP).

$$P : \text{Find Max } \{t_{ijk} : x_{ijk} > 0 \text{ and } x_{ijk} \text{ satisfies constraints (1)}\}$$

$$\begin{matrix} 1 \leq i \leq m \\ 1 \leq j \leq n \\ 1 \leq k \leq q \end{matrix}$$

Then the cost minimizing fuzzy GMTP can be formulated as follows:

$$P_1 : \text{Find } x_{ijk} (\geq 0) ; (1 \leq i \leq m, 1 \leq j \leq n, 1 \leq k \leq q)$$

subject to the constraints,

$$\begin{aligned} \sum_{j=1}^n \sum_{k=1}^q d_{ijk}^1 x_{ijk} &\leq a_i ; 1 \leq i \leq m, \\ b_j^* &\leq \sum_{i=1}^m \sum_{k=1}^q x_{ijk} \leq b_j ; 1 \leq j \leq n, \\ \sum_{i=1}^m \sum_{j=1}^n d_{ijk}^2 x_{ijk} &\leq c_k ; 1 \leq k \leq q, \\ \text{and} \quad \sum_{i=1}^m \sum_{j=1}^n \sum_{k=1}^q r_{ijk} x_{ijk} &\leq Z_1 \end{aligned} \tag{1}$$

Some times there may arise emergency situation, eg, hospital managements, fire services, police services etc., where the time of transportation is of greater importance than that of cost. Then time minimizing transportation problem arises. The time minimizing transportation problem can be written as:

$$P^1 : \text{Min } T = \text{Max } \left\{ t_{ijk} : x_{ijk} > 0 \right\}$$

$$\begin{matrix} 1 \leq i \leq m \\ 1 \leq j \leq n \\ 1 \leq k \leq q \end{matrix}$$

Subject to the constraints (1).

Combining the problem  $P_1$  and  $P^1$ , the fuzzy BGMTP appears as:

$$\mu D_j(x) = \begin{cases} \frac{\sum_{i=1}^m \sum_{k=1}^q x_{ijk} - (B_j^* - \Delta b_j)}{\Delta b_j} & ; \text{if } B_j^* - \Delta b_j \leq \sum_{i=1}^m \sum_{k=1}^q x_{ijk} < B_j^* ; \\ \frac{(B_j^* + \Delta b_j) - \sum_{i=1}^m \sum_{k=1}^q x_{ijk}}{\Delta b_j} & ; \text{if } B_j^* < \sum_{i=1}^m \sum_{k=1}^q x_{ijk} \leq B_j^* + \Delta b_j ; \\ 0 & ; \text{if } \sum_{i=1}^m \sum_{k=1}^q x_{ijk} > B_j^* + \Delta b_j \text{ and } \\ & \sum_{i=1}^m \sum_{k=1}^q x_{ijk} < B_j^* - \Delta b_j \end{cases} \tag{2}$$

where  $b_j^*$  and  $b_j$  are the lower tolerance limit and upper tolerance limit respectively of the demand  $j$  ( $1 \leq j \leq n$ ) and

subject to the constraints (1).

### Difference between Classical Multi-index Transportation Problem (MTP) and Generalized Multi-index Transportation Problem (GMTP):

There are several important differences between classical MTP and GMTP which are given below:

- (i) The rank of the co-efficient matrix  $[x_{ijk}]_{m \times n \times q}$  is in general  $m + n + q$  rather than  $m + n + q - 2$ , ie, all the constraints are in general independent.
- (ii) In GMTP the value of  $x_{ijk}$  may not be integer, though it is integer in classical MTP.
- (iii) The activity vector in GMTP is

$$P_{ijk} = d_{ijk}^1 e_i + e_{m+j} + d_{ijk}^2 e_{m+n+k}$$

Whereas in classical MTP it is

$$P_{ijk} = e_i + e_{m+j} + e_{m+n+k}$$

- (iv) In GMTP it need not be true that cells corresponding to a basic solution form a tree. Or in other words vectors in the loop are linearly independent. But in classical MTP vectors in the loop are linearly dependent.

The problem consists of two parts,

$P_1$  : the problem of solving the fuzzy GMTP

$P^1$  : the problem of minimizing the time.

To solve the problem  $P$ , the following technique is used.

The triangular membership function for the fuzzy demand constraints are

$$\Delta b_j = \frac{b_j - b_j^*}{2}, \quad B_j^* = \frac{b_j + b_j^*}{2}$$

The linear membership function of the fuzzy budget goal can be written as:

$$\mu R(x) = \begin{cases} 1 & ; \text{ if } \sum_{i=1}^m \sum_{j=1}^n \sum_{k=1}^q r_{ijk} x_{ijk} \leq Z_1, \\ \frac{Z^* - \sum_{i=1}^m \sum_{j=1}^n \sum_{k=1}^q r_{ijk} x_{ijk}}{\Delta Z} & ; \text{ if } Z_1 < \sum_{i=1}^m \sum_{j=1}^n \sum_{k=1}^q r_{ijk} x_{ijk} < Z^*, \\ 0 & ; \text{ if } \sum_{i=1}^m \sum_{j=1}^n \sum_{k=1}^q r_{ijk} x_{ijk} \geq Z^* \end{cases} \quad (3)$$

Where  $Z^*$  is the upper tolerance limit of the budget goal and  $\Delta Z = Z^* - Z_1$ .

## II. SOLUTION PROCEDURE

The fuzzy programming model of problem  $P_1$  is equivalent to the following linear programming problem as:

Max  $\lambda$   
 subject to the constraints

$$\left. \begin{aligned} \sum_{j=1}^n \sum_{k=1}^q d_{ijk}^1 x_{ijk} &\leq a_i && ; \quad 1 \leq i \leq m, \\ \sum_{i=1}^m \sum_{j=1}^n d_{ijk}^2 x_{ijk} &\leq c_k && ; \quad 1 \leq k \leq q, \\ \lambda &\leq \mu D_j(x) && ; \quad 1 \leq j \leq n, \\ \lambda &\leq \mu R(x), \\ \lambda &= \min[1 \leq j \leq n, \mu D_j(x), \mu R(x)] \\ \text{and } \lambda &\in [0,1] \end{aligned} \right\} \quad (4)$$

After solving the problem the optimum solution

$X_1^*$  and the corresponding optimum cost  $Z_1^*$  at the first iteration are obtained. Next the problem  $P^1$  is solved for minimizing the time.

$$\text{Let } T_1^* = \text{Min} \left[ \text{Max} \left\{ t_{ijk} : x_{ijk} > 0, x_{ijk} \in X_1^* \right\} \right]$$

subject to the constraints (1)

So, for the first iteration the time-cost trade-off pair is  $(Z_1^*, T_1^*)$ . Using re-optimizing technique and replacing  $Z_r$  by  $Z_{r+1}$ , ( $1 \leq r \leq h-1$ ) where  $Z_r < Z_{r+1} < Z^*$ ;  $\forall r$  and  $1 \leq r \leq h-1$ . All efficient time-cost trade-off pairs are obtained as:

$$(Z_1^*, T_1^*), (Z_2^*, T_2^*), \dots, (Z_r^*, T_r^*), \dots, (Z_h^*, T_h^*)$$

(say)

$$\text{where } Z_1^* < Z_2^* < \dots < Z_r^* < \dots < Z_h^*$$

$$\text{and } T_1^* > T_2^* > \dots > T_r^* > \dots > T_h^*$$

The pair  $(Z_1^*, T_h^*)$  is termed as the ideal solution.

Let,

$$\left. \begin{aligned} d_r &= Z_r^* - Z_1^* \\ d_{h+r} &= T_r^* - T_h^* \end{aligned} \right\} \quad 1 \leq r \leq h \quad (5)$$

So,

$$\begin{aligned} (D_1)_{opt} &= \text{Min}_{1 \leq r \leq h} (D_1)_r \\ &= \text{Min}_{1 \leq r \leq h} (d_r + d_{h+r}) \\ &= d_s + d_{h+s} \text{ (say)} \\ &= (D_1)_s \end{aligned}$$

Since equal priority to cost as well as time is given, so  $(Z_s^*, T_s^*)$  attains the optimum trade-off pair.

**The Algorithm:**

Step - 1: Set  $b = 1$ , where  $b$  is the number of iteration.

Step - 2: Solve problem  $P_1$ . Let  $Z_1^*$  be the optimum total cost corresponding to the optimum solution  $X_1^*$ .

Step - 3: Find  $T_1^*$  where,  

$$T_1^* = \text{Max}_{\substack{1 \leq i \leq m \\ 1 \leq j \leq n \\ 1 \leq k \leq q}} \{ t_{ijk} : x_{ijk} > 0 \text{ according to } X_1^* \}$$

Then  $(Z_1^*, T_1^*)$  is called time-cost trade-off pair at the first iteration.

Step - 4: Define

$$r_{ijk}^{b+1} = \begin{cases} M & \text{if } t_{ijk} \geq T_b^* \\ r_{ijk} & \text{if } t_{ijk} < T_b^* \end{cases}$$

$$\text{and } Z_{b+1} < \sum_{i=1}^m \sum_{j=1}^n \sum_{k=1}^q r_{ijk}^{b+1} x_{ijk} < Z^*$$

Where  $Z_{b+1} > Z_b$

Where  $M$  is a sufficiently large positive number. Let  $P_{b+1}$  be the fuzzy GMTP with the cost values  $r_{ijk}^{b+1}$ ,  $Z_{b+1}$  is the aspiration level of cost and other constraints are same as in (1).

Step - 5: Find optimum solution of the problem  $P_{b+1}$ . Let  $Z_{b+1}^*$  be the total cost of problem  $P_{b+1}$ .

Step - 6: If  $Z_{b+1}^* \geq M$ , the algorithm terminates and go to step 8 if  $b + 1 > 2$  otherwise go to step 10. Otherwise in  $(b+1)$ th iteration the time-

cost trade-off pair is  $(Z_{b+1}^*, T_{b+1}^*)$ .

Obviously  $Z_{b+1}^* > Z_b^*$  and  $T_{b+1}^* < T_b^*$ .

Step - 7: Set  $b = b + 1$  and go to step 4.

Step - 8: Let after the  $h$ -th step the algorithm terminates, ie,  $Z_{h+1}^* \geq M$ , then the complete set of time-cost trade-off pairs,

$$(Z_1^*, T_1^*), (Z_2^*, T_2^*), \dots, (Z_r^*, T_r^*), \dots, (Z_h^*, T_h^*)$$

is identified.

Among the trade-off pairs  $(Z_1^*, T_h^*)$  is recognized as the ideal solution.

Step - 9: Find  $(D_1)_{opt} = \text{Min}_{1 \leq r \leq h} (D_1)_r = \text{Min}_{1 \leq r \leq h} (d_r + d_{h+r}) = d_s + d_{h+s}$  (say)

Then  $(Z_s^*, T_s^*)$  offers the best compromise solution.

Step - 10: If  $Z_2 \geq M$ , ie, if  $h = 1$ , then  $Z_1^*$  is the absolute minimum cost and  $T_1^*$  is the absolute minimum time for the optimum transportation plan.

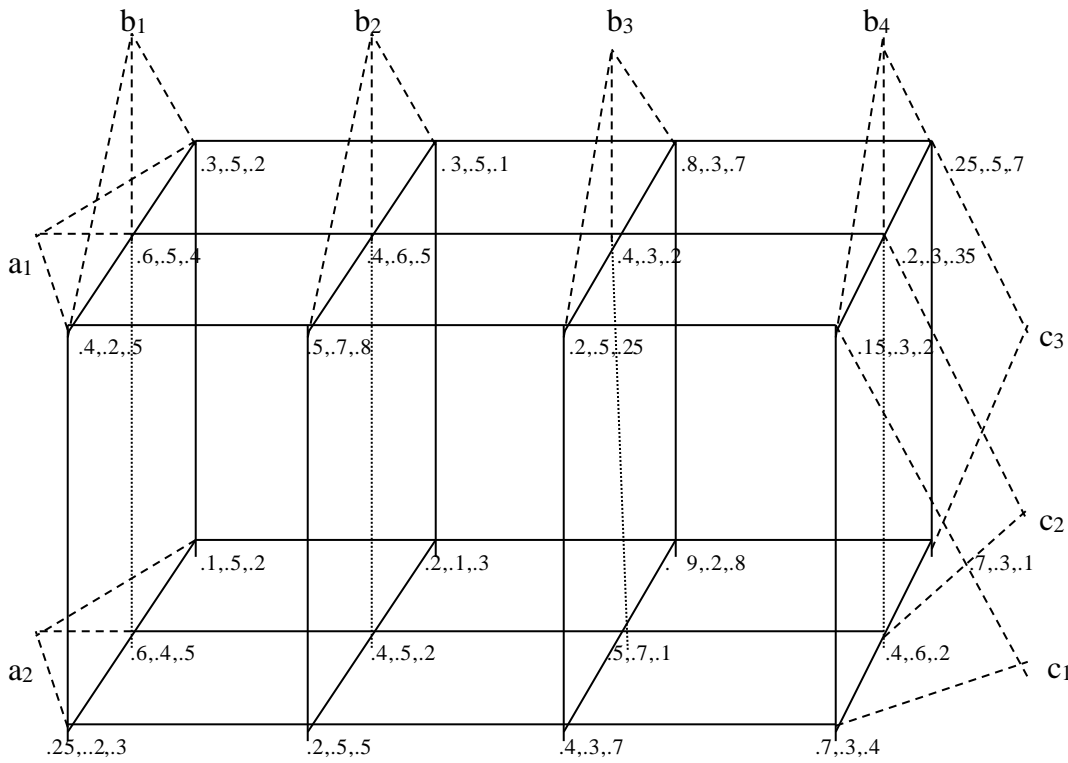
**Numerical Examples:**

A manufacturing company produces three types of products at two factories. They supply their products at four destinations. The corresponding data are given in **Table - 1**.

Table - 1

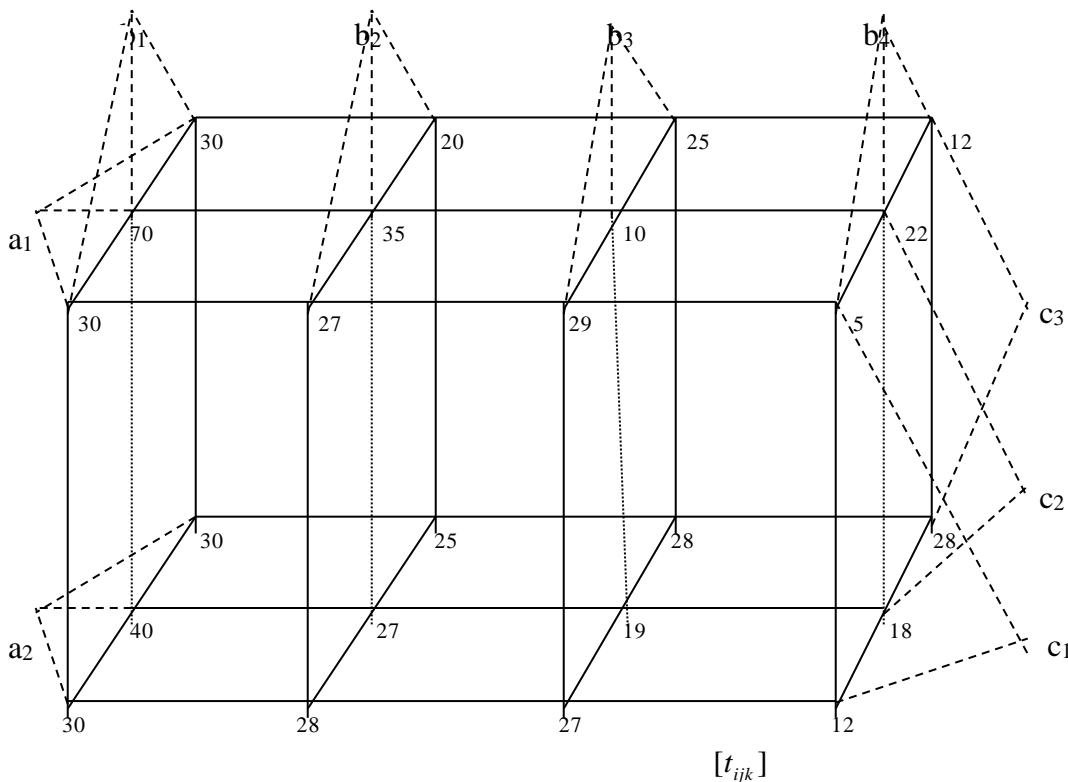
$a_1 = 1300$ $a_2 = 1200$	$b_1^* = 250, b_1 = 300$	$c_1 = 500$ $c_2 = 1200$ $c_3 = 1000$
	$b_2^* = 600, b_2 = 700$	
	$b_3^* = 325, b_3 = 400$	
	$b_4^* = 250, b_4 = 500$	

The proposed problem is explained by considering 2 □ 4 □ 3 costs and time minimizing transportation problem, where  $[d_{ijk}^1, d_{ijk}^2, r_{ijk}]_{2 \times 4 \times 3}$  values and  $[t_{ijk}]_{2 \times 4 \times 3}$  values are given in **Figure - 1** and **Figure - 2** respectively.



$$[d_{ijk}^1, d_{ijk}^2, r_{ijk}]$$

Figure - 2

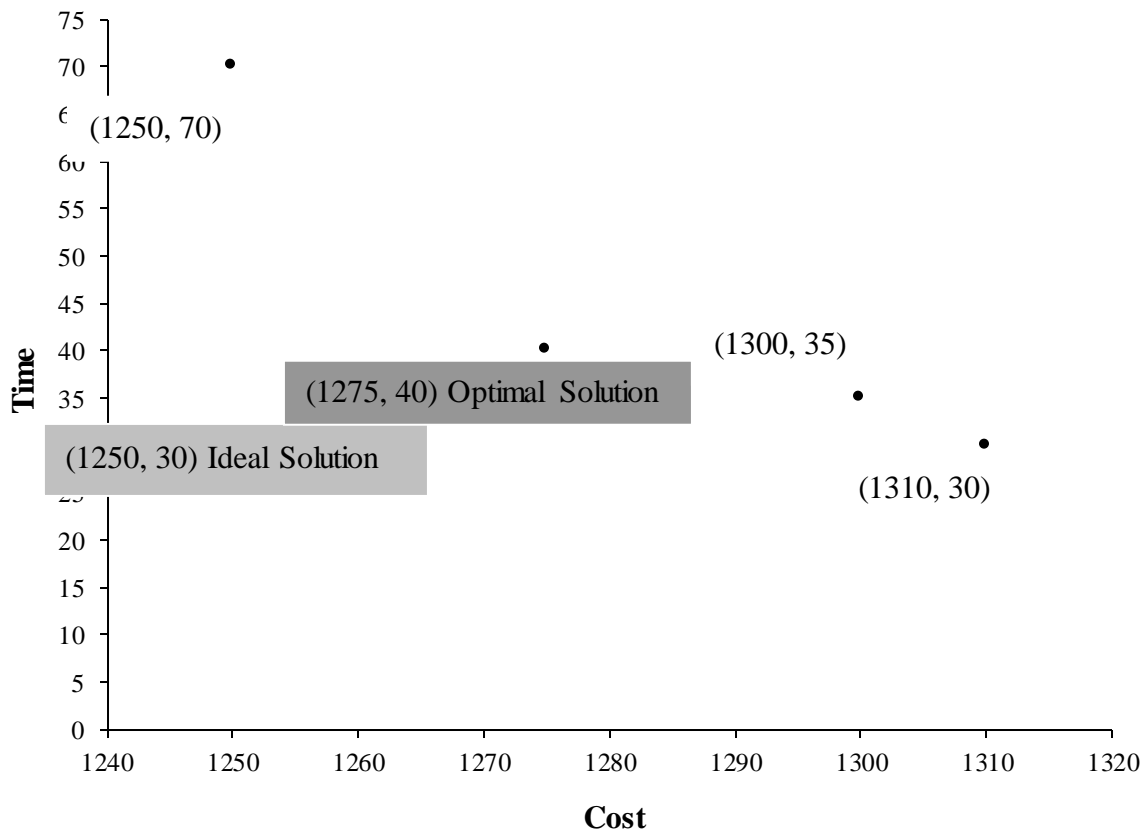


$$[t_{ijk}]$$

Four time-cost trade-off pairs (1250, 70), (1275, 40), (1300, 35), (1310, 30) are obtained. The result shows that the ideal solution is (1250, 30). The  $(D_1)$  distance of the trade-off pairs from the ideal solution is presented in the **Table - 2**.

Table – 2

Trade-off pairs	Ideal Solution	Distance $(D_1)_r$ between ideal solution and the trade-off pair	$(D_1)_{opt}$	Optimum time-cost trade-off pair
(1250, 70)	(1250, 30)	40	35	(1275, 40)
(1275, 40)		35		
(1300, 35)		55		
(1310, 30)		60		



Time - Cost Graph

So the optimum time-cost trade-off pair is (1275, 40).

**REFERENCES**

[1] Bala, E., Ivanescu, P. L. (1964): “On the generalized transportation problem”. Management Science, Vol. 11, p. 188 - 202.

[2] Balachandran, V. (1976): “An integer generalized Transportation model for optimal job assignment in computer networks, Operation Research, Vol. 24, p. 742 - 759.

[3] Basu, M., Pal, B. B., Kundu, A. (1993): “An algorithm for the optimum time cost trade-off in three dimensional transportation problem”, Optimization, Vol. 28, p. 171 - 185.

[4] Basu, M., Acharya Debiprasad (2000) : “An algorithm for the optimum time cost trade-off in generalized solid transportation problem, International Journal of Management Science, Vol. 16, No. 3, p. 237 - 250.

- [5] Basu, M., Acharya Debiprasad (2002): "On Quadratic fractional generalized Solid bi-criterion transportation problem", *Journal of Applied Mathematics and Computing*, Vol. 10 No. 1 - 2, p. 131 - 143.
- [6] Bellman, R. E. and Zadeh, L. A., (1970): 'Decision making in a Fuzzy Environment', *Management Science*, Vol. 17, B141 - B164.
- [7] Charnes, A., Cooper, W. W. (1957), "Management models and industrial application of linear programming", *Management Science*, Vol. 4, p. 38 - 91.
- [8] Cohon, J. L., (1978), "Multiobjective programming and planning, Academic Press,
- [9] Elseman, E. (1964) : "The generalized stepping stone method to the machine loading model, *Management*, Vol. 11, p. 154 - 178.
- [10] Ferguson, A. R., Dantzig, G. B. (1956): The allocation of aircraft to routes. An example of linear programming under uncertain demand". *Management Science*, Vol. 6, p. 45 - 73.
- [11] Fisher, M. L. (1981): "A generalized assignment heuristic for vehicle routing networks, Vol. 11, p. 109 - 124.
- [12] Freeling, A. M. S. (1980): *Fuzzy Sets and Decision Analysis*, *IEEE Transaction on Systems. Man and Cybernetics*, Vol. 10, p. 341 - 354.
- [13] Gunginger, W. (1976): "An algorithm for the solution of multi-index transportation problem. M. Roubens (Ed.) *Adv In Ops. Res. Proceedings of Euro.*, Vol. 11, p. 229 - 295.
- [14] Hadley, G. (1987): *Linear Programming*, Narosa Publishing House, New Delhi.
- [15] Halley, K. B. (1962) : The solid transportation problem", *Ops. Res.* Vol. 10, p. 448 - 463.
- [16] Halley, K. B. (1963): "The existence of solution to the multi-index problem", *Ops. Res. Quart.*, Vol. 16, p. 471 - 474.
- [17] Haman, E. L. (1982): "Contrasting Fuzzy goal programming and Fuzzy multicriteria Programming", *Decision Science*, Vol. 13, p. 337 - 339.
- [18] Hamen, P. L. (1969): "Time minimizing transportation problem", *Nav. Res. Logis. Quart.*, Vol. 16, p. 345 - 357.
- [19] L. A. Zadeh, (1965): 'Fuzzy Sets', *Information Control*, Vol. 8, p. 338 - 353.
- [20] Luhandjula, M. K., (1984): 'Fuzzy approaches for Multiple Objective Linear Fractional Optimization, "Fuzzy Sets and System, Vol. 13, p. 11 - 23.
- [21] Negoita, C. V. and Roiescu, D. A., (1977) : 'On Fuzzy Optimization' *Kybernetes*, Vol. 6, p. 193 - 196.
- [22] Negoita, C. V., (1981): 'The Current Interest in Fuzzy optimization', 'Fuzzy Sets and Systems', Vol. 6 (1981), p. 261 - 269.
- [23] Negoita, C. V., Sularia, M., (1976), 'On Fuzzy Mathematical Programming and Tolerances in planning', *Economic Computer and Economic Cybernetic Studies and Researches*, Vol. 8, p. 3 - 15.
- [24] Oheigeartaigh, M. (1982): 'A Fuzzy Transportation Algorithm *Fuzzy Sets and Systems*, Vol. 8, p. 235 - 243.

# Factors that Impede the Formation of Self-Directed work teams in Mexican Organizations

Martha Patricia Quintero-Fuentes<sup>1</sup>, Montserrat Gómez-Márquez<sup>2,4</sup>, Alejandra Martínez-Orencia<sup>3</sup>, Jesús Gerardo LLanillo-Navales<sup>2,4</sup>, Martha Marín-Ramos<sup>2,5</sup>, Luz del Carmen García-Arroyo<sup>2</sup>, María Isela Eurrieta-Ortiz<sup>2</sup>, Claudia Olivia Carrera-Salazar<sup>2</sup>, Fernando Agustín Romo-Celis<sup>2</sup>, José Luíz Calderón-Palomares<sup>4</sup>, Juan Manuel Méndez-Cervantes<sup>7</sup> Manuel González-Pérez<sup>1,6,8</sup>

<sup>1</sup>Ph.D.-researcher at Colegio Interdisciplinario de Especialización A. C. (CIES)

<sup>2</sup>Ph.D.-student in Strategic Management Sciences at Colegio Interdisciplinario de Especialización A. C. (CIES).

<sup>3</sup>Professor -researcher at Colegio Interdisciplinario de Especialización A. C. (CIES).

<sup>4</sup>Professor -researcher at Instituto Tecnológico Superior de Huatusco (ITSH).

<sup>5</sup>Professor -researcher at Telebachillerato Comunitario del Estado de Veracruz.

<sup>6</sup>Ph.D -researcher at Universidad Popular Autónoma del Estado de Puebla A.C. (UPAEP).

<sup>7</sup>Master-student in Public administration at Colegio Interdisciplinario de Especialización A. C. (CIES).

<sup>8</sup>Ph.D.-researcher SNI1. México.

**Abstract** — *The most efficient work teams are self-directed work teams (SDWTs). In the United States, seventy-five percent of medium and large companies use SDWTs. The United States has a higher economic performance than Mexico. In Mexico, SDWTs have not been successful. The objective of this document is to identify the factors that impede the formation of SDWTs in Mexican organizations. Qualitative research was carried out with a cross-correlational design. The sample consisted of 32 employees from Mexican companies. The chi-square statistical test was used to evaluate the relationship between the variables. The dependent variable was the formation of the SDWTs, and the independent variables were the multidisciplinary knowledge of the individuals, the empowerment of team members and multidisciplinary work teams (work teams with members from a variety of disciplines). The results showed that only the multidisciplinary knowledge of the individuals and multidisciplinary work teams are dependent variables in the formation of SDWTs. Therefore, the conclusion is that empowerment has been exercised in Mexican companies and it is not an impediment to the formation of SDWTs.*

**Keywords**— *Empowerment, Mexican organizations, Multidisciplinary knowledge of the individuals, Multidisciplinary work teams, Self-directed work teams.*

## I. INTRODUCTION

Work teams have been an element that drives the performance of organizations [1]. Unfortunately, not all work teams have generated benefits for the organization, and, in some cases, they have even become a burden on the organization.

The competitiveness of organizations relates to the effectiveness of the teams [1]. The structure and management of the teams determine their efficiency [2]. However, the current structures are traditional and require a change due to the dynamic nature of work environments of businesses today [3].

The most efficient work teams are self-directed work teams [4-6]. Self-directed work teams are “non-hierarchical groups of individuals with different and complementary experiences and knowledge to whom they are responsible for a specific job” [7]. Therefore, work teams have particular characteristics (Table 1).

Table.1: Particular characteristics of SDWTs

Author	Multidisciplinary knowledge of the individuals	Empowerment	Multidisciplinary teams
Johnson, Hollenbe.	o		o

DeRue, Barnes, and Jundt, 2013 [8].			
Wang, & Hicks, 2015 [9].	◦		◦
Robbins, 2013 [10].	◦	◦	◦
Millikin, Hom, and Manz, 2010 [11].		◦	◦
Lambe, Webb, and Ishida, 2009 [12].		◦	
Blanchard, 2007 [13].			
Hopp, 2004 [14].		◦	
Roy, 2003 [15].		◦	

The literature on self-directed work teams marks its particular characteristics. The members of the self-directed works teams are multidisciplinary and interrelate their knowledge to solve problems [16]. This collective knowledge of self-directed work teams generates improvements and innovation [16].

The members of the SDWTs execute their tasks, control the results obtained and take responsibility for the innovations achieved [17]. Therefore, the tasks performed by the self-directed work teams are interdependent and benefit from the synergy of the group [5].

Flexible work increases productivity and improves competitiveness. SDWTs operate through flexible jobs to generate a competitive advantage [6]. The autonomy of self-directed work teams allows them to monitor their environment interactively and quickly change their strategies to adapt to the dynamic environment and improve performance [8].

#### The Culture of the United States and Mexico

The United States is the second most competitive country worldwide [18]. Seventy-five percent of medium and large companies in the United States use a structure based on self-directed work teams [19].

In Mexico, there is a lack of formation of self-directed work teams in organizations. The majority of the organizations where the SDWTs operate are transnational

companies from the United States that permeate their organizational cultures. Some companies where they work in this way are PepsiCo and GM. A Mexican company that has acquired the scheme of SDWTs is Bimbo. However, only a minority of Mexican companies have implemented structures based on SDWTs.

Trejo (2009) points out that the primary challenge for Mexico is the formation of SDWTs. To form them, it is necessary to have an atmosphere with trust, leadership, excellent communication and a clear understanding of the objectives. Moreover, each team member must exert their full effort to maximize their strengths [20].

The cultures of the United States and Mexico are different (Table 1). The culture of a country influences the effectiveness of empowerment [21, 22]. Empowerment is a characteristic of self-directed work teams.

Table.2: Differences between the United States and Mexico

	United States	Mexico
Economic Development GDP per capita (2016 USD)	57,436.4	8,554.6
Power Distance Range 0-100	40	81
Individualism / Collectivism Range 0-100	91	30

Sources: [18, 23].

The United States has a better economic performance compared to Mexico. The GDP of the United States is 57, 436.4 USD per year, and for its part, Mexico has a GDP of 8,554.6 USD [18].

Mexico has a power distance of 81 on the Hofstede scale [23]. Therefore, Mexico is a hierarchical population. Individuals in Mexico understand that everyone has a position and subordinates wait for the indications from their superiors. For its part, the United States has a power distance of 40 on the Hofstede scale [23]. Therefore, the hierarchy in the United States is not essential for the completion of activities.

Mexico has a score of 30 in individualism on the Hofstede scale [23]. Mexico is a collectivist society. Individuals have a long-term commitment to group members. Mexican employees are loyal to each other. The United States is an individualist country with a score of 91 on the Hofstede scale [23]. Individualism is the highest value in the United States [24]. Therefore, employees are self-sufficient and proactive [23].

**II. METHOD**

The instrument used for data collection was a questionnaire [25]. The questionnaire consisted of 16 items covering the three dimensions respectively. A multivariable analysis was conducted of a dependent variable (formation of self-directed work teams) and three independent variables (multidisciplinary knowledge of the individuals, empowerment, and multidisciplinary work teams), of which six, five, and five items were included respectively (Table 3).

Table.3: Classification of the dimensions that affect the formation of self-directed work teams

Multidisciplinary knowledge of the individuals	Empowerment	Multidisciplinary work teams
They have knowledge different from their area.	They have the authority to make changes in their area without having repercussions with their boss.	The members of the work teams are made up of personnel with different knowledge.
The knowledge provided by the company (institution) helps them make decisions.	Their boss allows them to comment on their area of work.	The collaborators of the different areas meet to solve problems in a specific area.
They have knowledge of maintenance regarding their work area.	Their boss allows them to make decisions in their area of work	The members of their work team recognize that the tasks are interdependent.
They have knowledge of quality regarding their work area.	Their boss allows them to stop activities if they do not comply with any work procedure.	They have meetings with staff from other departments.
They have knowledge of occupational safety in their work area.	If there is a problem in their area of work, they can make decisions to improve the situation.	Solutions to problems in their work area are obtained by including the knowledge of all team members.
They have knowledge of productivity in their work area.		

The Questionnaire used the Likert scale. The Likert scale showed the beliefs and attitudes of the respondents [26]. The response options were from one to five where one does not influence the dimension in the formation of the self-directed work teams, and five reflects the influence of the aspect in the formation of the self-directed work teams.

To verify the reliability of the instrument, 32 employees from different companies in the state of Veracruz in Mexico answered a pilot questionnaire using the designed instruments. The instrument was validated through the Pearson correlation (Table 4) and the internal alpha consistency method of Cronbach (Table 5) [27].

Table.4: Validation of the instrument through the Pearson correlation.

	I 1	I 2	I 3	I 4	I 5	I 6	I 7	I 8	I 9	I 10	I 11	I 12	I 13	I 14	I 15	I 16
I 1	1															
I 2	0	1														
I 3	0	0	1													
I 4	0	0	0	1												
I 5	0	0	0	0	1											
I 6	0	0	0	0	0	1										
I 7	0	0	0	0	0	0	1									
I 8	0	0	0	0	0	0	0	1								
I 9	0	0	0	0	0	0	0	0	1							
I 10	0	0	0	0	0	0	0	0	0	1						
I 11	0	0	0	0	0	0	0	0	0	0	1					
I 12	0	0	0	0	0	0	0	0	0	0	0	1				
I 13	0	0	0	0	0	0	0	0	0	0	0	0	1			
I 14	0	0	0	0	0	0	0	0	0	0	0	0	0	1		
I 15	0	0	0	0	0	0	0	0	0	0	0	0	0	0	1	
I 16	0	0	0	0	0	0	0	0	0	0	0	0	0	0	0	1



			significant.
Empowerment of the employees	0.613	3.8415	The empowerment that employees possess is not statistically significant.
Multidisciplinary work teams	14.385	3.8415	The presence of multidisciplinary work teams is statistically significant.

The calculated chi-square is distant from the theoretical chi-square and outside the normal Pearson curve for 1 degree of freedom. The dependence is considered a p-value of almost zero and an independence with a p-value of 1 (Figure 1, 2 and 3).

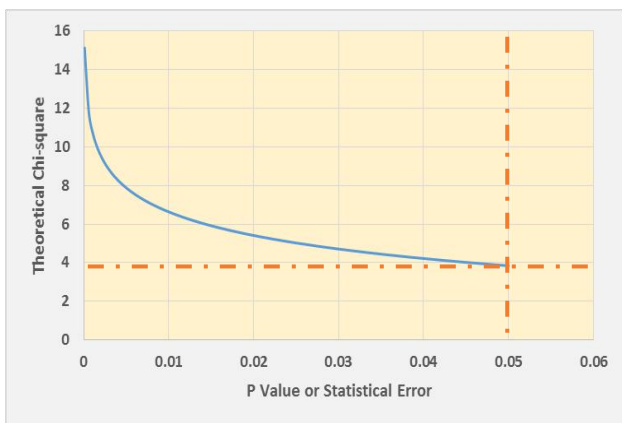


Fig.1: Graph of the theoretical inverse function: p-value vs theoretical chi-square of 1 degree of freedom.

For a 95% confidence for independence, the intercession presented by the theoretical chi-square is (0.05, 3.84); therefore, 5% of statistical error was considered for dependence (Figure 1).

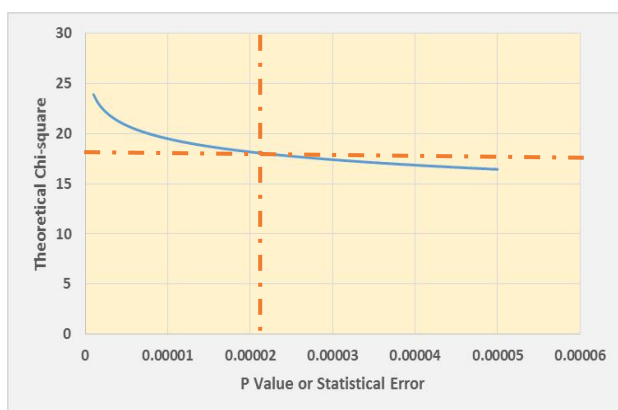


Fig.2: Graph of the theoretical inverse function: p-value vs observed chi-square, independent variable multidisciplinary knowledge of the individuals of 1 degree of freedom.

The intercession of p-value and observed chi-square is (0.00002354, 17.8790357). Therefore, it shows almost 100% confidence for the dependence of the variables: multidisciplinary knowledge of the individuals (independent variable) and the formation of the SDWTs (dependent variable) (Figure 2).

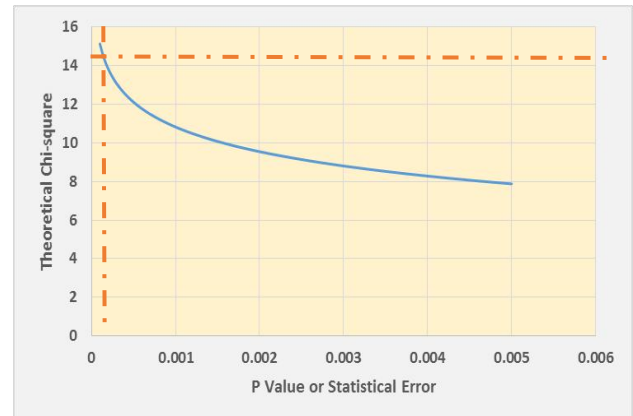


Fig.3: Graph of the theoretical inverse function: p-value vs observed chi-square, independent variable multidisciplinary work teams of 1 degree of freedom.

The intercession of the p-value and observed chi-square is (0.000149, 14.384803). Therefore, it shows an almost 100% confidence for the dependence of the variables: multidisciplinary work teams (independent variable) and the formation of the SDWTs (dependent variable) (Figure 3).

#### IV. CONCLUSIONS

The results revealed that the factors that impede the formation of SDWTs in Mexican organizations are the lack of multidisciplinary knowledge of the individuals and the lack of multidisciplinary work teams. On the other hand, the empowerment of these employees from these Mexican companies does not influence the formation of self-directed work teams. The tests were performed with a 95% confidence.

Technical knowledge is essential for the performance of an organization. The most competitive countries are at the top of the indicators of education and efficiency of the labor market. Mexico is in position 80 and 70 respectively of 135 countries [18]. Therefore, Mexico needs to train its workers with multidisciplinary knowledge for complex tasks in order to respond quickly to changes in their work environments. The work teams that are formed in the Mexican organizations must be multidisciplinary, that is, the members must be experts in different areas than their teammates.

Despite Mexico having a high score on the scale of power distance index [23], this study has shown that Mexican workers have empowerment. The leaders of Mexican organizations are delegating authority to their employees.

Therefore, the empowerment of these Mexican employees does not influence the formation of self-directed work teams.

The limitations of the present investigation were several. The sample was made only in Mexico. The sample was of 32 employees from Mexican companies from different states of the Mexican Republic. The questionnaire was applied to one collaborator per company.

Future studies could be to analyze other factors that prevent the formation of (SDWTs) in other countries. On the other hand, the United States and Mexico are different nations. Therefore, the different dimensions between countries can be studied for the formation of self-directed work teams.

### REFERENCES

- [1] Alavi, M., & Tiwana, A. (2002). Knowledge integration in virtual teams: The potential role of KMS. *Journal of the Association for Information Science and Technology*, 53(12), 1029-1037.
- [2] Cummings, T. G., & Worley, C. G. (2007). *Desarrollo organizacional y cambio* (No. Sirsi) i9789706866349).
- [3] Rico, R., Alcover de la Hera, C. M., & Taberner, C. (2010). Efectividad de los equipos de trabajo: Una revisión de la última década de investigación (1999-2009). *Revista de Psicología del Trabajo y de las Organizaciones*, 26(1), 47-71.
- [4] Palamary, R. E. (2012). "Formación de equipos de alto desempeño y estrategias gerenciales en proyectos de empresas publicitarias", *Estudios Gerenciales*, vol. 28, núm. 22, enero-marzo, pp. 69-81.
- [5] Martínez Martínez, A., García Gamica, A., & Santos Navarro, G. (2014). Nuevas formas de organización laboral en la industria automotriz: los equipos de trabajo en General Motors, Complejo Silao. *Análisis Económico*, 29(70).
- [6] Rubio M.A., Gutiérrez S. B., Montoya M. J., (2010). Los equipos autodirigidos como ventaja competitiva. *Leadership*. 7 (24) 22-23.
- [7] Johnson, M. D., Hollenbeck, J. R., DeRue, D. S., Barnes, C. M., & Jandt, D. (2013). Functional versus dysfunctional team change: Problem diagnosis and structural feedback for self-managed teams. *Organizational Behavior and Human Decision Processes*, 122(1), 1-11.
- [8] Wang, J., & Hicks, D. (2015). Scientific teams: Self-assembly, fluidness, and interdependence. *Journal of Informetrics*, 9(1), 197-207.
- [9] Robbins, S. (2013). *Comportamiento organizacional* (10ª ed.). México: Pearson.
- [10] Millikin, J. P., Hom, P. W., & Manz, C. C. (2010). Self-management competencies in self-managing teams: Their impact on multi-team system productivity. *The leadership quarterly*, 21(5), 687-702.
- [11] Lambe, C. J., Webb, K. L., & Ishida, C. (2009). Self-managing selling teams and team performance: The complementary roles of empowerment and control. *Industrial Marketing Management*, 38(1), 5-16.
- [12] Blanchard, K. (2007). *Liderazgo al más alto nivel: cómo crear y dirigir organizaciones de alto desempeño*. Bogotá: Grupo Editorial Norma.
- [13] Holpp, L. (2004). *Dirija el mejor equipo de trabajo*. Madrid: McGraw-Hill, Interamericana de España.
- [14] Roy, M. (2003). Self-directed workteams and safety: a winning combination?. *Safety Science*, 41(4), 359-376.
- [15] Andrés, M., R.; Broncano, S., G.; Monsalve, J. N. (2014). Los equipos autodirigidos como ventaja competitiva: Estudio de un liderazgo efectivo. *Leadership: Magazine for Managers*. dic2010, Vol. 7 Issue 24.
- [16] García, J. M., Jiménez, G. A., & Ramírez, J. A. M. Implementación de un equipo de alto desempeño en una línea de producción para Mars México en el estado de Querétaro y su impacto en los indicadores de eficiencia y 5 S. *Competitividad y gestión del conocimiento en organizaciones con proyección internacional*, 237.
- [17] Schwab Klaus, (2017). *The Global Competitiveness Report 2017-2018* World Economic Forum. Geneva.
- [18] Hernández, J. (2011). *Desarrollo organizacional, enfoque latinoamericano*. México: Pearson.
- [19] Trejo, D. (2009). Identificación, análisis y aprovechamiento de la administración del conocimiento para la empresa y organización mexicana del siglo XXI. México: Editor Daniel Trejo Medina.
- [20] Child, J. (1981), "Culture, contingency, and capitalism in the cross national study of organizations", in Cummings, L. and Staw, B. (Eds), *Research in Organizational Behavior*, Vol. 3, pp. 303-56.
- [21] Barrett, G. and Bass, B. (1976), "Crosscultural issues in industrial and organizational psychology", in Dunnette, M. (Ed.), *Handbook of Industrial and Organizational Psychology*, Rand McNally, Chicago, IL.
- [22] Hofstede, (2018). Compare countries. Retrieved from <https://www.hofstede-insights.com/product/compare-countries/>

- [23] Chambers, D. and Hamer, S. (2012), "Culture and growth: some empirical evidence", *Bulletin of Economic Research*, Vol. 64 No. 4, pp. 549-564.
- [24] Clifford J. Drew, Michael L. Hardman, John L. Hosp. (2008). *Designing and Conducting Research in Education*. California, Estados Unidos. Sage
- [25] Hartas, D. (Ed.). (2015). *Educational research and inquiry: Qualitative and quantitative approaches*. Bloomsbury Publishing.
- [26] Yockey Ronald D. (2016). *SPSS DEMYSTIFIED A Step-by-Step Guide to Successful Data Analysis*. USA. Routledge.
- [27] Stowell, S. (2014). *Using R for statistics*. Apress.

# Effectiveness of Guided Inquiry Model Student Worksheet to Improve Critical thinking Skill on Heat Material

Heri Nurdin<sup>1</sup>, Tri Jalmo<sup>2</sup>, Chandra Ertikanto<sup>2</sup>

<sup>1</sup>Master Degree Program Student of Physics Education

<sup>2</sup>Master Degree Program Lecturer of Physics Education, Faculty of Teacher Training and Education, University of Lampung

[herigisting@yahoo.co.id](mailto:herigisting@yahoo.co.id)

**Abstract**—This research aims to describe the effectiveness of guided inquiry model student worksheet to improve critical thinking skill on heat material in terms of learning outcomes. The research used Control Group Pretest-Posttest Quasi-Experimental Design. The subjects of this research were VII grade of U1 and U2 students of Junior High School 1 with a total of 60 students. The research subjects were determined by using purposive sampling technique. Data collection was conducted by performing test. The results of data analysis with Independent Samples t-Test showed sig. value of 0,022. Because sig. value  $\leq 0,05$ ,  $H_0$  was rejected or  $H_1$  was accepted. Product effectiveness level based on the mean of normalized gain from pretest and posttest value of experimental and control groups demonstrated that N-gain of experimental group was 0,48 and N-gain of control group was 0,38. Therefore, it can be stated that the improvement of students' critical thinking skill of experimental group or group which used development product student worksheet was higher than the improvement of students' critical thinking skill of control group which used conventional student worksheet. It can be concluded that the learning which uses guided inquiry model student worksheet is more effective in improving critical thinking skill than the learning which uses conventional student worksheet.

**Keywords**— student worksheet, guided inquiry, critical thinking skill.

## I. INTRODUCTION

The quality of education in Indonesia, especially Natural Science (science), is still low. Based on PISA data, Indonesia, in terms of science literacy, always scores far below the international average score. Indonesia can only occupy the top 10 lowest rank of the participating countries (PISA, 2012). The low quality of science education in Indonesia is a manifestation of the application of teaching patterns which are less suited to the demands and the needs of students. The partially applied learning process still uses lecture method that causes students to

play a passive role and tend to be the only recipients of science products. The learning process needs to be changed, which is initially teacher-centered, to learning which involves students and challenges them using scientific methods in problem-solving so that it can increase the participation and generate curiosity in learning, improve understanding and mindset as well as help students to develop critical thinking skill. According to Wardani, et al. (2013), students do not only listen to lectures from teachers about a material, but students can also experience the process to get the concept, so that students' understanding of a concept or principle will be greater.

The efforts of government to improve the quality of education are conducted by improving the curriculum, from the Education Unit Level Curriculum (KTSP) 2006 to the 2013 Curriculum. The 2013 curriculum obliges to provide the essence of the scientific approach in learning of science. The scientific approach is an approach that will shape individuals to have critical and characterized attitudes. In order to build the critical and characterized attitudes in students, an appropriate learning model such as scientific discovery learning model, problem-based learning model, and other learning model that build critical and characterized attitudes of the students are needed (Rizqi, et al., 2013; Afidah, et al. 2013).

This scientific approach can be integrated in one of the learning tool components in the form of Student Worksheet (LKS). Student Worksheet, according to Wijayanti, et al. (2015), is a printed material in the form of sheets of paper containing materials, summaries, and instructions on the learning task implementation that must be done by the students, which refers to the basic competencies that must be achieved.

One of the purposes of the use of Student Worksheet in science learning is to provide opportunity for students to actively involve themselves in finding a concept through observation and experimental activities, so that the

learning becomes more meaningful. In developing the teaching materials (Student Worksheet) a proper model is also needed. Learning model which is considered quite effective in science learning is inquiry model (BSNP, 2006).

Inquiry is derived from the word "inquire" which means "seeking" or "questioning". Learning by using inquiry approach, according to Wenning (2011): When taught using the levels of inquiry approach, students have the opportunity to make observation, formulate prediction, collect and analyze, develop scientific principle, synthesize laws, and make and test hypotheses to generate explanation. Guided inquiry learning is more constructive, it gives students the opportunity to ask questions and share learning experiences, as well as to improve students' knowledge and develop critical thinking skill. Guided inquiry learning can make students to think critically. The ability to think critically can tackle the cognitive, affective and psychomotor aspects. It is in accordance with Azwar's research (2015), that students' critical thinking can influence learning outcomes. Critical thinking stimulates each student's cognitive structure to capture ideas, concepts and to organize the knowledge they owned to improve the development of students' proficiency and readiness.

Inquiry is applied in order to make students participate more actively in learning and to find knowledge in their own way. Knowledge that is found by constructing the knowledge itself through real experience will be more meaningful than the knowledge which is remembered or memorized (Sanjaya, 2012). Learning by using inquiry model that is suitably applied to junior high school students is guided inquiry model. The use of guided inquiry is chosen because students have not been accustomed to learn to use inquiry model beforehand.

According to Sagala (2013), thinking is the process of describing the characteristics of an object, placing two relationships between two verbally formulated definitions, and drawing conclusion as the work of reason in the form of a new opinion based on the existing opinion. The ability to think is the basic in a learning process (Heong, et al., 2011). In addition, according to Rustaman (2005), thinking habituation needs to be instilled at the early age through science learning. Critical thinking skill is needed in the current science and technology (IPTEK) development era because the result of Science and Technology (IPTEK) development not only can be enjoyed, but also can generate some impacts that create problems for human life and the environment. The problem is complex enough that it needs high-level thinking skill to solve the problem.

Critical thinking is thinking based on reasons and thinking reflectively by emphasizing decision-making on what should believe or do, Ennis (in Costa ed., 1985). The ability of critical thinking has an important role because it is a provision of life success that prepares students to be clever to explain the reasons, able to make good information assessment and able to solve problems that have not been known (Cheong and Cheung, 2008). Critical thinking skill is included in one of the 21st-century learning and innovation skills that enable students to effectively address social, scientific and practical issues in the future (Snyder and Snyder, 2008).

Students who are accustomed to conduct critical thinking training know more about how to think in a purposeful, planned and logical way according to the facts that have been known so that it can result in the acquisition of more optimal learning outcomes (Haseli & Rezaei, 2013). Indicators of critical thinking skill are divided into 5 groups (Ennis in Costa ed., 1985) namely: 1) Providing a simple explanation (*elementary clarification*), 2) Building basic skills (*basic support*), 3) Making inferences (inferring), 4) Generating further explanation (*Advanced clarification*), and 5) Setting strategies and tactics (*strategy and tactics*).

This research aims to describe the effectiveness of guided inquiry model student worksheet to improve critical thinking skill on heat material in terms of learning outcomes.

## II. RESEARCH METHOD

This research was *quasi-experimental* research. The design used in this research was *Pretest-Posttest Control Group Design*. The subjects of the study were VII grade of U1 and U2 students of SMPN 1 Gisting with a total of 60 students. Research subject was determined by using purposive sampling technique. Research data were collected through critical thinking skill tests. The data analysis of test result was used to measure the effectiveness level of the usage trial (*Pretest-posttest Control Group Design*) with *Independent Sample t-Test*. Prior to data analysis, normality test were performed using *Kolmogorov-smirnov* and homogeneity test with *Levene's* test.

## III. RESULTS AND DISCUSSION

### The Results of the Research

The implementation of guided inquiry model student worksheet to improve critical thinking skill was performed during three meetings for the subject of heat, two meetings for the learning and one meeting for the test. There were five stages of learning approach with inquiry model as stated by Wena (2009), namely: (1) problem

presentation; (2) Collection of verification data; (3) Collection of experiment data; (4) organization of data and formulation of conclusions; and (5) analysis of inquiry processes.

The level of the concept mastery of students was measured by using the concept mastery instrument in the form of *essay* test as many as 10 items concerning on heat material. The test instruments used to measure the critical thinking skill were based on indicators of critical thinking skill and, according to Ennis (in Costa ed., 1985), they were outlined from the four dimensions of critical thinking skill namely providing simple explanation (*elementary clarification*), building basic skills (*basic support*), inferring (*inference*), and generating further explanation (*advanced clarification*).

The result of descriptive statistics test of *posttest* value data in experimental and control groups can be seen in Table 1.

Table.1: Descriptive Statistics of Posttest Result Value Data

		Posttest Experimental Group	Posttest Control Group
<i>N</i>	<i>Valid</i>	30	30
	<i>Mising</i>	0	0
<i>Mean</i>		70,83	67,18
<i>Std. Deviation</i>		6,86	5,01
<i>Minimum</i>		58	55
<i>Maximum</i>		90	75

Table 1 demonstrates that the *posttest* mean value of experimental group is 70,83 and the *posttest* mean value of control group is 67,18. This results shows that the *posttest* mean value of experimental group is higher than the *posttest* mean value of control group.

The result of *posttest* data normality and homogeneity tests of experimental and control groups are presented in Table 2 and Table 3.

Table.2: The Result of Posttest Data Normality Test

Group	Sig. (2-tailed)	Conclusion
Experimental	0,200	Sig. $\geq 0,05$ = Normal

Control	0,200	Sig. $\geq 0,05$ = Normal
---------	-------	---------------------------

Table 2 depicts that the significance value of experimental group and control group is the same, which is 0,200. It means that sig. (significance) value or probability value of both groups  $\geq 0,05$ , so that  $H_0$  is accepted, which means that the research data are derived from normally distributed data.

Table.3: The Result of Posttest Data Homogeneity Test

Levene	df1	df2	Sig
1,826	1	58	,182

Table 3 demonstrates that the significance value of *posttest* data homogeneity test of experimental and control groups is 0,182. Because sig. (significance) value or probability value  $\geq 0,05$ , so  $H_0$  is accepted, which means that both groups have the same or homogeneous variance.

The qualification result of students' critical thinking skill of experimental and control groups based on the mean score of *posttest* value can be seen in the Table 4.

Table.4: The Qualification of Critical Thinking Skill

Group	Mean Score	Category
Experimental	65,5	Critical
Control	60,68	Less Critical

Source: Dwijananti (2000)

Table 4 demonstrates that after conducting a learning using guided inquiry model student worksheet, the result of experimental group development obtains a mean score of 65,5 with 'critical' category, while in the control group, after conducting a learning using conventional student worksheet, a mean score of 60,68 with critical thinking skill category of 'less critical' is obtained.

The result of difference test of two means between experimental group and control group using t-test (*Independent Samples t-Test*) can be seen in Table 5.

Table.5: The Difference of Posttest Data Mean

		Paired Differences							
		Mean	Std. Deviation	Std. Error Mean	95% Confidence Interval of the Difference		T	df	Sig.(2-tailed)
					Lower	Upper			
Pair									
1	Experimental Group	70,83	6,865	1,253	0,545	6,755	2,4	58	0,022
	Control Group	67,18	5,008	0,914					

Table 5 shows that the sig value. (2-tailed) <0,05, so that it rejects  $H_0$  and accepts  $H_1$ . This result indicates that there is a significant difference between the mean value of critical thinking skill of experimental group students and the mean value of critical thinking skill of the control group students. The level of product effectiveness based on the mean of normalized gain of the pretest and posttest values of the experimental and control group is obtained as it is in Table 6.

Table.6: N-gain Value of Experimental Group

Group	< g > (N-gain)	Classification	Effectiveness Level
Experimental	0,48	Moderate	Quite Effective
Control	0,38	Moderate	Quite Effective

Source: Hake (2000)

Table 6 shows that the N-gain value of experimental group is 0,48 and the N-gain value of control group is 0,38. N-gain value of experimental group is higher than the N-gain value of control group.

The increase of N-gain in each dimension of critical thinking skill for each student group is presented in Figure 1.

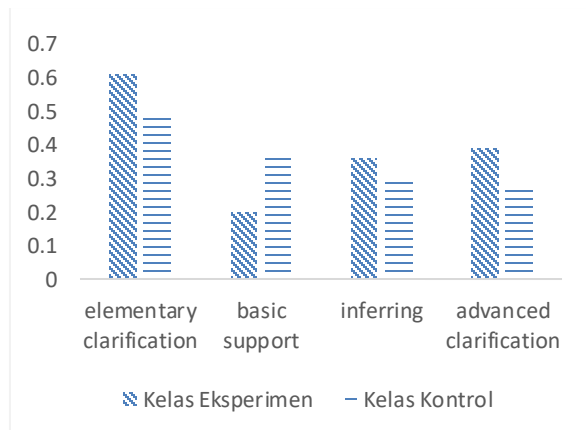


Fig.1: The Increase of N-gain in Each Dimension of Students' Critical Thinking Skill

Figure 1 above indicates that the highest N-gain value of critical thinking skill is in the dimension of elementary clarification (providing simple explanation) either in experimental group or in control group. While, the lowest N-gain of experimental group is in the dimension of basic support (building basic skills).

#### IV. DISCUSSION

Hypothesis testing in this research was conducted by using SPSS 21 program.

The results of descriptive statistical test of pretest-posttest value data in the experimental and control groups were obtained that; the mean pretest value of experimental group was 33,17 and the mean of pretest value of control group was 35,07 while the mean of value of experimental group was 70,83 and the mean of posttest value of control group was 67,18. These results indicated that the mean value of experimental group posttest has increased. The mean value of the experimental group posttest was bigger than the mean value of the control group posttest.

The implementation of guided inquiry model student worksheet resulted in the improvement of student learning outcomes. The student learning outcomes of experimental group which used guided inquiry model student worksheet was greater than the student learning outcomes of control group which used conventional student worksheet. This result also means that students' critical thinking skill in the experimental group were better than the students' critical thinking skill in the control group. The implementation of guided inquiry model student worksheet in the experimental group could improve students' critical thinking ability. This was in accordance with the research conducted by Sohibin's (2009) that the guided inquiry model can improve students' understanding of concepts and develop students' critical thinking skill. The research of Tindangen (2007); Azizmalayeri (2012); Fuad, et al. (2017) proved that

inquiry learning contributes in improving critical thinking skill.

The student learning outcomes in the experimental group were improved due to the learning which used guided inquiry model student worksheet which allows students to be actively involved both physically and mentally in the learning process. Students gained the experience directly, students were more interested in learning, and student learning motivation increased. These things were supported by previous research conducted by Winarni (2009) who stated, "Through inquiry, teachers invite students to be more active both physically and mentally in the learning process". Rachman et al (2012) stated, "The application of guided inquiry model can improve student learning activities". Laubach et al (2010) said, "With inquiry learning, students can be more interested in the learning that is taught because students get the experience directly". Patrick et al. (2009) said that guided inquiry can improve students' motivation in the learning of science.

The results of *Posttest* data normality and homogeneity test of experimental and control group in Table 2 and Table 3 showed that *posttest* data of both groups were derived from the same or homogeneous and normally distributed variance. Based on this reason, t-test (*Independent Samples t-Test*) was conducted. Prior to analysis of product effectiveness level using t-test (*Independent Sample t-Test*), *pretest* and *posttest* result data on critical thinking skill assessment were analyzed. The analysis was performed to find out the value of students' critical thinking ability. Having obtained the value of critical thinking skill, the category of critical thinking skill of each student was determined. Category giving aimed to know the qualification of critical thinking ability. The result of the students' critical thinking skill qualification in Table 4 showed that experimental group which used guided inquiry model student worksheet obtained the mean score of the *posttest* value of 65.5 with 'critical' category, while the control group which used the conventional student worksheet obtained the mean score of the *posttest* value of 60,68 with 'less critical' critical thinking skill category.

The result of t-test (*Independent Sample t-Test*) in Table 5 showed that the sig. value obtained was 0.022. Because the sig. value  $\leq 0.05$  then  $H_0$  was rejected or  $H_1$  was accepted, so it could be stated that the learning using guided inquiry model student worksheet improved critical thinking skill more effectively than the learning using conventional student worksheet. Guided inquiry model student worksheet packaged in the student worksheet improved critical thinking skill more effectively. This was in accordance with the research conducted by Damayanti, et al. (2012) and Sudarmini, et al. (2015).

The product effectiveness level based on the mean of the normalized *N-gain* from *pretest* and *posttest* value of the experimental group and control group obtained the result of the experimental group *N-gain* value of 0.48 with classification of 'moderate' and effectiveness level of 'quite effective', while the control group *N-gain* value was 0.38 with classification of 'moderate' and effectiveness level of 'quite effective'. Based on the calculation of *N-gain* value, it was known that the *N-gain* value of experimental group was bigger than the *N-gain* value of the control group. Therefore, it can be stated that the improvement of students' critical thinking skill of experimental group or group which used guided inquiry model student worksheet was higher than the improvement of students' critical thinking skills of the control group.

Based on the comparison of *N-gain* increase in each critical thinking skill dimension for each group of students, the development result of *elementary clarification* critical thinking skill of experimental group which used guided inquiry model student worksheet was higher than the development result of control group which used conventional student worksheet. The mean of *posttest* value from *pretest* value of experimental group on the critical thinking skill dimension of *elementary clarification* increased because the learning which used guided inquiry model student worksheet allowed students to understand and observe problems from various aspects, to train students to learn in finding problems then make problem formulation based on the facts found. The critical thinking ability of the students was trained and developed by always asking and questioning the various phenomena being studied. It can be attributed to Gengarely's (2009) research which stated that inquiry could teach students how to ask questions in the classroom and to get their own answers. Inquiry could encourage students' scientific thinking habits and students were more open to new ideas in groups or classes, with the hope that students think about the process, not just the final result. An example of problem formulation by student is shown in Figure 2.

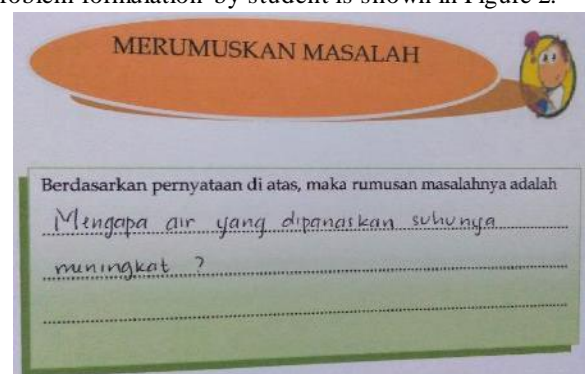


Fig.2: An Example of Problem Formulation

The problem formulation written by the student is correct. The formula is in accordance with the purpose of the experiment, namely the influence of heat towards the rise in temperature. The orientation stage (guiding the students) of learning steps in using guided inquiry model student worksheet model inquiry has trained students to think critically.

The learning by using guided inquiry model student worksheet also allowed the students to use the knowledge they have in the form of temporary answers or hypotheses before conducting experiments. Students' critical thinking skill could be trained and developed through the stage of formulating the problem. This was in accordance with Bilgin's (2009) research that guided inquiry learning model could train students to build answers and think smartly in finding alternative solutions to problems given by teachers, develop understanding skills, and train the delivery process of the concepts found. An example of a temporary answer by a student is shown in Figure 3.

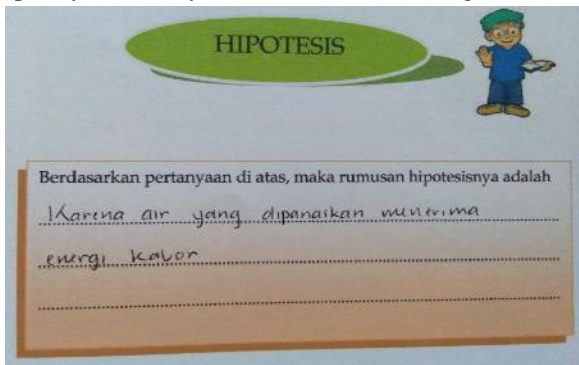


Fig.3: An Example of Hypothesis Formulation

The temporary answer towards the hypothesis formulation put forward by the student is also appropriate. The temperature of an object when heated increased due to the receiving / absorbing energy of heat. Formulating problem stage of learning step in using guided inquiry model student worksheet has trained the students to think critically in using the knowledge they have in the form of temporary answer or hypothesis.

Based on the comparison in *N-gain* increase in each dimension of critical thinking skill for each group of students, the critical thinking skill dimension of *basic support* of experimental group was still lower than control group has (Figure 2), this was possible because students were less accustomed to being trained to think critically in solving problem. Snyder & Snyder (2008) revealed that like any other skills, critical thinking requires training, practice and patience.

The low result of *basic support* dimension strengthens that, in the learning which uses guided inquiry model, the teacher does not just let go of the activities undertaken by the students. Teachers still provide guidance and direction

in the learning activities so that students who think slowly still able to follow the activities that are being held and the students who have the ability to think fast do not monopolize the activities.

The next step of learning is the collection of verification data. In this step, the students collect the data or information through literature review. An example of collection of verification data by a student is shown in Figure 4.

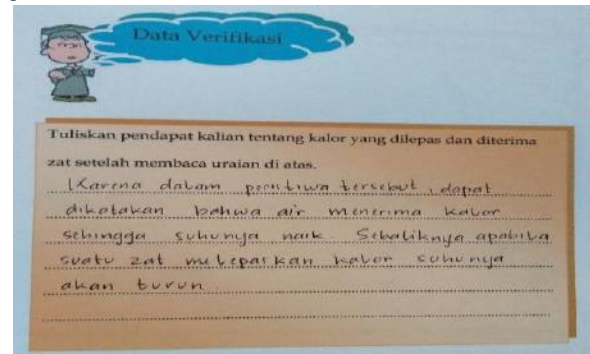
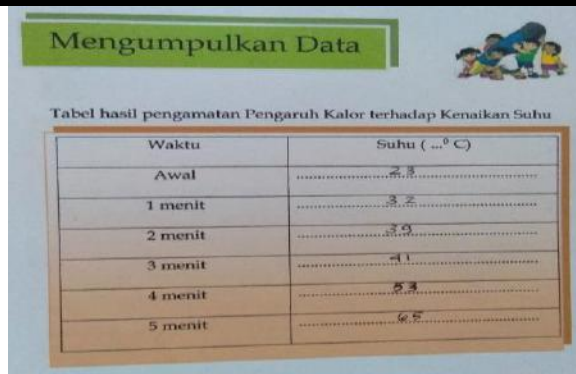


Fig.4: An Example of Verification

#### Data Collection

Verification data which have been collected by the student is exactly in accordance with the concept, the water receives / absorbs the heat so that the temperature rises. The verification data trains students to think critically and to sort and choose the correct concept according to the objectives which will be achieved through experiment.

The next step is experimental data collection. Students perform experiments in accordance with the existing procedures, followed by recording the data of experimental results. Experimental activities can help students to understand the material more easily and to gain real experience by taking an active role in learning activities and it can train them to practice investigative skills. This is in accordance with Hackling's (2005) statement that the practice of observation or conducting experiment gives students the opportunity to practice and develop investigative skills as well as to gain real-life experience about natural phenomena as the basis of conceptual learning. Experimental activities can also help students to solve problems and to find their own knowledge. This is in line with Ketpichainarong, Panijpan & Ruenwongsa (2010) research that students collect data through experimental activities to solve problems so that students are able to build and discover their own concepts of knowledge. An example of data collection by a student is shown in Figure 5.



Tabel hasil pengamatan Pengaruh Kalor terhadap Kenaikan Suhu

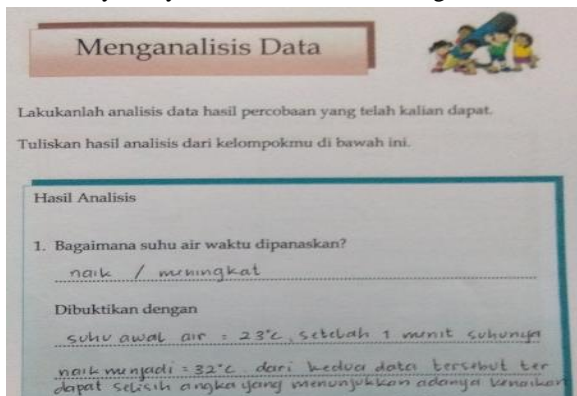
Waktu	Suhu ( $^{\circ}\text{C}$ )
Awal	23
1 menit	32
2 menit	39
3 menit	41
4 menit	53
5 menit	65

Fig.5: An Example of Experimental

### Data Collection

The resulting data of the experiment collected by the student is correct. The longer the heating time, the higher the temperature rise of the object. The high temperature of the object indicates that the amount of heat received by the object increases.

Based on the experimental data, the students performed data analysis. There is a possibility that the resulting data of experiment and the theory is different, so students need to analyze it. Data analysis begins by examining data and ideas, as well as identifying opinions and supporting reasons. Data analysis activity can be performed by building and using ideas that students owned. This is in accordance with the statement of Callahan, et. Al. (1992: 293-294) that data analysis activity can be done by building and using ideas owned by students. An example of data analysis by a student is shown in figure 6.



Lakukanlah analisis data hasil percobaan yang telah kalian dapat.  
Tuliskan hasil analisis dari kelompokmu di bawah ini.

Hasil Analisis

1. Bagaimana suhu air waktu dipanaskan?  
naik / meningkat

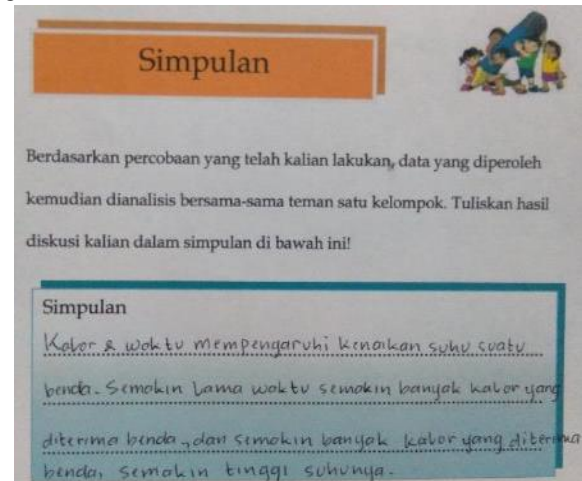
Dibuktikan dengan  
suhu awal air =  $23^{\circ}\text{C}$  setelah 1 menit suhunya  
naik menjadi  $32^{\circ}\text{C}$  dari kedua data tersebut ter  
dapat selisih angka yang menunjukkan adanya kenaikan

Fig.6: An Example of Analyzing Experimental Data

The analysis of experimental data conducted by the student is correct, water temperature rises when heated, the amount of heat received by the object increases. Data collection and analysis stage of the learning step in using guided inquiry model student worksheet has trained the students to think critically and to summarize a number of raw data into information that can be interpreted.

The next learning step is data organization and conclusion formulation. In this step, the teacher guides students to arrange or interpret the experimental results.

Teachers also guide students to make a conclusion. An example of conclusions drawn by a student is shown in Figure 7.



Berdasarkan percobaan yang telah kalian lakukan, data yang diperoleh kemudian dianalisis bersama-sama teman satu kelompok. Tuliskan hasil diskusi kalian dalam simpulan di bawah ini!

Simpulan  
Kalor & waktu mempengaruhi kenaikan suhu suatu benda. Semakin lama waktu semakin banyak kalor yang diterima benda, dan semakin banyak kalor yang diterima benda, semakin tinggi suhunya.

Fig.7: An Example of Conclusion

The conclusion written by the student based on interpretation towards the results of the research is correct. Heat affects the rise in the temperature of the object, the more heat it receives, the higher the temperature of the object. The implementation of guided inquiry model student worksheet in the experimental class can increase the critical thinking skill dimension of *inference*.

Based on the comparison in *N-gain* increase for each group of students, the development result of average increase in *inference* critical thinking skill of experimental group which uses guided inquiry model is higher than the development result of control group which uses conventional student worksheet. The mean of *posttest* value from *pretest* value of experimental group on the critical thinking skill dimension of *inference* increases because the learning which uses guided inquiry model student worksheet allows students to describe the findings obtained based on hypothesis testing. To reach an accurate conclusion, students should be able to demonstrate relevant data.

Based on the comparison of the increase of *N-gain* in each critical thinking skill dimension for each group of students, the comparison of *pretest* and *posttest* results of critical thinking skills of the experimental and control groups in the *advanced clarification* critical thinking skill dimension (generating further explanation) and the critical thinking sub defined the terms, considered the definition of classification and range. There was an increase in the mean of *posttest* value from *pretest* value in *advanced clarification* critical thinking skill dimension of 2.85 in experimental group and of 1.95 in control group. The development result of the increase in mean value of *advanced clarification* critical thinking skill of experimental class which used guided inquiry model

student worksheet was higher than the development result of the control group which used conventional student worksheet. The mean of *posttest* value from *pretest* value of experimental group on *advanced clarification* critical thinking skill dimension increased because the learning which used guided inquiry model student worksheet allowed the students to be actively involved in finding their own concept through observation or experiment so that learning activities became more meaningful.

The average increase of *posttest* value from *pretest* value in all dimensions of critical thinking skill in the experimental group showed that the learning using guided inquiry model can improve students' academic proficiency. This is supported by the research conducted by Sari & Sutiadi (2008) that the observed academic abilities were improved after applying guided inquiry learning model. Jannah *et al* (2012) stated that the implementation of guided inquiry could improve the quality of students' conceptual understanding and was able to embed the characters in the students. Wirtha (2008); Suma (2010); Handhika (2010) said that guided inquiry learning could develop the mastery of physics concept.

The average increase of *posttest* value from *pretest* value in all dimensions of critical thinking skill in the experimental group also showed that the learning using guided inquiry model student worksheet improved students' critical thinking skill. This was supported by Hasruddin' (2009) research which stated that the application of inquiry learning can empower students' thinking skill so that it could maximize the critical thinking skill. Prabowo *et al* (2015) stated that the critical thinking skill of students who were taught with inquiry learning model has increased.

## V. CONCLUSION AND SUGGESTION

### Conclusion

Based on the results of research and discussion, it can be concluded that learning by using guided inquiry model student worksheet packaged in student worksheet is quite effective to improve critical thinking skill. The results of *N-gain* calculation showed that the *N-gain* value of group which used development product student worksheet was higher than the value of the group which used conventional student worksheet. *N-gain* value of experimental group was 0.48 and *N-gain* value of control group was 0.38. The implementation of guided inquiry model student worksheet in the experimental group can improve students' critical thinking skill.

### Suggestion

Suggestions from this development research are: (1). Teachers and students should be able to use guided inquiry model student worksheet as a means to improve critical thinking skill. (2). This new development research is conducted on a small scale, hence, further research on large-scale groups should be carried out to determine the feasibility of this product to be applied to large-scale groups.

## REFERENCES

- [1] Afidah, A.R.R., Erman, B., & Budiyanto, M. 2013. Penerapan Model Pembelajaran Berdasarkan Masalah pada Pembelajaran IPA Terpadu Tema Korosi Besi untuk Siswa Kelas VII SMP Negeri 1 Bungah Gresik. *Jurnal Pendidikan Sains*, 1 (1): 66-70.
- [2] Amilasari, A. & Sutiadi, A. 2008. Peningkatan Kecakapan Akademik Siswa SMA Dalam Pembelajaran Fisika Melalui Penerapan Model Pembelajaran Inkuiri Terbimbing. *Jurnal Pengajaran MIPA, FPMIPA UPI*, 12 (2): 1-8.
- [3] Azizmalayeri, K., MirshahJafari, E., Sharif, M., Asgari, M., & Omid, M. (2012). The Impact of Guided Inquiry Methods of Teaching on The Critical Thinking of High School Student. *Journal of Education and Practice*, 3 (10): 1-7.
- [4] Azwar, M. 2015. Pengaruh Pembelajaran Inkuiri Terbimbing dan Inkuiri Bebas Termodifikasi Terhadap Prestasi Belajar Ditinjau dari Berpikir Kritis dan Kedisiplinan Belajar Siswa Kelas X MIA SMA Negeri 8 Surakarta Tahun Pelajaran 2014/2015. *Jurnal Inkuiri*, 4 (3): 127-135.
- [5] Badan Standar Nasional Pendidikan. 2006. *Panduan Penyusunan Kurikulum Tingkat Satuan Pendidikan Jenjang Pendidikan Dasar dan Menengah*. Jakarta: Depdiknas.
- [6] Bilgin, I. 2009. The Effect of Guided Inquiry Instruction Incorporation a Cooperative Learning Approach an University Student, Achievement Acid and Based Concepts and Attitude Toward Guided Inquiry Instruction. *Academics Journal Scientific Research and Essay*, 4 (10): 1038-1046.
- [7] Callahan, J.F., Clark, L.H., & Kellough, R.D. (2002). *Teaching in The Middle And Secondary Schools*. New York: Macmillan Publishing Company.
- [8] Cheong, C.M., & Cheung, W.S. 2008. Online Discussion and Critical Thinking Skill: A Casestudy in a Singapore Secondary School. *Australasian Journal of Educational Technology*, 24 (5): 556-573.
- [9] Costa, A.L. 1985. The Prinscipal's Role in Enhancing Thinking Skill. Dalam Costa A.L. (ed). *Developing*

- Mind: A Resource Book for Teaching thinking.* Alexandria: ASCD.
- [10] Damayanti, D.S., Ngzizah, N. & K.E., Setyadi. 2012. Pengembangan Lembar Kerja Siswa (LKS) dengan Pendekatan Inkuiri Terbimbing untuk Mengoptimalkan Kemampuan Berpikir Kritis Peserta Didik pada Materi listrik Dinamis SMA Negeri 3 Purworejo Kelas X ahun Pelajaran 2012/2013. *Jurnal Radiasi*, 3. (1): 58-62.
- [11] Dwijananti, P., & Yulianti, D. 2010. Pengembangan kemampuan berpikir Kritis mahasiswa melalui pembelajaran problem based instruction pada mata kuliah fisika lingkungan. *Jurnal Pendidikan Fisika Indonesia (Indonesian Journal of Physics Education)*, 6 (2): 108-114.
- [12] Fuad, N.M., Zubaidah, S., Mahanal, S., & Suarsini, E. (2017). Improving Junior High Schools Critical Thinking Skills Based on Test Three Different Models of Learning. *International Journal of Instruction*, 10 (1): 101-116.
- [13] Gengarely, L.M. & Abrams, E.D. (2009). Closing the Gap: Inquiry in Research and the Secondary Science Classroom. *Journal of Science Education and Technology*. 18 (1): 74-84.
- [14] Hackling, M.W. (2005). *Working Scientifically: Implementing and Assessing Open Investigation Work in Science*. Western Australia: Departement of Education and Training.
- [15] Hake, R.R. 2000. Interactive-engagement vs traditional methods: A six thousand student survey of mechanics test data for introductory physics courses. *American Journal of Physics*, 66, p. 64-74.
- [16] Handhika, J. 2010. Pembelajaran Fisika Melalui Inkuiri Terbimbing dengan Metode Eksperimen dan Demonstrasi ditinjau dari Aktivitas dan Perhatian Mahasiswa, *JP2F*, 1 (1): 9-23.
- [17] Haseli, Z., & Rezaii, F. 2013. The Effect of Teaching Critical Thinking on Educational Achievement and Test Anxiety among Junior High School Student in Saveh. *European Online Journal of Natural and Social Sciences*, 2(2): 168-175.
- [18] Hasruddin. 2009. Memaksimalkan Kemampuan Berpikir Kritis Melalui Pendekatan Kontsktual. *Jurnal Tabularasa PPS UNIMED*. 6(1): 48-60. Diperoleh 12 April 2018, dari: <http://digilib.unimed.ac.id/public/UNIMED-Article-24572-Hasruddin.pdf>.
- [19] Heong, Y.M., Yunos, J.M., Hassan, R.B., Othman, W.B., Kiong, T.T. 2011. The Perception of The Level Of Higher Order Thinking Skills among Technical Education Student. *International Conference on Social Science and Humanity Journal*. Faculty of Technical Education, Universiti Tun Hussein Onn Malaysia, 5 (2): 281-285.
- [20] Jannah, M., Sugianto & Sarwi. 2012. Pengembangan Perangkat Pembelajaran Berorientasi Nilai Karakter Melalui Inkuiri Terbimbing Materi Cahaya Pada Siswa Kelas VIII Sekolah Menengah Pertama. *Journal of Innovative Science Education*, 1 (1): 54-60.
- [21] Ketpichainarong, W., Panijpan, B., & Ruenwongsa, P. 2010. Enhanced Learning of Biotechnology Student by An Inquiry-based Cellulase Laboratory. *International Journal of Environmental & Science Education*, 5(2): 169-187.
- [22] Laubach, T.A., Elizondo, L.A., McCann, P.J., & Gilani, S. 2010. Quantum Dotting the “i” of Inquiry: A Guided Inquiry Approach to Teaching Nanotechnology. *The Physics Teacher Journal*. University of Oklahoma, Norman, OK, 48: 186-188.
- [23] Patrick, H., Mantzicopoulos, P. & Samarapungavan, A. 2009. Motivation for Learning Science in Kindergarten: Is There a Gender Gap and Does Integrated Inquiry and Literacy Instruction Make a Difference. *Journal Of Research In Science Teaching*, 46 (2): 166-191.
- [24] PISA, 2012. *Organisation for Economic Cooperation and Development (OECD)*. [Online]. Tersedia: [oecd.org/statistic/statlink](http://oecd.org/statistic/statlink). [12 Desember 2014].
- [25] Prabowo, L.S.B. & Sunarti, T. 2015. Penerapan Model Pembelajaran Inkuiri pada Materi Alat Optik untuk Meningkatkan Keterampilan Berpikir Kritis Siswa Kelas VIII SMP Cendekia Sidoarjo. *Jurnal Inovasi Pendidikan Fisika*, 4 (1): 6-11.
- [26] Rachman, N.D., Sudarti, & Supriadi, B. 2012. Penerapan Model Inkuiri Terbimbing (Guided Inquiry Approach) Pada Pembelajaran Fisika Siswa Kelas VII-B SMP Negeri 3 Rogojampi Tahun Ajaran 2012/2013. *Jurnal Pembelajaran Fisika*, 1(3): 143-151
- [27] Rizqi, A., Parmin, P., & Nurhayati, S. 2013. Pengembangan Modul Ipa Terpadu Berkarakter Tema Pemanasan Global untuk Siswa SMP/MTs. *Unnes Science Education Journal*, 2 (1): 203-208.
- [28] Rustaman, N.Y. 2005. Perkembangan Penelitian Berbasis Inkuiri Dalam Pendidikan Sains. *Makalah disampaikan dalam seminar Nasional II Himpunan Ikatan Pascasarjana dan Pemerhati Pendidikan IPA*. FP MIPA UPI. Bandung 22-23 Juli 2005.
- [29] Sagala, S. 2013. *Konsep dan Makna Pembelajaran*. Bandung: Alfabeta.
- [30] Sanjaya, I.P.H. 2012. Pengaruh Model Pembelajaran Inkuiri Laboratorium terhadap Keterampilan Berpikir

- Kreatif dan Keterampilan Proses Sains Siswa Ditinjau dari Kemandirian Belajar Siswa. *Jurnal Penelitian Pascasarjana Undiksha*, 2(2): 1-15.
- [31] Sudarmini, Y., Kosim & Hadiwijaya, A.S. 2015. Pembelajaran Fisika Berbasis Inkuiri Terbimbing dengan Menggunakan LKS untuk Meningkatkan Keterampilan Berpikir Kritis Ditinjau dari Sikap Ilmiah Siswa Madrasah Aliyah Qamarul Huda Bagu Lombok Tengah. *Jurnal Penelitian Pendidikan IPA*, 1. (1): 35-48.
- [32] Snyder, L.G., & Snyder, M.J. 2008. Teaching Critical Thinking and Problem Solving Skills. *The Delta Pi Epsilon Journal*, L(2): 90-99.
- [33] Sohibin, A., Dwijananti, P., & Marwoto, P. 2009. Penenrapan Model Pembelajaran Inkuiri Terpimpin untuk Peningkatan Pemahaman dan Keterampilan Berpikir Kritis Siswa SD. *Universitas Negeri Semarang (Unnes), Semarang, Indonesia. Jurnal Pendidikan Indonesia*, 5: 96-100.
- [34] Suma, K. 2010. Efektivitas Pembelajaran Berbasis Inkuiri dalam Peningkatan Penguasaan Konten dan Penalaran Ilmiah Calon Guru Fisika. Fakultas MIPA, Universitas Pendidikan Ganesha, *Jurnal Pendidikan dan Pengajaran*, 43 (6): 47-55.
- [35] Tindangen, M. (2007). Implementasi Strategi Inkuiri Biologi SMP serta Pengaruhnya terhadap Kemampuan Berpikir Tingkat Tinggi. *Jurnal Pendidikan*, 8 (2): 1-9.
- [36] Wardani, S., Anna, P., Asep, K., & Buchari. 2013. Kecerdasan *Logical Mathematics* Berbasis Aktivitas Inkuiri Laboratorium. *Jurnal Inovasi Pendidikan Kimia*, 7(3): 1129-1137.
- [37] Wena, Made. 2009. *Strategi Pembelajaran Inovatif Kontemporer*. Jakarta: Bumi Aksara.
- [38] Wenning Carl, J. 2011. Level of Inquiry Model of Science Teaching: Learning Sequences to Lesson Plan. Department of Physics. Illinois University, Normal, IL, USA. *Journal Physics Teacher Education online*, 6(2), 17-20.
- [39] Wijayanti, P.I., & Hindarto, N. 2010. Eksplorasi Kesulitan Belajar Siswa pada Pokok Bahasan Cahaya dan Upaya Peningkatan Hasil Belajar Melalui Pembelajaran Inkuiri Terbimbing. *Jurnal Pendidikan Fisika Indonesia*, 6: 1-5.
- [40] Winarni, E. 2009. Pengembangan Model Pembelajaran Inkuiri Terbimbing dan Masyarakat Belajar untuk Meningkatkan Pemahaman Konsep dan Life Skill Siswa Sekolah Dasar. *Jurnal Pendidikan Dasar*, 10 (1): 1-7.
- [41] Wirtha, N.K. 2008. Pengaruh Model Pembelajaran dan Penalaran Formal terhadap Penguasaan Konsep Fisika dan Sikap Ilmiah Siswa SMA Negeri 4 Singaraja. JPPP, Lembaga Penelitian Undiksha, *Jurnal Penelitian dan Pengembangan Pendidikan*, 1 (2): 15-29.

# Facile fabrication and characterizations of nanostructured Fe<sub>2</sub>O<sub>3</sub>-TiO<sub>2</sub> composite from Ilmenite ore

Chinh Van Tran<sup>1</sup>, Phuong T.H Nguyen<sup>1</sup>, Duy Anh Nguyen, Bac Thanh Le, Tuan Ngoc Truong, Duong Duc La<sup>1,\*</sup>

<sup>1</sup>Institute of Chemistry and Materials, Hoang Sam, Hanoi, Vietnam, 100000

**Abstract**— Fe<sub>2</sub>O<sub>3</sub>-TiO<sub>2</sub> nanoparticles promises as a highly effective material for adsorption of heavy metals and used as photocatalyst for the removal of organic dye pollutants. In this study, nanostructured Fe<sub>2</sub>O<sub>3</sub>-TiO<sub>2</sub> composite was successfully fabricated by one-step reaction of ilmenite ore at the high temperature in ambient condition. The resultant Fe<sub>2</sub>O<sub>3</sub>-TiO<sub>2</sub> composite was characterized by using X-ray diffraction (XRD), Fourier Transform Infrared spectroscopy (FTIR), Scanning electron microscopy (SEM), nitrogen adsorption-desorption isotherm. The effects of sintered temperature and time on the formation of the Fe<sub>2</sub>O<sub>3</sub>-TiO<sub>2</sub> nanocomposite were investigated in detail. The Fe<sub>2</sub>O<sub>3</sub>-TiO<sub>2</sub> was formed from ilmenite ore after calcination at the temperature of 700°C in 3 hours, followed by a ball-milled process in 4 hours. The obtained Fe<sub>2</sub>O<sub>3</sub>-TiO<sub>2</sub> composite has an average diameter of from 50 - 100 nm with the BET surface area of 7 m<sup>2</sup>/g.

**Keywords**—Ilmenite, Fe<sub>2</sub>O<sub>3</sub>-TiO<sub>2</sub>, nanocomposite, mixed oxides, ore processing.

## I. INTRODUCTION

In recent years, nanostructured Fe<sub>2</sub>O<sub>3</sub>-TiO<sub>2</sub> particles have been extensively studied by many researchers for application of photocatalytic oxidation<sup>1-3</sup> and adsorption processes.<sup>4-6</sup> Various synthetic approaches for fabrication Ti /Fe oxides composites have been reported in the literature.<sup>1, 4, 7-8</sup> One of the most employed methods to synthesize nanostructured Fe<sub>2</sub>O<sub>3</sub>-TiO<sub>2</sub> composite is co-precipitation. The co-precipitation technique is related to the dissolving of a salt precursor such as a chloride, oxychloride or nitrate. The precipitation of corresponding metal hydroxides is occurred during addition of base solution such as sodium hydroxide or ammonium hydroxide solution. The residues are then washed and calcined to obtain the final products. This preparation method is effective for synthesis of metal oxide composites. Other processes such as hydrothermal deposition,<sup>8-9</sup> impregnation<sup>8, 10</sup> and sol-hydrolysis<sup>9</sup> have been also employed to improve the distribution of FeII/III

into the TiO<sub>2</sub> lattice. The sources of Ti and Fe in fabrication of mixed oxides composite have been utilized including titanium tetra-isopropoxide,<sup>8, 10</sup> titanium IV tetra-tert-butoxide<sup>9</sup> and powdered TiO<sub>2</sub> anatase as Ti pre-cursors and iron nitrate,<sup>8</sup> FeIII acetylacetonate<sup>10</sup> and FeII/III chloride as Fe pre-cursor materials.<sup>9</sup>

There are several parameters affecting to the formation of TiO<sub>2</sub> and Fe<sub>2</sub>O<sub>3</sub> such as the use of synthetic method, calcination temperature and relative ratio of Ti and Fe oxides. For example, calcination temperatures of Fe:Ti (1:1 ratio) mixtures at 700°C and 900°C, lead to the information of rutile and of pseudo-brookite (Fe<sub>2</sub>TiO<sub>5</sub>) due to the diffusion of FeIII into TiO<sub>2</sub> at higher temperature whereas only amorphous anatase and traces of rutile were found at calcination temperature of 500°C.<sup>10</sup>

Ilmenite ore (FeTiO<sub>3</sub>) is an important raw material for titanium dioxide production due to cheapness and abundance in nature for the titanium source.<sup>2, 11</sup> Because of the attractively unique properties of nanoilmenite, it has received considerable attention for the utilization in wide range of applications such as supercapacitor,<sup>12</sup> oxygen carrier in a chemical-looping combustion reactor,<sup>13</sup> gas sensor, solar cells, chemical catalysts and photocatalysts.<sup>14-18</sup> Ilmenite ore has been employed to fabricate the Fe<sub>2</sub>O<sub>3</sub>-TiO<sub>2</sub> mixed oxides by many researchers.<sup>3, 19-22</sup> Smith *et al.* successfully fabricated sulfated Fe<sub>2</sub>O<sub>3</sub>-TiO<sub>2</sub> by treatment of ilmenite ore with sulfuric acid and the prepared sulfated mixed oxides show the photocatalytic activity toward oxidation of 4-chlorophenol (4-CP) in aqueous medium under UV-vis and visible light irradiation.<sup>22</sup> The same procedure was also employed to synthesize sulfated Fe<sub>2</sub>O<sub>3</sub>-TiO<sub>2</sub> and used as a catalyst for conversion of vegetable oil to biodiesel.<sup>3</sup> Recently, nano FeTiO<sub>3</sub>-TiO<sub>2</sub> had been successfully prepared from ilmenite ore as raw material by simple modified sulfate route.<sup>19</sup> This nano FeTiO<sub>3</sub>-TiO<sub>2</sub> samples showed significant effectiveness of catalyst under Fenton-like process. However, most of these Fe<sub>2</sub>O<sub>3</sub>-TiO<sub>2</sub> composites prepared from ilmenite ore contains sulfate groups and related to toxic fabricating process (treatment

with concentrated acid). In order to address these disadvantages, we present a facile approach to fabrication of nanostructured  $\text{Fe}_2\text{O}_3/\text{TiO}_2$  composite from ilmenite ore by calcinating of raw ilmenite ore at high temperature and followed by a ball mill process. The prepared  $\text{Fe}_2\text{O}_3/\text{TiO}_2$  composite are thoroughly characterized by XRD, SEM, FTIR, and BET. The The effects of calcination conditions are also studied in detail.

## II. EXPERIMENTAL SECTION

### Synthesis of nanostructured $\text{Fe}_2\text{O}_3/\text{TiO}_2$ composite

In the typical procedure, 10g of raw ilmenite ore 52% was washed with 100 ml sulfuric acid several times. The  $\text{Fe}_2\text{O}_3/\text{TiO}_2$  mixed oxides were prepared by sintering 10 g of washed ilmenite at various temperature of 500, 600, 700, 800 and 900°C in different periods of time in air condition. The calcinated products were then cooled naturally to room temperature before underwent a ball-milled process with 150 and 200 g of 2 and 5 mm-diameter zirconia ball in the milling cell and filled with 80 ml deionized water. The milling process was operated at room temperature for 24 h. The milled  $\text{Fe}_2\text{O}_3/\text{TiO}_2$  mixed oxides were filtered and dried at temperature of 60°C for 12 h to obtained nanostructured  $\text{Fe}_2\text{O}_3/\text{TiO}_2$  composite.

### Characterization

Particle size, morphology and surface topology of samples were observed by using a Hitachi S-4600. The surface area was evaluated from the  $\text{N}_2$  adsorption isotherm at 77 K using a BET TriStar II Plus 377. XRD patterns for all samples were measured using X'Pert PRO PANalytical with 0.15405 nm  $\text{Cu-K}\alpha$  radiation source. Fourier transform infrared spectroscopy (FTIR, TENSOR II, Bruker) was employed to investigate the surface functional group adsorbent of prepared nanostructured  $\text{Fe}_2\text{O}_3/\text{TiO}_2$  composite samples.

## III. RESULTS AND DISCUSSION

Illustrated in Figure 1 is the XRD patterns for the Ilmenite ore and the  $\text{Fe}_2\text{O}_3\text{-TiO}_2$  mixed oxides obtained from calcination of ilmenite ore at temperature of 700°C in 3 hours. In the XRD pattern of ilmenite ore, all diffraction peaks were assigned to the Ilmenite ( $\text{FeTiO}_3$ ) phase (JCPDS card No. 98-010-4235). After sintering at 700°C in 3 hours in air condition and followed by ball mill process,  $\text{FeTiO}_3$  completely converted to  $\text{TiO}_2/\text{Fe}_2\text{O}_3$  mixed oxides, which is clearly shown in the XRD pattern. All diffraction peaks in the XRD pattern of prepared  $\text{TiO}_2\text{-Fe}_2\text{O}_3$  were denoted to the  $\text{TiO}_2$  rutile (JCPDS card No. 98-006-2553) and  $\text{Fe}_2\text{O}_3$  (hematite, JCPDS card No. 98-005-3677) phases.

The formation of  $\text{TiO}_2\text{-Fe}_2\text{O}_3$  mixed oxides was further confirmed by FTIR spectrum. Figure 2 shows the FTIR

spectra of Ilmenite ore and the  $\text{Fe}_2\text{O}_3/\text{TiO}_2$  mixed oxides obtained from calcination of ilmenite ore at temperature of 700°C in 3 hours. In these spectra, the large and broad absorption peak at  $3432\text{ cm}^{-1}$  is related to the stretch region of the surface hydroxyl groups with hydrogen bonds and chemisorbed water.<sup>23-24</sup> The

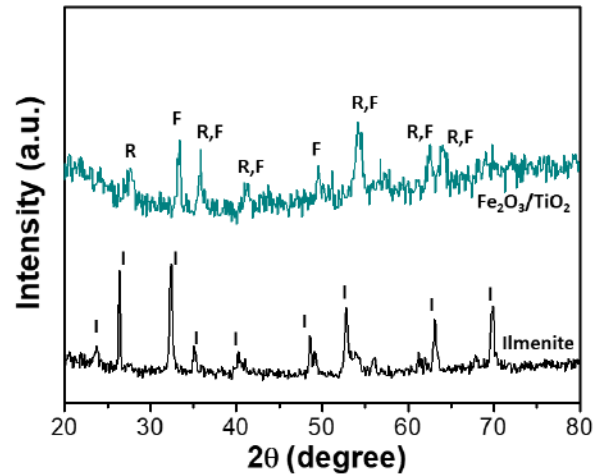


Fig. 1: XRD patterns of Ilmenite ore (black line) and as-prepared  $\text{Fe}_2\text{O}_3/\text{TiO}_2$  composites (blue line). The peaks are indexed with standard JCPDS cards, I – Ilmenite ore, R – Rutile, F –  $\text{Fe}_2\text{O}_3$ .

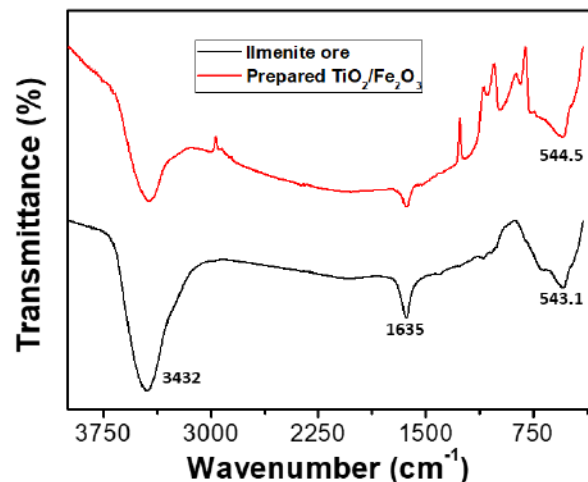


Fig. 2: FTIR spectra of Ilmenite ore (black curve) and as-prepared  $\text{Fe}_2\text{O}_3/\text{TiO}_2$  composites (red curve).

broad absorption peak at  $1635\text{ cm}^{-1}$  can be assigned to the O–H bending of molecularly physisorbed water.<sup>25</sup> In the FTIR spectrum of ilmenite ore (black curve), the absorption peak at  $543.1\text{ cm}^{-1}$  can be attributed to the Fe–O bond in the ilmenite ( $\text{FeTiO}_3$ ).<sup>26</sup> A broad absorption peak at around this position was also observed in the FTIR spectrum of the prepared mixed oxides, which indicate the presence of the F–O stretching. However, this absorption peaks was at higher wavenumber of  $544.5\text{ cm}^{-1}$  comparing to that of ilmenite, which indicates the formation of  $\text{Fe}_2\text{O}_3$ . In the FTIR curve of mixed oxides, the appearance of the

large absorption in the range of 600  $\text{cm}^{-1}$  to 800  $\text{cm}^{-1}$ , which is characteristic of the O–Ti–O bond,<sup>24</sup> confirm the formation of  $\text{TiO}_2$  oxide. The above results indicate that under the high temperature of 700°C in the ambient condition, the  $\text{FeTiO}_3$  reacted with oxygen to form  $\text{Fe}_2\text{O}_3$  and  $\text{TiO}_2$  oxides.

The surface morphology of nanostructured  $\text{Fe}_2\text{O}_3/\text{TiO}_2$  composite was investigated by using scanning electron microscopy. Illustrated in Figure 3 is the SEM images of raw ilmenite ore and the  $\text{Fe}_2\text{O}_3/\text{TiO}_2$  composites

obtained from calcination of ilmenite ore at 700°C in 3h and followed by a ball-milled process for 8 hours. The figure 3A shows that ilmenite ore is in form of microparticles with the diameter ranging from 100 - 500  $\mu\text{m}$ . After formation of  $\text{Fe}_2\text{O}_3/\text{TiO}_2$  oxides, the particle sizes are significantly decreased with particle diameter down to 50 - 100 nm. This result indicates that the nanostructured  $\text{Fe}_2\text{O}_3/\text{TiO}_2$  composite was successfully fabricated from ilmenite microparticles by simple calcination and ball-milled approach.

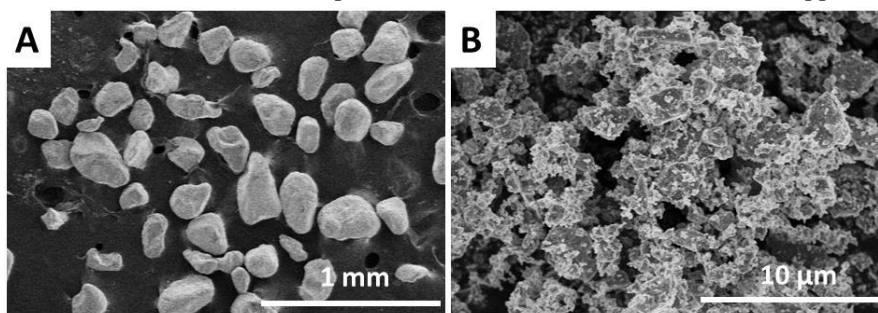


Fig.3 :SEM images of Ilmenite ore (A) and as-prepared  $\text{Fe}_2\text{O}_3/\text{TiO}_2$  composites (B)

The total surface areas of the nanostructured  $\text{Fe}_2\text{O}_3/\text{TiO}_2$  composite were obtained with reference to the Brunauer–Emmett–Teller (BET) multi-point and single-point methods [35] using the  $\text{N}_2$  adsorption/desorption isotherm data. All samples were pretreated with degassing at 90 °C for 1 h followed by 105 °C overnight with ultra high purity nitrogen purge before the measurement. The pore volume data were calculated by using BJH method which is the procedure for calculating pore size distribution using the Kelvin equation and DH methods. Figure 4 shows the  $\text{N}_2$  adsorption/desorption isotherm plot and inset is the BET surface area plot. The parameters of BET surface area analysis are summarized in Table 1. It is clear from the table that the obtained  $\text{Fe}_2\text{O}_3/\text{TiO}_2$  composite has the BET surface area of 6.9645  $\text{m}^2/\text{g}$  with pore volume of 0.023686  $\text{cm}^3/\text{g}$  and the pore size of 15.7380 nm.

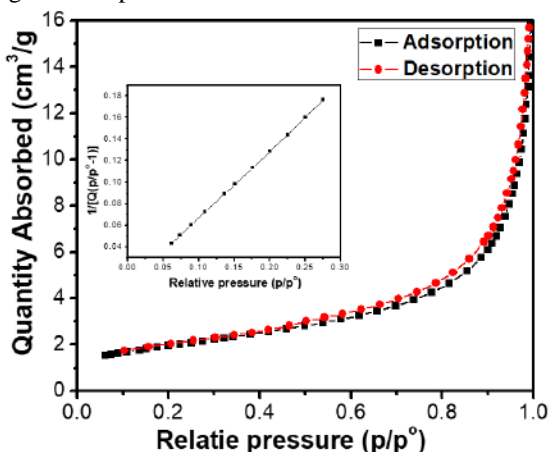


Fig.4 :Nitrogen adsorption plot and inset is the BET surface area plot

Table 1: BET surface area values

Surface area ( $\text{m}^2/\text{g}$ )	Pore volume ( $\text{cm}^3/\text{g}$ )	Pore size (nm)
6.9645	0.023686	15.7380

The effect of the sintering temperature on the formation of nanostructure  $\text{TiO}_2\text{-Fe}_2\text{O}_3$  composite was investigated by employing the X-ray diffraction pattern. Figure 5 shows the XRD patterns of products obtained from the calcination of ilmenite ore at various temperature in 3 hours. In the XRD pattern of ilmenite sintered at the sintered temperature of 500°C, all diffraction peaks were consistent with ilmenite phase (JCPDS card No. 98-010-4235), which indicates that no oxides were formed from  $\text{FeTiO}_3$  under this temperature. When the sintered temperature was further increased to 600°C, the diffraction peaks in the XRD pattern show the presences of  $\text{TiO}_2$  (rutile) and  $\text{Fe}_2\text{O}_3$  (hematite) phases. There still exists the diffraction peaks of ilmenite phase. However, no diffraction peaks of ilmenite was observed when calcined ilmenite at temperature of 700°C, which indicates that  $\text{FeTiO}_3$  completely reacted with oxygen to form  $\text{TiO}_2\text{-Fe}_2\text{O}_3$  mixed oxides. When calcined temperature was further increase to 800°C, diffraction peaks were assigned to the formation of  $\text{TiO}_2$  (rutile),  $\text{Fe}_3\text{O}_4$  (magnetite), and  $\text{Fe}_2\text{TiO}_5$  (pseudobrookite) (JCPDS card No. 98-001-2310, 98-010-8716, and 98-001-2289, respectively). Interestingly, at the higher calcined temperature, all diffraction peaks was denoted to the  $\text{Fe}_2\text{TiO}_5$  (pseudobrookite) phase, which shows that at this temperature  $\text{FeTiO}_3$  reacted with oxygen in air to

form  $\text{Fe}_2\text{TiO}_5$ . From these results, the calcined temperature of  $700^\circ\text{C}$  was selected as optimized temperature to obtain  $\text{TiO}_2/\text{Fe}_2\text{O}_3$  composite from ilmenite ore.

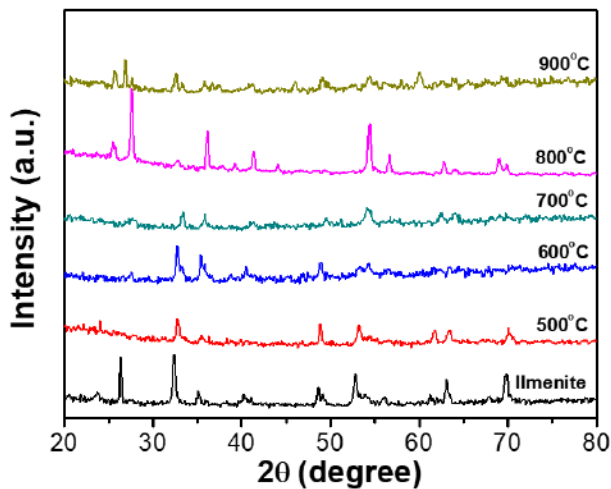


Fig.5 : XRD patterns of ilmenite ore sintered in 3h at various temperatures in air condition.

The sintered time also greatly affects to the formation of  $\text{TiO}_2\text{-Fe}_2\text{O}_3$  composite. Figure 6 exhibits the XRD patterns of ilmenite calcined at temperature of  $700^\circ\text{C}$  in different period of time. After only 30 minute of calcination, majority of the ilmenite already converted to  $\text{TiO}_2$  and  $\text{Fe}_2\text{O}_3$ . This indicates that reaction of ilmenite with oxygen to form oxides at this temperature occurred

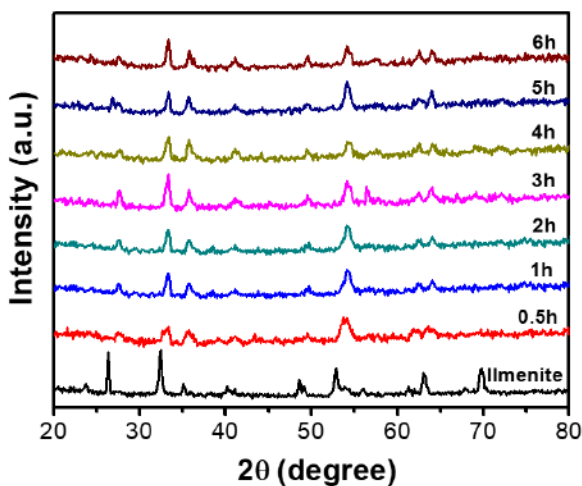


Fig.6 : XRD patterns of ilmenite ore sintered at temperatures of  $700^\circ\text{C}$  in various time points in air condition. relatively quick. It is obvious from the XRD patterns that further increase of the sintering time did not significantly affect to phase of the calcined product, the phase and crystallinity of the mixed oxides were almost unchanged after 2 hours of the calcination time.

#### IV. CONCLUSION

In summary, we have employed a simple one-step approach for successful fabrication of nanostructured  $\text{Fe}_2\text{O}_3\text{-TiO}_2$  composite. The  $\text{Fe}_2\text{O}_3\text{-TiO}_2$  nanocomposite was synthesized from ilmenite ore by calcination at the temperature of  $700^\circ\text{C}$  in 3 hours, followed by a ball-milled process in 4 hours. The obtained  $\text{Fe}_2\text{O}_3\text{-TiO}_2$  composite has an average diameter of from 50 - 100 nm with BET surface area of around  $7 \text{ m}^2/\text{g}$ . While temperature greatly affects to the formation of  $\text{Fe}_2\text{O}_3\text{-TiO}_2$  nanocomposite from ilmenite ore, the sintering time does not significantly affect to the formation of nanocomposite. The success of fabrication of nanostructured  $\text{Fe}_2\text{O}_3\text{-TiO}_2$  composite from ilmenite ore by a simple approach of calcination will certainly introduce a cost-effective way to synthesize the metal oxides nanocomposite, which can be use in adsorption, photocatalysis and energy storage. In the next study, we will investigate the photocatalytic activity and adsorption properties of this resultant nanocomposite.

#### ACKNOWLEDGEMENTS

This work was financially supported by Inorganic Lab, Institute of Chemistry and Materials. The authors acknowledge the facilities, and the scientific and technical assistance, at Institute of Chemistry and Materials.

#### REFERENCES

- [1] Zhou, W.; Fu, H.; Pan, K.; Tian, C.; Qu, Y.; Lu, P.; Sun, C.-C., Mesoporous  $\text{TiO}_2/\alpha\text{-Fe}_2\text{O}_3$ : bifunctional composites for effective elimination of arsenite contamination through simultaneous photocatalytic oxidation and adsorption. *J. Phys. Chem. C* 2008,**112** (49): 19584-19589.
- [2] Su, H.; Lv, X.; Zhang, Z.; Yu, J.; Wang, T., Arsenic removal from water by photocatalytic functional  $\text{Fe}_2\text{O}_3\text{-TiO}_2$  porous ceramic. *J. Porous Mater.* 2017,**24** (5): 1227-1235.
- [3] Anuradha, S.; Raj, K.; Vijayaraghavan, V.; Viswanathan, B., Sulphated  $\text{Fe}_2\text{O}_3\text{-TiO}_2$  catalysed transesterification of soybean oil to biodiesel. *Indian J. Chem.* 2014,**53A**: 1493 - 1499.
- [4] D'Arcy, M.; Weiss, D.; Bluck, M.; Vilar, R., Adsorption kinetics, capacity and mechanism of arsenate and phosphate on a bifunctional  $\text{Fe}_2\text{O}_3\text{-TiO}_2$  bi-composite. *J. Colloid Interface Sci.* 2011,**364** (1): 205-212.
- [5] Yu, L.; Peng, X.; Ni, F.; Li, J.; Wang, D.; Luan, Z., Arsenite removal from aqueous solutions by  $\gamma\text{-Fe}_2\text{O}_3\text{-TiO}_2$  magnetic nanoparticles through simultaneous photocatalytic oxidation and adsorption. *J. Hazard. Mater.* 2013,**246**: 10-17.

- [6] Beduk, F., Superparamagnetic nanomaterial Fe<sub>2</sub>O<sub>3</sub>-TiO<sub>2</sub> for the removal of As (V) and As (III) from aqueous solutions. *Environ. Technol.* 2016,**37** (14): 1790-1801.
- [7] Gupta, K.; Ghosh, U. C., Arsenic removal using hydrous nanostructure iron (III)-titanium (IV) binary mixed oxide from aqueous solution. *J.Hazard. Mater.* 2009,**161** (2-3): 884-892.
- [8] Kang, M.; Choung, S.-J.; Park, J. Y., Photocatalytic performance of nanometer-sized Fe<sub>x</sub>O<sub>y</sub>/TiO<sub>2</sub> particle synthesized by hydrothermal method. *Cat. Today* 2003,**87** (1-4): 87-97.
- [9] Zhu, J.; Zheng, W.; He, B.; Zhang, J.; Anpo, M., Characterization of Fe-TiO<sub>2</sub> photocatalysts synthesized by hydrothermal method and their photocatalytic reactivity for photodegradation of XRG dye diluted in water. *J. Mol. Cat. A Chem.* 2004,**216** (1): 35-43.
- [10] Pal, B.; Sharon, M.; Nogami, G., Preparation and characterization of TiO<sub>2</sub>/Fe<sub>2</sub>O<sub>3</sub> binary mixed oxides and its photocatalytic properties. *Materials Chemistry and Physics* 1999,**59** (3): 254-261.
- [11] Zhang, W.; Zhu, Z.; Cheng, C. Y., A literature review of titanium metallurgical processes. *Hydrometallurgy* 2011,**108** (3-4): 177-188.
- [12] Tao, T.; Glushenkov, A. M.; Liu, H.; Liu, Z.; Dai, X. J.; Chen, H.; Ringer, S. P.; Chen, Y., Ilmenite FeTiO<sub>3</sub> nanoflowers and their pseudocapacitance. *J. Phys. Chem. C* 2011,**115** (35): 17297-17302.
- [13] Adánez, J.; Cuadrat, A.; Abad, A.; Gayán, P.; de Diego, L. F.; García-Labiano, F., Ilmenite activation during consecutive redox cycles in chemical-looping combustion. *Energy Fuels* 2010,**24** (2): 1402-1413.
- [14] Lind, F.; Berguerand, N.; Seemann, M.; Thunman, H., Ilmenite and nickel as catalysts for upgrading of raw gas derived from biomass gasification. *Energy Fuels* 2013,**27** (2): 997-1007.
- [15] García-Muñoz, P.; Pliego, G.; Zazo, J.; Barbero, B.; Bahamonde, A.; Casas, J., Modified ilmenite as catalyst for CWPO-Photoassisted process under LED light. *Chem. Eng. J.* 2017,**318**: 89-94.
- [16] Halpegamage, S.; Ding, P.; Gong, X.-Q.; Batzill, M., Ordered Fe (II) Ti (IV) O<sub>3</sub> mixed monolayer oxide on rutile TiO<sub>2</sub> (011). *ACS Nano* 2015,**9** (8): 8627-8636.
- [17] Zhang, X.; Li, T.; Gong, Z.; Zhao, H.; Wang, L.; Wan, J.; Wang, D.; Li, X.; Fu, W., Shape controlled FeTiO<sub>3</sub> nanostructures: Crystal facet and photocatalytic property. *J. Alloy. Comp.* 2015,**653**: 619-623.
- [18] Truong, Q. D.; Liu, J.-Y.; Chung, C.-C.; Ling, Y.-C., Photocatalytic reduction of CO<sub>2</sub> on FeTiO<sub>3</sub>/TiO<sub>2</sub> photocatalyst. *Catal. Commun.* 2012,**19**: 85-89.
- [19] Phooinkong, W.; Yimwan, W.; Mekprasart, W.; Pecharapa, W., Preparation of nanoFeTiO<sub>3</sub>-TiO<sub>2</sub> catalyst from ilmenite ore for catalytic degradation of methylene blue. *Suranaree J. Sci. Technol.* 2016,**23** (4).
- [20] Raj, K.; Prakash, M.; Shanmugam, R.; Krishnamurthy, K.; Viswanathan, B., Surface acidic properties of sulphated Fe<sub>2</sub>O<sub>3</sub>-TiO<sub>2</sub>. *Indian J. Chem.* 2011,**50A**: 1050-1055.
- [21] Raj, K. J. A.; Prakash, M.; Viswanathan, B., Selective ortho butylation of phenol over sulfated Fe<sub>2</sub>O<sub>3</sub>-TiO<sub>2</sub>. *Catal. Sci. Technol.* 2011,**1** (7): 1182-1188.
- [22] Smith, Y. R.; Raj, K. J. A.; Subramanian, V. R.; Viswanathan, B., Sulfated Fe<sub>2</sub>O<sub>3</sub>-TiO<sub>2</sub> synthesized from ilmenite ore: a visible light active photocatalyst. *Coll. Surf. A Phys. Chem. Eng. Asp.* 2010,**367** (1-3): 140-147.
- [23] Kuvarega, A. T.; Krause, R. W.; Mamba, B. B., Nitrogen/palladium-codoped TiO<sub>2</sub> for efficient visible light photocatalytic dye degradation. *J. Phys. Chem. C* 2011,**115** (45): 22110-22120.
- [24] Zou, J.; Gao, J.; Xie, F., An amorphous TiO<sub>2</sub> sol sensitized with H<sub>2</sub>O<sub>2</sub> with the enhancement of photocatalytic activity. *J. Alloys Comp.* 2010,**497** (1-2): 420-427.
- [25] Wu, J. C.; Lin, H.-M.; Lai, C.-L., Photo reduction of CO<sub>2</sub> to methanol using optical-fiber photoreactor. *Appl. Cat. A Gen.* 2005,**296** (2): 194-200.
- [26] Hong, T.; Mao, J.; Tao, F.; Lan, M., Recyclable Magnetic Titania Nanocomposite from Ilmenite with Enhanced Photocatalytic Activity. *Molecules* 2017,**22** (12): 2044.